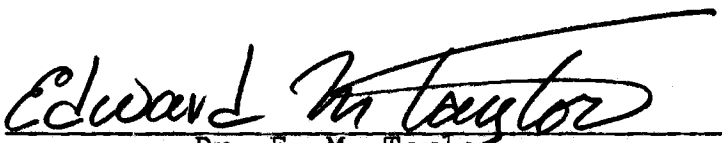


AN ABSTRACT OF THE THESIS OF

Debra May Cannon for the degree of Master of Science in
the Department of Geology presented on May 4, 1984

Title: The Stratigraphy, Geochemistry, and Mineralogy of
Two Ash-Flow Tuffs in the Deschutes Formation, Central
Oregon

Abstract approved:


Dr. E. M. Taylor

Two ash-flow tuff units of the late Miocene-early Pliocene Deschute Formation in central Oregon were studied in detail because of the widespread distribution, diverse compositions, and stratigraphic importance.

The Lower Bridge tuff is a double-flow simple cooling unit that is poorly welded. The upper flow grades from rhyolite in the lower part to dacite in the upper part. A white 1.5 to 5-foot accretionary lapilli air-fall deposit often underlies the two ash-flow sequences. Phenocrysts in the pumice lumps are plagioclase (An 35-45), pargasite, hypersthene, augite, ilmenite, apatite, and magnetite. The compositional change from rhyolite to dacite in the upper flow suggests

that it was formed by eruption of successively lower parts of a zoned magma body.

The McKenzie Canyon tuff is a multiple flow compound cooling unit that overlies the Lower Bridge tuff. It may have covered 160 square km and had a volume of 0.7 km^3 . It was erupted onto irregular terrain resulting in variable thicknesses. Up to three light-colored, rhyolitic ash-flow deposits are overlain by two red columnar-jointed units. The red color and welding of the upper two members are the distinguishing physical features of the McKenzie Canyon tuff. The lower nonresistant silicic flows are often absent in the northern part of the study area. The facts that the units decrease in thickness and in elevation northward and that the average pumice size becomes smaller suggests a source to the south. Another distinguishing feature of the upper red flow(s) is the prevalence of white (rhyolite), black (andesite), banded (rhyolite and andesite), and collapsed pumices. A few dacite pumice clasts (mixed) are also present. In the lower silicic flows black or banded pumices are only found in minor amounts and collapsed pumices are absent. Collapsed pumices in the upper flow(s) only occur throughout the welded section in nearly horizontal orientations.

The white pumice is a high-K rhyolite with phenocrysts of oligoclase/andesine (An 29-31),

hypersthene, augite, magnetite, ilmenite, and zircon.

The black pumice is medium-K, hi-Ti and -Fe andesite that contains labradorite (An 60-65), olivine (Fo₈₂), augite, hypersthene, and magnetite. The percentage of black pumice increases upward in the upper flow. Banded pumice is a combination of rhyolite and andesite magmas and represents the coeruption of these two compositions.

Evidence of complete mixing of the magmas i.e., homogeneous dacite pumice, is minor. Collapsed pumices have the same composition as rhyolite or banded pumices.

The McKenzie Canyon tuff was possibly derived from two separate magmas. As mafic magma was injected into a silicic magma chamber, ensuing convection and vesiculation probably caused the formation of banded pumice. This hypothesis is based on the following relationships: 1) phenocrysts and bulk chemistry of rhyolite and andesitic pumices are of distinct compositions, 2) a paucity of phenocrysts occur in the andesitic pumices, and 3) Harker diagrams of major element chemistries show that the two magmas have divergent regression lines.

The McKenzie Canyon tuff upper flows are unusual among banded pumice-bearing tuffs because of the aphyric nature of the andesite and the probability that the rhyolite and andesite magmas are not derived from the same magma chamber.

THE STRATIGRAPHY, GEOCHEMISTRY, AND MINERALOGY OF TWO
ASH-FLOW TUFFS IN THE DESCHUTES FORMATION,
CENTRAL OREGON

by

Debra May Cannon

A THESIS

submitted to

Oregon State University

In partial fulfillment of the
requirements for the
degree of

Master of Science

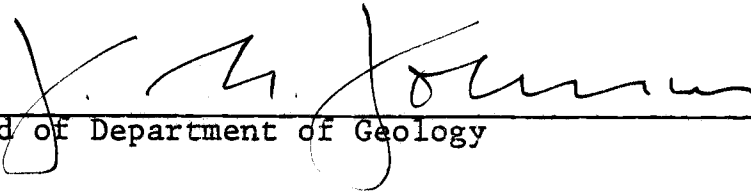
Completed May 4, 1984

Commencement June 1985

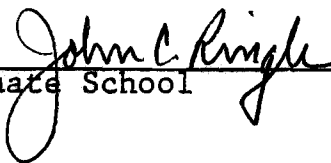
APPROVED:



Associate Professor of Geology in charge of major



Head of Department of Geology



Dean of Graduate School

Date thesis is presented May 4, 1984

Typed by Carol I. Barnett for Debra May Cannon

ACKNOWLEDGEMENTS

I am deeply indebted to Dr. Ed Taylor, whose encouragement and "fast turnaround time", enabled me to take the job with Boise Cascade. His willingness to help is appreciated.

Rich Conrey, and Scott Hughes deserve special thanks for reviewing the first draft of my thesis and providing words of encouragement.

The following people provided their friendship and support and made my time in graduate school a little easier and much more enjoyable: Dan Mumford, Brit Hill, Max Rosenberg, Dave Thormalin, Doug Bonelli, Bob Casacelli, and Larry Freeman. Many other friends have also provided enumerable hours of advice and incentive.

This thesis is dedicated to my parents who have given me the freedom, and most of all, their love and support that has enabled me to complete my course of study.

TABLE OF CONTENTS

	Page
INTRODUCTION	1
Purposes of Study.	1
Location, Access, Topography, and Climate. . .	3
Previous Work.	6
Methods.	9
GEOLOGIC SETTING AND STRUCTURE	14
Geologic Setting	14
Structure.	18
ASH-FLOW TUFF DESCRIPTIONS.	25
General Characteristics of Ash-flow Tuffs. . .	25
Deschutes Formation Ash-flow Tuffs	28
STRATIGRAPHY AND DISTRIBUTION	28
LOWER BRIDGE TUFF	30
MCKENZIE CANYON TUFF.	35
General Description	35
Clasts of McKenzie Canyon Tuff	
Below McKenzie Canyon Tuff	47
LATERAL VARIATIONS AND SOURCE	49
WELDING, ZONING, AND COOLING UNITS. . . .	51
TEMPERATURE, VOLUME, TRANSPORT, SPEED, AND FLOW MECHANISMS	55
Temperature	55
Volume and Transport	56
Speed and Flow Mechanisms.	61
MINERALOGY.	63
Introduction	63
Lower Bridge Tuff Pumice	68
McKenzie Canyon Tuff White Pumice	71
McKenzie Canyon Tuff Black Pumice	74
GEOCHEMISTRY.	79
Introduction	79
Harker Diagrams	86
Calcalalic Rocks and Ternary Diagrams	92
Lateral and Vertical Chemical Variation. . . .	101
Conclusion	104

	Page
INTERPRETATION AND CONCLUSIONS.	111
The Zoned Magma Chamber	114
Two Separate Magmas.	117
Conclusions.	118
REFERENCES.	119
APPENDIX 1	128
APPENDIX 2	133

LIST OF FIGURES

Figure		Page
1.	Location map of study area.	4
2.	Orange MCT exposed in the walls of the Deschutes River Canyon.	5
3.	Location of Stensland's (1970) thesis area and geochemical sample locations for LBT and MCT	10
4.	Two lower silicic flows of MCT overlain by the upper red unit on the south side of "Clarno Hill".	20
5.	Orange MCT cut by a channel of sediments.	22
6.	In the foreground MCT thickens and fills a channel	23
7.	Proximal and distal facies of intermediate to large pyroclastic flow units. . .	27
8.	Idealized columnar section of LBT and MCT	32
9.	Accretionary lapilli bed at the base of LBT	33
10.	Basal zone of upper flow of MCT	37
11.	Three lower silicic flows of MCT overlain by an upper red resistant flow.	38
12.	Columnar jointed MCT; note ten foot thick pumice-rich layer in foreground at base of red flow	39
13.	Gravel-laden spiracles found in the lower silicic flows of MCT.	41
14.	Horizontal lineation of black collapsed pumice in upper MCT flow.	43
15.	Mixed black and white pumice in upper flow MCT.	45

Figure		Page
16.	Clasts of a red upper flow of MCT in an epiclastic deposit below the upper flow of MCT.	48
17.	Possible location of source volcano for LBT and MCT	52
18.	Clinopyroxenes in the system $\text{CaMgSi}_2\text{O}_6$ - $\text{CaFeSi}_2\text{O}_6$ - $\text{Mg}_2\text{Si}_2\text{O}_6$ - $\text{Fe}_2\text{Si}_2\text{O}_6$. . .	66
19.	Nomenclature of orthorhombic pyroxenes and MCT microprobe orthopyroxene analyses using weight % oxides	67
20.	Photomicrograph of a plagioclase crystal from LBT pumice (#247).	69
21.	The suite of mafic minerals in LBT under a binocular microscope.	71
22.	Photomicrograph under crossed nicols of plagioclase from MCT white pumice (#251), southern Deep Canyon.	73
23.	Photomicrograph of plagioclase under crossed nicols from a black MCT pumice (#252), southern Deep Canyon sample location.	75
24.	Nomenclature and chemical composition of olivines	77
25.	An olivine crystal coated with idding-site taken from a black MCT pumice (#201)	78
26.	Southernmost sample location of MCT, (35 feet thick)	83
27.	Harker diagram of % K_2O versus % SiO_2 with linear regression lines.	89
28.	Harker diagram of % TiO_2 versus % SiO_2 with linear regression lines.	91
29.	Harker diagram of % FeO versus % SiO_2 with linear regression lines.	93
30.	Harker diagram of % CaO versus % SiO_2 with linear regression lines.	94

Figure		Page
31.	Chemical classification of volcanic rocks	95
32.	The definition of tholeiitic (TH) versus calcalkaline (CA) andesites.	97
33.	Relation of FeO and CaO versus SiO ₂ in black andesite pumice of MCT.	98
34.	Arrows represent 10% fractional crystallization.	99
35.	Arrows represent fractional crystallization of black MCT	100
36.	AMF diagram of oxide whole rock percentages by weight	102
37.	Plot of whole rock percentages.	103
38.	Vertical variation in chemistry, LBT at Deep Canyon sample location.	105
39.	Vertical variation in chemistry, LBT at Deep Canyon and Deschutes River sample location.	106
40.	Vertical variation in chemistry, MCT at Squaw Creek Butte sample location.	107
41.	Vertical variation in chemistry of MCT white pumice at Deep Canyon and Lower Bridge sample location.	108

LIST OF TABLES

Table		Page
1.	Estimated volumes and distances traveled by pyroclastic flows from their source.	58
2.	Emplacement data on large pyroclastic flows	60
3.	Analyzed mineral content of MCT and LBT relative to vertical position in the flow.	64
4.	Average chemical compositions and standard deviations for LBT and MCT	81
5.	A comparison of black and white pumice chemistries from blocks of MCT in sediments with the overlying MCT flow	85
6.	A comparison of the chemistries of the components of MCT banded pumice with similar MCT pumice compositions	87
7.	Characterization of the MCT and LBT	112

LIST OF PLATES

Plate

1. Outcrop map of the two ash-flow tuff units in the Deschutes Basin, Jefferson and Deschutes Counties, Oregon in pocket
2. The stratigraphy, geochemistry, and mineralogy of two ash-flow tuffs in the Deschutes Formation, Central Oregon in pocket

THE STRATIGRAPHY, GEOCHEMISTRY, AND MINERALOGY OF TWO
ASH-FLOW TUFFS IN THE DESCHUTES FORMATION,
CENTRAL OREGON

INTRODUCTION

Purposes of Study

The purposes of this study are to identify and interpret two unique ash-flow tuff units by determining the areal distribution, lateral and vertical variation, mineralogy, and major element geochemistry. These required geologic mapping, and petrographic and geochemical analyses.

Two ash-flow tuffs of the Deschutes Formation were chosen for detailed study because of the unique characteristics, broad areal extent, and common occurrence together. The McKenzie Canyon tuff is unusual because of the red, columnar jointed, upper flow top and banded black and white pumice. The underlying Lower Bridge tuff is distinguished by the light color, a basal accretionary lapilli layer, and lack of resistance to weathering and erosion.

Ash-flow tuffs furnish a quenched inverted look into

the upper reaches of a magma chamber, indicate the sequence of eruption, and are a key to flow mechanisms of ash-flow tuff deposition. An ash flow represents an instant in geological time. It is important as a marker bed within a formation because it may extend for long distances in volcanic and sedimentary terrains that commonly have lensing, tonguing, and facies changes (Smith, 1960b). The two tuffs selected lie stratigraphically in the middle of the formation as well as lying in the center of the Deschutes Basin. Consequently, this study will permit correlation of units lying both to the north and to the south in the basin.

The nearly flat lying Deschutes Formation has been incised by numerous streams and rivers, and provides a unique opportunity to study the geological environment existing 7.6 to 4 million years (m.y.) ago in central Oregon. Stratigraphic relations and major element chemistries of lava flows, ash-flow tuffs, and epiclastic deposits of the Deschutes Formation have been and continue to be studied by Oregon State University graduate students (Jay, 1982; Hayman, 1983; Conrey, [M.S.,] Dill, [M.S.,] McDannel, [M.S.,] Wendland, [M.S.,] Yogodzinski, M.S. theses in progress, Smith, Ph.D. thesis in progress).

Location, Access, Topography, and Climate

The Deschutes Basin of north-central Oregon has been a repository for volcanic ash and epiclastic material throughout the Neogene. It is physiographically bounded by the Cascade Range to the west and the Ochoco Mountains to the east. The 160 square mile study area encloses parts of Deschutes and Jefferson counties and is located five miles west and northwest of Redmond, Oregon between latitude $44^{\circ} 16' 30''$ N. and $44^{\circ} 31' 0.2''$ N., and longitude $121^{\circ} 12' 30''$ W. and $121^{\circ} 27' 30''$ W. (Fig. 1).

Access is provided by state highway 126 from the south and U.S. highway 97 from the east. Entrance is gained on the southeast through Lower Bridge Road and on the west by Squaw Flat Road. Roads on the Crooked River Ranch, a recent housing development between the Deschutes and Crooked Rivers on "The Peninsula" (see Fig. 1), permit access to the rims of the Deschutes and Crooked River Canyons. Animal trails can be followed to the bottoms of the canyons. Exposures are excellent in the canyon walls of Deschutes and Crooked Rivers and the tributaries (Fig. 2). Redmond, with a population of 6,250 (Oregon Department of Economic Development, 1977), is the closest town for supplies; it lies at an elevation of 3,010 feet. Most land in the thesis area is privately owned and used for farming and ranching.

Broad, elongate lava-capped mesas trending

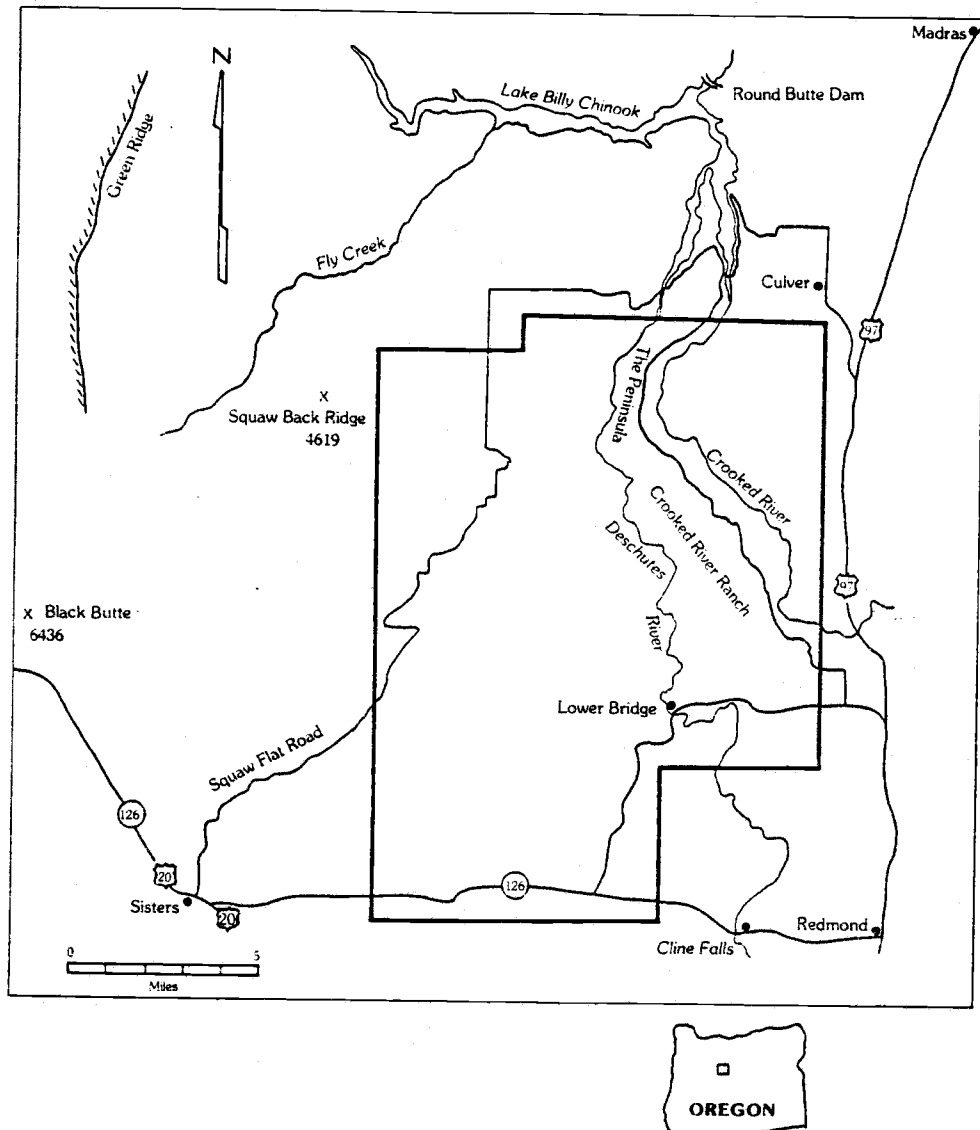


Figure 1. Location map of study area.



Figure 2. Orange MCT exposed in the walls of the Deschutes River Canyon. Looking north from NW1/4, Sec. 5, T.13S., R.12E.

northeast-southwest and gently sloping to the northeast characterize the topography of the study area. The Deschutes and Crooked Rivers have cut steep-walled canyons up to 700 feet deep into the surrounding tablelands. Tributary streams have formed less spectacular, although deep, chasms. More than 500 large volcanoes, cinder cones, or volcanic vents lie within Deschutes County (Peterson et al., 1976), providing some of the best examples of volcanic landforms in the United States.

A rain shadow formed by the High Cascades causes a semi-arid climate in the Deschutes Basin. Redmond has an average annual precipitation of eight inches per year (Oregon Department of Economic Development, 1977), most of which falls during the winter months. Agricultural products produced within the Redmond area consist of potatoes, mint, timber, and various livestock including dairy cattle. Vegetation in the Cascade foothills consists of Douglas fir, Western hemlock, and Ponderosa pine with scattered juniper, sagebrush, and rabbit brush occupying lower, more arid areas to the east.

Previous Work

The Deschutes Formation was first described by I. C. Russel (1905) during his study of the geology and water resources of central Oregon. He correctly assigned the

thick sedimentary deposits below the rim rock basalts to a Tertiary age and proposed that the unit be named the "Deschutes Sands". A diatomite deposit at Lower Bridge (Sec. 16, T.14S., R.12E.) was described by Dr. A. C. Boyle, Jr. (1921) in his report to the Union Pacific Railroad Co. He suggested that it originated from a broad "spring-fed fresh-water lake, probably caused by lava damming a watercourse during the deposition of the Deschutes Formation". Ira A. Williams (1924) noted the varied lithology and renamed the entire sequence "Deschutes Formation" during his study of dam sites for the Columbia Valley Power Co. Hodge (1928, 1940) gave the name "Madras Formation" to correlative rocks in the vicinity of Madras, Oregon, and later (1942) proposed the name "The Dalles Formation" for these units.

The geology and water resources of the middle Deschutes River Basin were studied by Stearns (1930) during an investigation of dam sites on the Crooked River for the Federal Power Commission. Fossil plants studied by Chaney (1938) from the Deschutes Formation on the vanora Grade north-northwest of Madras were dated as early to middle Pliocene. H. Williams (1957) mapped the geology of the 30-minute Bend quadrangle at a scale of 1:125,000 and A. C. Waters (1968) mapped the geology of the adjacent 30-minute Madras quadrangle.

Hewitt (1970) mapped the geology of Fly Creek

quadrangle and the north half of Round Butte Dam quadrangle. Hales (1975) mapped the geology of the adjacent Green Ridge area in the Whitewater River quadrangle. Both areas are located north of latitude $45^{\circ} 30'$ N. and provide information for correlating units north of the present study area. The geology of Deschutes County, Oregon, was described in a recent study by Peterson and others (1976) during an evaluation of low cost industrial mineral resources. Volcanic rocks in the central Cascade Range of Oregon were dated by K-Ar methods by Armstrong, Taylor, Hales, and Parker (1975). Robinson and Stensland (1979) mapped an area between $121^{\circ} 15'$ W. and $121^{\circ} 00'$ W. longitude and $44^{\circ} 15'$ N. and $44^{\circ} 30'$ N. latitude at a scale of 1:48,000, and used the term "Madras Formation". A regional geologic summary of the central Western and High Cascades, and Deschutes Basin subprovinces was presented by Taylor (1980). Stensland (1970) made an excellent geologic map of an area between latitude $44^{\circ} 15'$ N. and $44^{\circ} 30'$ N., and longitude $121^{\circ} 7' 3''$ W. and $121^{\circ} 3'$ W. (Fig. 3). He described most Deschutes Formation ash-flow tuffs and lavas in the field area and his map serves as the basis for this study.

Farooqui and others (1981) reviewed the nomenclature for Neogene formations overlying the Columbia River Basalt Group in north-central Oregon. They formally established the name Deschutes Formation for the late

Miocene to middle Pliocene age "interbedded volcanic, volcanoclastic, pyroclastic, and epiclastic rocks" which occur in the Madras Basin. The boundaries of the basin are defined by the Mutton Mountains to the north, the Cascade Range to the west, the High Lava Plains to the south, and the Blue and Ochoco Mountains to the east.

Methods

Geology was mapped at a scale of 1:24,000 directly onto 7.5-minute U.S. Geological Survey topographic maps that include Cline Falls, Henkle Butte, Squaw Back Ridge, Steelhead Falls, Opal City, and Round Butte Dam quadrangles. Outcrops of McKenzie Canyon tuff and Lower Bridge tuff were located from Stensland's map (1970) and verified in the field. Contacts outside his thesis area were mapped by the author during the summer of 1981. Most exposures of the tuff are believed to have been identified and mapped, and 32 vertical sections were measured for thickness and unique characteristics. Widths of outcrop on the geologic map (Plate 1) are exaggerated at some localities in order to represent small outcrops.

Five sample locations for chemical analyses of the McKenzie Canyon tuff were chosen at the farthest azimuthal extremes and in the center of the flow (Fig. 3) to pick up lateral variations in chemistry. Four sample

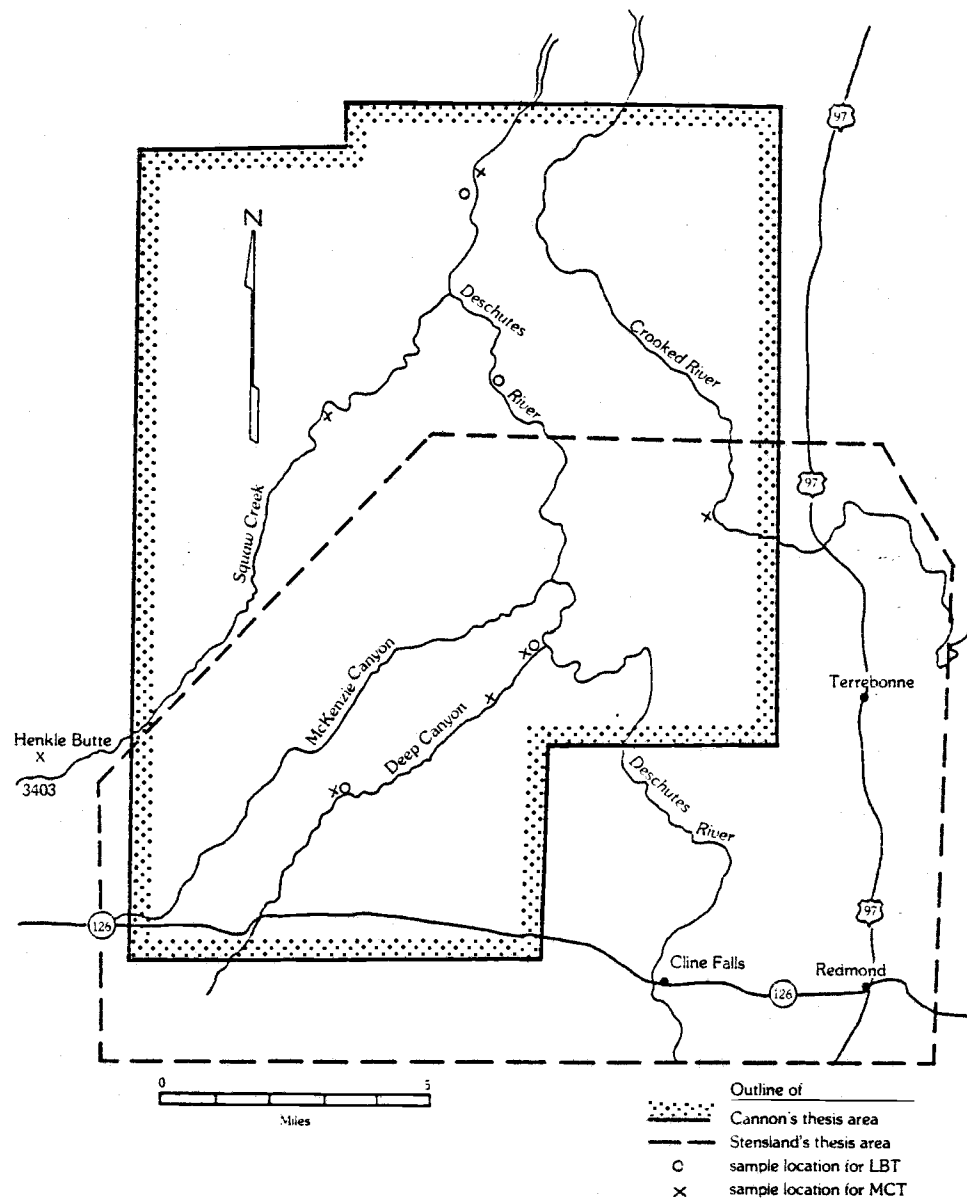


Figure 3. Location of Stensland's (1970) thesis area and geochemical sample locations for LBT and MCT.

locations distributed between the southern and northern exposures were selected for chemical analyses of the Lower Bridge tuff. In order to reveal vertical variation in chemistry, the base, middle, and top of individual flows were sampled at each location. Each flow within a single cooling unit was sampled separately in this matter. Distinct pumice varieties, including black, white, and banded (black and white) of McKenzie Canyon tuff, or light grey and dark grey of Lower Bridge tuff, were sampled at the base, middle, and top of the flow.

Paleomagnetic polarity of oriented samples of ash-flow tuffs was checked using a fluxgate magnetometer.

Sixty-three samples of McKenzie Canyon tuff and Lower Bridge tuff from the nine sample locations (Fig. 3) and two samples of unit 0 were analyzed for major elements using X-ray fluorescence (XRF) and atomic absorption spectrophotometry (AAS). Samples were pulverized in a Pitchford ball mill and dehydrated by heating one hour at 450° C in ceramic crucibles. Powders were mixed with lithium metaborate (flux) in a ratio of 2:10 rock to flux, fused at 1050° C in graphite crucibles and cooled to form glass buttons. The buttons were ground flat and analyzed by XRF for K_2O , SiO_2 , Al_2O_3 , FeO , TiO_2 , and CaO . The buttons were repulverized and 0.15 grams of glass powder mixed with 200 milliliters of 0.5 N nitric acid. This solution was analyzed using AAS

for MgO and Na_2O . For this study the divisions between andesite and dacite and between dacite and rhyolite were placed at 63% and 69% silica respectively (Ewart, 1979).

Optical methods were used to determine the crystal habit and zoning of plagioclase and the compositions of orthopyroxene and plagioclase. Plagioclase grain mounts were analyzed from three samples of Lower Bridge tuff pumice (24 crystals), three samples of McKenzie Canyon tuff white pumice (20 crystals), and four samples of McKenzie Canyon tuff black pumice (24 crystals). Large grains with subhedral to euhedral morphology were picked using a binocular microscope and mounted on a glass slide on the [001] cleavage face. The upper crystal faces were ground flat, the glue remelted, grains turned over and pressed onto the slide surface, and the grains ground to about 30 microns thick. Zoning patterns, abundance of inclusions, resorption, and crystal habit were observed.

A suite of 14 samples was used for the remaining mineralogical analyses. Nine samples of McKenzie Canyon tuff were taken from the Squaw Creek section (five of white pumice and four of black pumice) and five samples of Lower Bridge tuff were taken from near the intersection of Deschutes River and Deep Canyon (Plate 1). Both the Lower Bridge tuff and McKenzie Canyon tuff samples were taken from a vertical section to reveal

vertical variation in mineralogy. Clean plagioclase (30-40 grains) was picked from each sample, ground to a fine powder, magnetically cleaned of Fe-Ti oxides, and fused to a bead. Anorthite (An) content of a sliver of the fused feldspar bead was determined (Schairer and others, 1956) using Cargile index oils and sodium light to obtain the refractive index. Advantages of this method include

the lack of any uncertainty as to the optical orientation of the grain. . . and its ability to give the average plagioclase composition for material with strong zoning or with exsolution intergrowths (Deer, Howie, and Zussman, 1967, p. 132).

Refractive indices of 3 to 4 slivers per sample were determined to optimize accuracy of the values.

Inclusion-free orthopyroxene grains were fractured, a sliver mounted on a spindle stage and the gamma refractive index checked. Leake (1968b) was used to compare the refractive index with the chemical composition of the orthopyroxene series. Two to four grains were analyzed from each sample to assure reproducibility. There was some variability which may be attributed to slight zoning of the orthopyroxene.

Microprobe work to obtain the composition of the grains was performed on olivine, clinopyroxene, orthopyroxene, and amphibole at the University of Idaho, Moscow, by Charles Knowles.

GEOLOGIC SETTING AND STRUCTURE

Geologic Setting

The Deschutes Basin in central Oregon extends from the city of Bend north to Warm Springs River, west to Green Ridge, and east to include the cities of Madras and Prineville (Farooqui et al., 1981). Pliocene and Pleistocene-Holocene composite and shield volcanoes of the High Cascade Range border the basin on the west; middle Miocene Columbia River Basalt, Oligocene and early Miocene John Day Formation, and late Eocene-early Oligocene Clarno Formation border it on the east. The Deschutes Basin is covered by mostly late Miocene to middle Pliocene (7.5-4.5 m.y. old, Smith and Snee, 1984) Deschutes Formation. Taylor (1980, 1981) noted that the younger central High Cascade Range is predominantly basalt and basaltic-andesite shield volcanoes, not a belt of andesite volcanoes typical of Pacific margin subduction zones.

The Clarno Formation in central Oregon overlies pre-Tertiary deposits with angular unconformity. The oldest Clarno rocks in the Mitchell area are reported to be 46 m.y. old (Enlows and Parker, 1972). Basalt, andesite, and rhyolite lava flows, mudflows, tuffs, and

tuffaceous sediments make up the units of this formation (Stensland, 1970). Volcanic sources for the Clarno rocks were scattered over central and eastern Oregon (Taylor, 1977). Eroded andesite covers about three square miles in the central part of the study area on the west side of the Deschutes River (Plate 1). Stensland (1970) correlated this mass with rocks of the Clarno Formation; however, the true age and origin of the andesite remain unknown. The nature of weathering of the Clarno Formation, the abundance of mudflows, and characteristic plant fossils found within it suggest a humid climate existed in central Oregon before elevation of the Cascade barrier. Folding probably occurred contemporaneously with Clarno deposition (Taylor, 1977). Clarno Formation volcanism probably ended about 36 m.y. ago (Robinson and Brem, 1981).

Volcanism continued from 36 to 18-20 m.y. ago (Robinson and Brem, 1981) producing the John Day Formation. The John Day Formation reaches a thickness of 4,000 feet, and the western facies extends into the northeastern Deschutes Basin, northeast of the study area. Dacite and andesite tuffs, air-fall tuffs, and tuffaceous claystone become thicker and coarser from east to west suggesting a source in the proximity of the present day Cascade Range. Domes located on the eastern margin of the Deschutes Basin (e.g., Juniper and Powell

Buttes) are possibly the sources for rhyolite ash-flow tuffs and lava flows so prevalent in the western facies. Northeast of these volcanic centers, alkali-olivine basalt and trachyandesite originated from scattered vents in the John Day basin. A humid climate still existed in central Oregon allowing three-toed horses, giraffe-camels, and giant pigs to roam the region. Folding was contemporaneous with John Day deposition (Taylor, 1977) and post-depositional folding and erosion caused an unconformity at the top of the John Day Formation (Robinson and Brem, 1981).

Large volumes of tholeiitic flood basalt of the Columbia River Basalt Group (Waters, 1961) were erupted from 17 to 6 m.y. ago (McKee et al. 1977); the largest volume erupted from 17 to 14 m.y. ago. Flows originated from dike swarms in Oregon, Washington, and Idaho. McBirney (1974) contends that volcanic activity throughout the circum-Pacific system was coincident with eruption of this massive volume of lava.

The Simtustus formation, found in the Deschutes Basin, contains mid-Miocene fossils and overlies the Columbia River Basalt Group and is interbedded with the upper most members of the Columbia River Basalt Group (Smith and Snee, 1984).

The Deschutes Formation lies unconformably on the Clarno Formation, John Day Formation, Columbia River

Basalt Group, and Simtustus formation. The thickness of the formation ranges from about 100 to 3,000 feet (Stensland, 1970; Hodge, 1940) and consists of andesitic to rhyolitic ash-flow and ash-fall tuffs, interbedded basalt flows, and epiclastic sediments of late Miocene to early Pliocene age (7.6 to 4.5 m.y. ago). The Deschutes Formation thickens toward the Cascades and easterly transport direction indicators suggest that the source volcanoes (the "Plio-Cascades") for this material were located where the modern High Cascades are today (Taylor, 1980).

As the "Plio-Cascades" built up, a semi-arid climate formed east of the Cascades which changed forests to grasslands that supported horses and camels. McBirney (1982) alternatively states that "no new chain of large andesitic volcanoes" formed after 14-13 m.y. ago (end of Columbian event in mid-Miocene) until the rise of the modern High Cascades and does not support the theory of a "Plio-Cascades".

Pliocene volcanic activity continued while rivers brought in sediments from the south, southeast, and west. Hot ash-flow tuffs spread across the Deschutes Basin originating from the "Plio-Cascades", occasionally preceded by beds of accretionary lapilli. Streams, locally blocked by lava flows, formed lakes and ponds which bloomed with diatoms and resulted in the production

of diatomite. Plateau-forming basalts (rim lavas) covered the majority of the Deschutes Formation, ensuring its preservation. A north-south fault system formed 4.5 m.y. ago, dropped down the "Plio-Cascades," and possibly initiated Pleistocene High Cascade volcanism. The earliest flows of open-textured basalt lavas were contained by the graben structure, forming a broad platform of overlapping shield volcanoes. Subsequent basaltic andesite composite volcanoes (e.g., Three Sisters, Mt. Jefferson) were built upon the platform. The total thickness of the volcanic pile is estimated to be greater than 4,000 feet (Taylor, 1980). The Deschutes Basin contains evidence of some Pleistocene eruptions (cones and lavas) and intracanyon lavas from Newberry Caldera. Volcanic activity has continued through Holocene time in the Three Sisters region.

Structure

The nearly flat-lying Deschutes Formation dips about 1-5° to the east on Green Ridge (Hales, 1975), 1-2° to the north-northeast in the central and southern parts of the depositional basin (Stensland, 1970), and is gently folded in the northern part of the basin (Gary Smith, pers. comm., 1983). Individual units locally have larger inclinations that reflect preexisting topography or represent the edge of a flow channel. The pre-Deschutes

Formation rocks have been folded and faulted such that the Clarno and John Day units make up a northeast-trending anticline east of the study area.

As mentioned before, a resistant outcrop directly underlying the Deschutes Formation northwest of Big Falls (SW1/4, SW1/4, Sec. 4 and SE1/4, SE1/4, Sec. 5, T.14S. R.12E.) is probably Clarno. McKenzie Canyon tuff flowed up the west side and back down the south side of the obstruction, forming multiple pumice flows each about six feet thick capped by the red, welded upper flow (Fig. 4); this produced a total McKenzie Canyon tuff thickness greater than 35 feet. McKenzie Canyon tuff on "Clarno Hill" dips 8° to the southwest away from the hill (McKenzie Canyon tuff normally dips 1-2° to the NNE). On the opposite side of this inlier (SW1/4, Sec. 33, T.13S., R.12E.) a thin eight foot layer of McKenzie Canyon tuff includes an unusually large percentage (5%) and size (up to 10 inches) of lithic clasts and dips 5° northeast. An energetic flow may have swept up "Clarno Hill" losing most of its volume and momentum on the ascent, thus allowing only a small amount of material to crest the hill and to be deposited on the far side. Stensland (1970) notes 45-60° dips of normally horizontal Deschutes sediment along the flank of the inlier. The "Clarno Hill" probably represented an obstruction to deposition

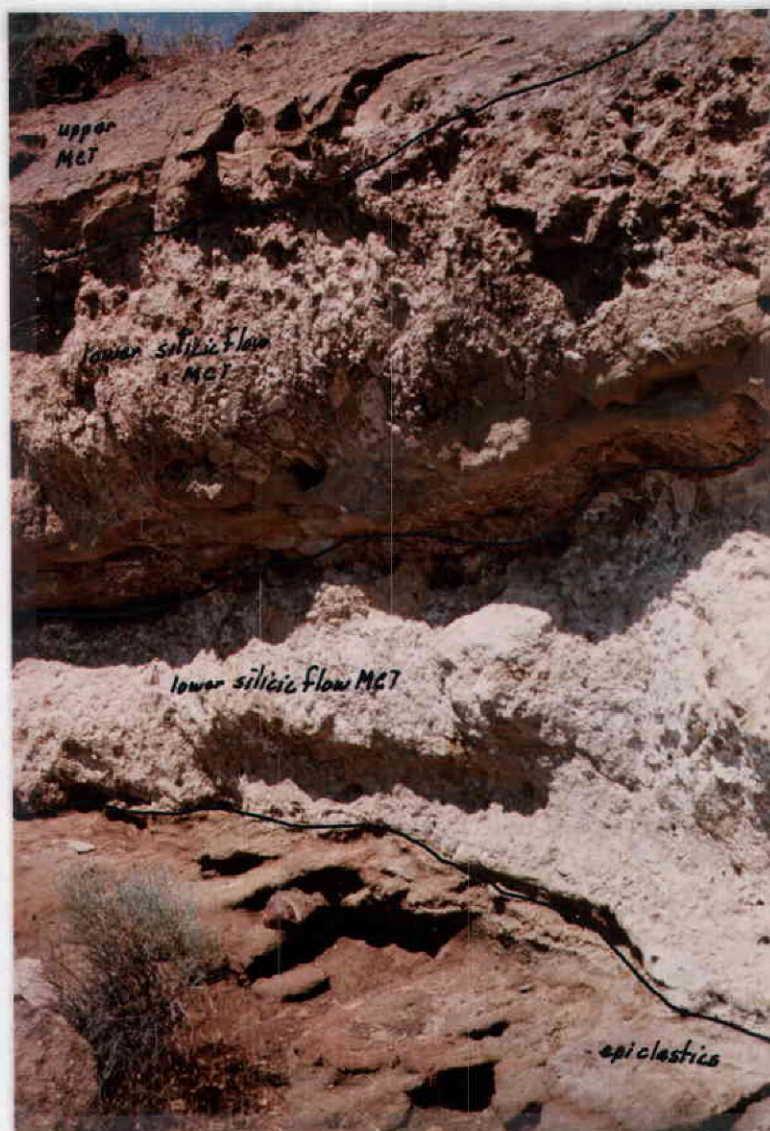


Figure 4. Two lower silicic flows of MCT overlain by the upper red unit on the south side of "Clarno Hill", (SE1/4, Sec. 5, T.14S., R.12E.). The middle flow of MCT is six feet thick.

as indicated by the change in thickness and dip of the McKenzie Canyon tuff.

McKenzie Canyon tuff and Lower Bridge tuff have many local discontinuities. Paleochannels filled with lava or sediment cut the McKenzie Canyon tuff at several locations (Fig. 5) while ash-flow tuffs, lava, and, most commonly, epiclastic sediments concordantly overlie the unit. The McKenzie Canyon tuff lies directly above Lower Bridge tuff in the southern part of the study area and is separated from Lower Bridge tuff by up to 40 feet of epiclastics in the northern part (Plate 2). The configuration of basal contacts of both units reflect topography at the time of deposition, whether a flat plain, a channel, or an existing obstruction (i.e., "Clarno Hill"). Thicknesses also reflect primary topography; for example, lens-shaped channels exposed in canyon walls (Fig. 6) show the thin channel edges.

Green Ridge lies ten miles northwest of the study area (Fig. 1) and is made up of Deschutes Formation lavas, ash flows, and sediments. Transport direction indicators in these units are to the east. Transport directions indicated by McKenzie Canyon tuff and Lower Bridge tuff in this study (Plate 1) are to the northeast. Both are thought to be derived from different parts of the "Plio-Cascade" range.

At the Green Ridge escarpment the Deschutes



Figure 5. Orange MCT cut by a channel of sediments, MCT is 19 feet thick and the LBT ash-flow and air-fall deposits are 10.5 feet thick. (East side of Deschutes River Canyon, looking north, SW1/4, Sec. 21, T.13S., R.12E.)



Figure 6. In the foreground MCT thickens and fills a channel, the relationship of Unit 0, LBT, and MCT to each other is also shown.
(Looking north at east side of Crooked River Canyon, SE1/4, Sec. 10, T.13S., R.12E.)

Formation lies 2,000 feet above the Pleistocene High Cascade platform. From 4.5 to 2.5 m.y. ago a 20 mile long, north-south fault system downdropped the eastern edge of the "Plio-Cascades" more than 3,000 feet (Taylor, 1980). The Tumalo Fault, a closely related feature with smaller displacement, extends southeast from Black Butte to Bend (Taylor 1980, 1981). Armstrong et al. (1975) reported K-Ar ages which show that west of the Green Ridge fault the oldest rocks are 2.8 m.y. old and east of the fault the rocks are much older. Because the Deschutes Formation on Green Ridge has a slope of only 1-5° east (Hales, 1975), uplift of the ridge is unlikely, supporting the theory of graben subsidence to the west. A 30 to 40 km wide graben formed beginning about 4.5 m.y. ago with magma using intragraben faults as pathways to the surface (Taylor, 1980). All evidence suggests that the Pliocene source volcanoes subsided into the graben and are now covered by recent High Cascades volcanics (Taylor, 1980).

ASH-FLOW TUFF DESCRIPTIONS

General Characteristics of Ash-flow Tuffs

Smith (1960a,b) and Ross and Smith (1961) made the first comprehensive studies of ash-flow tuffs in which they described mode of eruption, mechanism of deposition, development of zonation, and temperatures appropriate to welding. The volume of literature has expanded greatly since then (e.g., Moore and Peck, 1962; Peterson, 1970; Walker, 1971; Sheridan, 1971), especially by the USGS Special Paper 180 entitled "Ash-Flow Tuffs" (Chapin and Elston, eds., 1979), a comprehensive treatment of the subject.

Terminology for explosive volcanic rocks is extensive (e.g., Fisher, 1961, 1966); the present study follows the classification of Schmid (1981). Pyroclastic is a term used to describe material explosively ejected from a volcano. Three types of pyroclastic deposits are recognized: 1) fall, 2) surge, and 3) flow (Sparks and Walker, 1973; Wohletz and Sheridan, 1979). Air-fall deposits result from volcanic ejecta being carried by wind currents and eventually settling to form graded beds. A pyroclastic surge often precedes an ash flow as a base surge or directed blast (Sparks, 1976) forming

thin, fine-grained bedded deposits. Ash-flow tuffs, the most voluminous type of pyroclastic deposit, are confined to topographic lows. They fill canyons where confined, and form continuous sheets where unconfined. They have nearly horizontal upper surfaces and undulating basal contacts controlled by the topography (Smith, 1960a). The characteristically massive and unsorted features of ash-flow tuffs are normally attributed to a turbulent flow mechanism.

Idealized proximal and distal columnar sections for large pyroclastic units are described by Sheridan (1979) (Fig. 7). The proximal facies is characterized by an air-fall unit overlain by a cross-bedded, pyroclastic-surge deposit. This, in turn, is overlain by the poorly sorted pyroclastic-flow unit which includes reversely graded pumice lumps and normally grade lithic clasts. A thin basal layer of fine-grained pumice and ash (2 to 10 inches, not shown in Fig. 7) is commonly present in a pyroclastic-flow unit. The distal facies lacks the surge deposit and the pyroclastic flow becomes more homogenized, loses many of the large lithic fragments, and commonly has a concentration of coarse pumice lumps at the flow top.

Ash-flow deposits are generally composed of greater than 50% ash, in addition to fine pumice, scoria, lithic fragments, and crystals. The overall percentage of fine

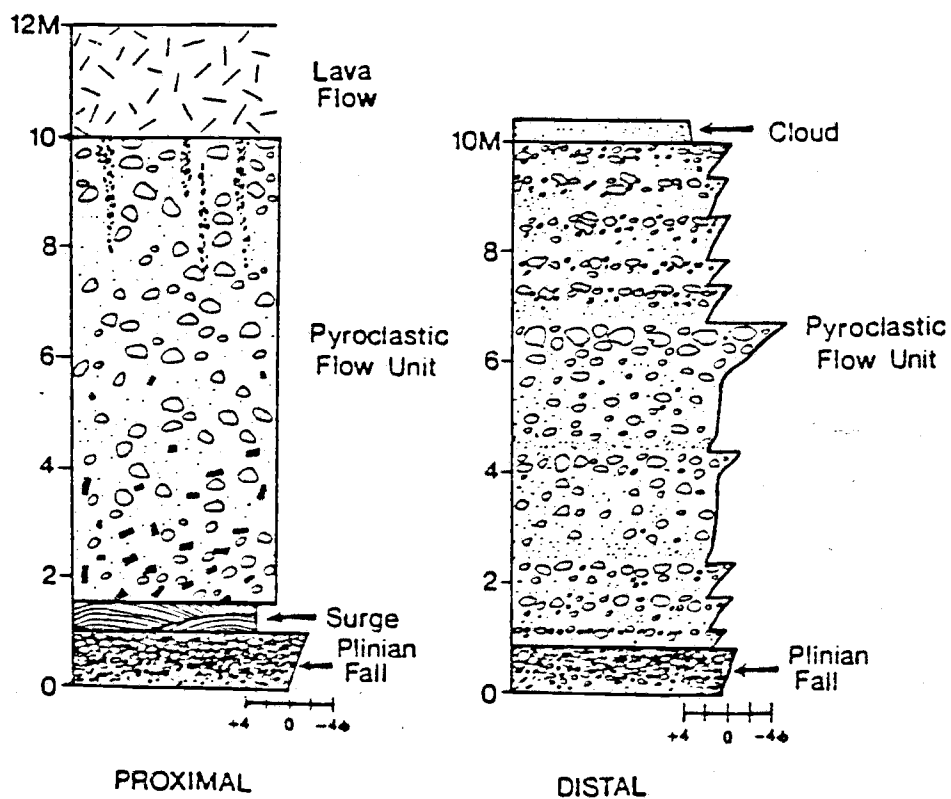


Figure 7. Proximal and distal facies of intermediate to large pyroclastic flow units.
(After Sheridan, 1979, p. 134)

material usually increases and heavy foreign lithic fragments become increasingly scarce away from the source.

Deschutes Formation Ash-flow Tuffs

STRATIGRAPHY AND DISTRIBUTION

The sequence of units covered in this study begins with the Lower Bridge tuff which consists of a lower air-fall unit and two overlying ash-flow tuffs. The Lower Bridge tuff in turn is overlain either by epiclastic deposits which locally include a thin interbedded air-fall unit or by the multiple flow units of McKenzie Canyon tuff. The McKenzie Canyon tuff overlies Lower Bridge tuff or epiclastic units except in Squaw Creek Canyon where it overlies a basalt lava and a white ash-flow unit.

A thick orange unit in the Crooked River Canyon wall, with the same reversed polarity and similar chemical composition as McKenzie Canyon tuff and Lower Bridge tuff, is called Unit 0 in this study; it was originally grouped with Lower Bridge tuff (Stensland, 1970). Detailed mapping proved that Unit 0 underlies the Lower Bridge tuff and McKenzie Bridge tuff. Figure 6 shows a thick sequence of Unit 0 directly underlying a channel of McKenzie Canyon tuff; Lower Bridge tuff has

either been removed or was never deposited. A lava flow separates Lower Bridge tuff from Unit 0 in at least two places in the Crooked River Canyon (NE1/4, Sec. 10, T.13S., R.12E.). Elsewhere epiclastic deposits lie between Unit 0 and Lower Bridge tuff or between Unit 0 and McKenzie Canyon tuff when Lower Bridge tuff is absent. Unit 0 is unique because the massive, dark purple or orange deposit (Fig. 6) forms characteristic hoodoos. Unit 0 ranges in thickness from 27 to 126 feet (Stensland, 1970) and contains pink and orange hard glassy pumice lumps. Lower Bridge tuff, in contrast, is 4 to 51 feet thick with gray pumice lumps.

The air-fall deposit that crops out between McKenzie Canyon tuff and Lower Bridge tuff is present in two and possibly three locations. At Lower Bridge (NE1/4, Sec. 16, T.14S., R.12E.) it is interbedded with epiclastic units that separate Lower Bridge tuff and McKenzie Canyon tuff. In the Crooked River Valley (Sec. 4, T.13S., R.12E.) a one foot thick air-fall unit occurs near the base of 25 feet of epiclastic deposits that separate McKenzie Canyon tuff and Lower Bridge tuff. In Squaw Creek (SW1/4, Sec. 23, T.13S., R.11E.) the airfall is in direct contact with the base of McKenzie Canyon tuff; Lower Bridge tuff is not present. The air-fall tuff units indicate that at least one explosive event occurred

between the deposition of Lower Bridge tuff and McKenzie Canyon tuff.

Plates 1 and 2 display the distribution of Lower Bridge tuff and McKenzie Canyon tuff. McKenzie Canyon tuff and Lower Bridge tuff form a nearly continuous outcrop from the southern part of Deep Canyon to the intersection of McKenzie Canyon and the Deschutes River Canyon. North of "Clarno Hill", outcrops of both units become isolated and show evidence of channel fill suggesting that they followed stream drainages. West of "Clarno Hill" the McKenzie Canyon tuff is continuously exposed over 4.5 square miles and probably represents a sheet flow where McKenzie Canyon tuff had sufficient volume to cover a wide area of low relief.

LOWER BRIDGE TUFF

The Lower Bridge tuff is best exposed at the intersection of the Deschutes River and Deep Canyon and northward down the Deschutes River to McKenzie Canyon. It is not as extensive as McKenzie Canyon tuff, because it is not present in southwest Squaw Creek. Nor is it as well exposed, because it is a less resistant unit. The tuff forms rounded, gullied low-angle slopes. Weathered surfaces are brown and fresh surfaces range from white to purple.

The Lower Bridge tuff consists of a lower accretionary lapilli-fall deposit 1.5 to 5.5 feet thick and two overlying ash-flow tuffs (Fig. 8). The ash flows were deposited directly onto the air-fall member. No surface weathering of the underlying air-fall member is evident which suggests nearly continuous deposition of the ash flow following the air fall. Geochemical analyses were not performed on the accretionary lapilli deposit because of the lack of large fresh pumice lumps. However, the air-fall deposit is probably related to the overlying ash-flow tuffs and probably was erupted immediately prior to the flows.

The Lower Bridge tuff accretionary lapilli air-fall deposit is internally stratified and is moderately to well sorted (Fig. 9). The thickness of the bed varies from 3 to 5 feet at the intersection of Deschutes and Deep Canyons to 1 to 2 feet in the northern Deschutes and Crooked River Canyons.

Accretionary lapilli are "pea-size structures composed entirely of clastic volcanic material, primarily glass or its alteration product" (Moore and Peck, 1962). Most lapilli are less than 0.5 inch in diameter and flattened in the plane of bedding. One or two concentric layers surround a spherical core of volcanic ash (Fig. 9); the grain size decreases from core to rim. Clouds rich in ash and water form during eruption.

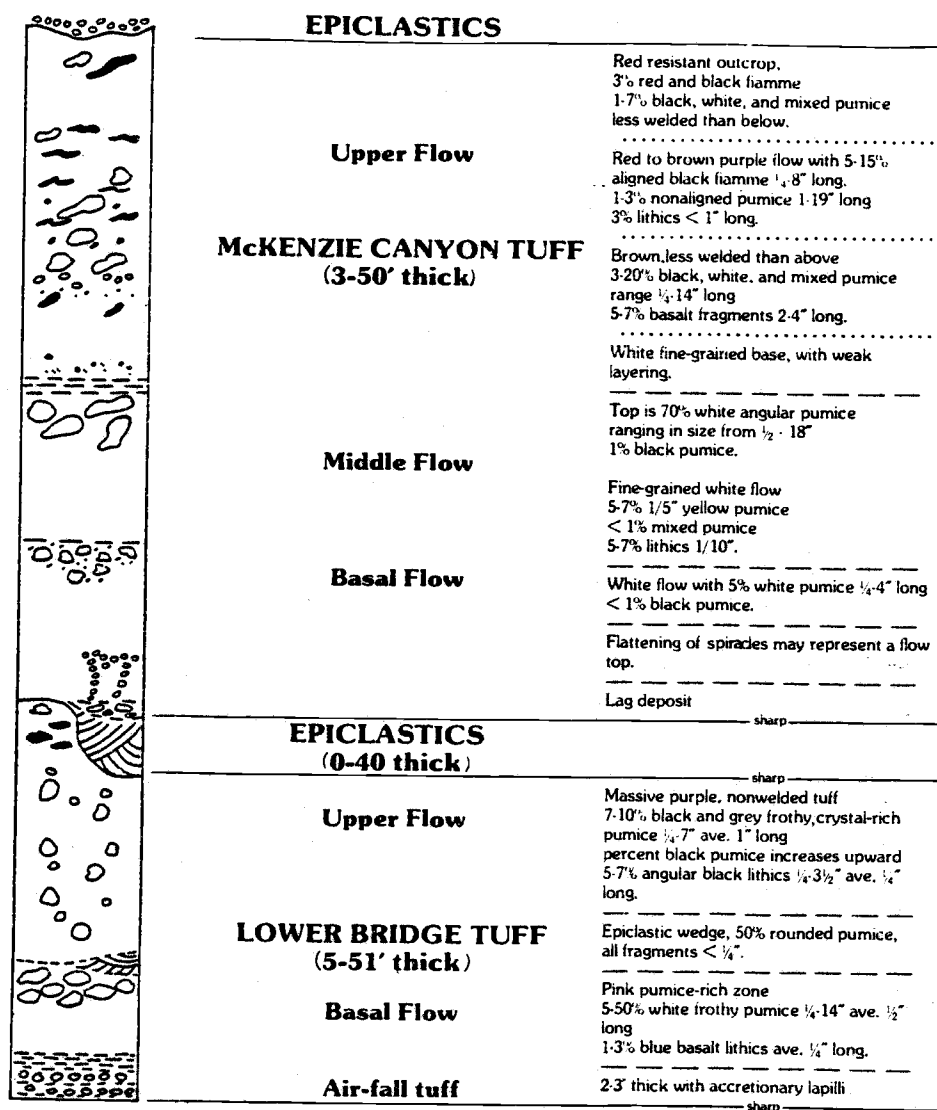


Figure 8. Idealized columnar section of LBT and MCT.



Figure 9. Accretionary lapilli bed at the base of LBT.
Pencil points to a fractured lapillus
fragment with internal concentric layering.

Condensation causes ash to adhere to cores of the lapilli. As the lapilli fall through the cloud, layers of ash accrete to their surfaces. Moore and Peck (1962) believe that accretionary lapilli suggest a source within 100 miles and probably within 10 miles. The Lower Bridge tuff accretionary lapilli bed extends for at least 8.5 miles in a north-south direction and is probably more than 22 miles from its source (Fig. 17).

Lower Bridge tuff ash-flow deposits are characterized by the light color, frothy pumice lumps, and lack of induration. Pumices and lithic clasts lie in a matrix (60% to 70%) composed of shards, clay, brown dust, and crystals. The lower flow is pink with white pumice lumps concentrated at the top (Fig. 8). Where a parting between the flows exists it may either be a thin 1 to 3 inch epiclastic layer or a change in clast size from 3 to 5 inch pumice lumps at the top of the lower unit to a fine basal layer of the upper member. The nonwelded gray to purple upper tuff contains 5% to 10% gray pumice throughout with 1% black pumice concentrated in the top of the unit. The black pumices on the average are larger (3 to 5 inches long) than the gray pumice lumps (0.5 to 1 inches long). Both colors of pumice lapilli in the upper flow are characterized by clusters of clear plagioclase crystals.

McKENZIE CANYON TUFF

The McKenzie Canyon tuff is the most extensive tuff unit studied and is distinguished by the red orange color, ledge-forming outcrops, and abundant banded (black and white) pumice lumps. The southernmost outcrop is situated just above the stream bed in Deep Canyon and extends 13.5 miles north where it crops out 200 feet above the Deschutes River in the canyon walls. This outcrop pattern may indicate that the Crooked and Deschutes Rivers have higher stream gradients today than in the Pliocene. The best exposures occur at the intersection of Deep Canyon and Lower Bridge Road and in the Deschutes Canyon between Lower Bridge and McKenzie Canyon. The maximum tuff thickness is 55 feet in Squaw Creek Canyon and generally decreases to the northeast (Plates 1 and 2). This may indicate, as does the northeastward decrease in mesa elevations, that the volcanic source was to the south-west. The unit may extend farther south and west but rivers and streams do not cut deeply enough to expose it.

General Description

The lower McKenzie Canyon tuff is made up of 1 to 3 white, poorly indurated flows that average 8 feet thick and are overlain by a red resistant flow which ranges from 8 to 50 feet thick. This upper unit is the most

distinctive and extensive member of the sequence. It has a thin white basal zone (Fig. 10) with very few mixed or black pumices that grades upward into a deep orange tuff exhibiting crude columnar jointing and black, white, and banded pumice blocks. All of the McKenzie Canyon tuff flows have a crystal-poor matrix.

Some of the lower silicic units of McKenzie Canyon tuff (Figs. 4 & 11) may be subflows (Smith, 1960a, p. 811) that originated within one original silicic flow. Subflows may develop from the overlapping of lobes at the front of a flow, by overriding of volume surges, or by the overlapping of flows on the far side of topographic barriers.

Individual units are separated by a change in clast size, a minor erosional unconformity, a change in color, or any combination of these partings. At many locations pumice fragments are reversely graded and form a concentrated two to ten foot thick layer at the top of a flow (Fig. 12) which is overlain by a fine basal layer of the next member. The layer of concentrated (80%) pumice lumps commonly is weathered sufficiently to form a distinct break between units (Fig. 11 & 12). Figures 11 and 12 also show partings at the level of change from the lower light-colored flows to the upper orange member.

Lower McKenzie Canyon tuff silicic flows are best exposed at the intersection of Deep Canyon and Lower



Figure 10. Basal zone of upper flow of MCT; note fine-grained light-colored base of MCT. Located at the intersection of Deep Canyon and Deschutes River.

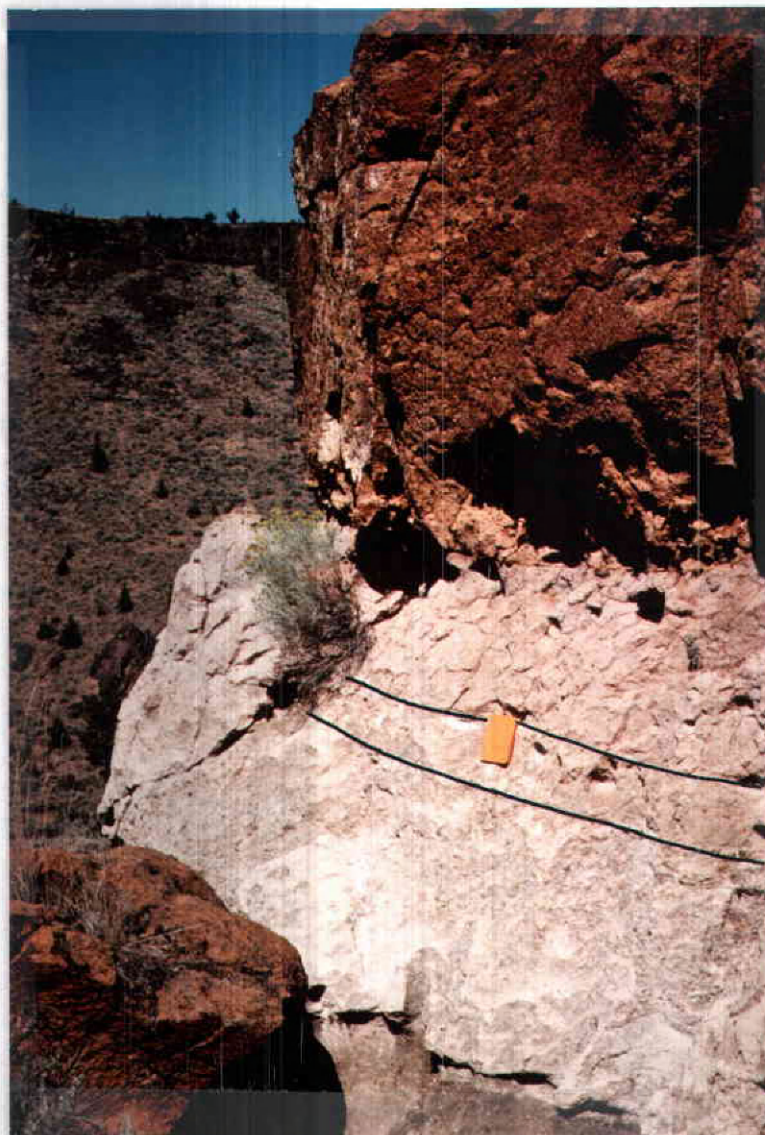


Figure 11. Three lower silicic flows of MCT overlain by an upper red resistant flow. This distal outcrop of MCT shows less welding than a proximal outcrop (Fig. 26). Denser welding near the top indicates that this is a compound cooling unit that had an increase in emplacement temperature. (Squaw Creek Butte, NW1/4, SE1/4, Sec. 23, T.13S., R.11E.)



Figure 12. Columnar jointed MCT; note ten foot thick pumice-rich layer in foreground at base of red flow. Photo taken looking north at west side of Deschutes River where it intersects McKenzie Canyon.

Bridge Road and at the sample site in Squaw Creek (Fig. 11). The units are either rich (50% to 80%) in white pumice lumps or have fine-grained matrix containing small lithic and white pumice clasts (Fig. 11). Black and banded pumices represent less than 1% of the pumice fragments in these lower members. All of the flows have a thin 1 to 2 inch fine-grained ashy basal layer that grades up into coarser material.

Basal features observed in the lower units include spiracles, flame structures, and the inclusion of blocks of Lower Bridge tuff. Spiracles are formed by explosions when hot ash clouds or lava flows come in contact with water (Williams, and McBirney, 1979). The gravel-laden spiracles (fumarolic vesicles) at the base of the McKenzie Canyon tuff suggest that the original pyroclastic material flowed over a wet, gravel-covered surface, probably a stream bed. Pebble-size debris from underlying sediments were carried upward into the spiracles by explosive action. Spiracles may be bent in the direction of flow movement. Those present in the McKenzie Canyon tuff are vertical (Fig. 13) and cannot provide information on the flow direction; however, the zone where they flatten out may represent a flow top (Fig. 8 & 13). The flame structure probably was formed by movement of the ash flow over plastic sediments that were pulled into the flow. Blocks of Lower Bridge tuff



Figure 13. Gravel-laden spiracles found in the lower silicic flows of MCT. (SE1/4, Sec. 17, T.14S., R.12E., west side of canyon.)

in the base of McKenzie Canyon tuff indicate that McKenzie Canyon tuff exerted an erosive force at some locations or that loose blocks of Lower Bridge tuff were lying on the surface and were picked up by the flow.

The red upper member of McKenzie Canyon tuff usually grades from a white nonindurated base up into a more resistant darker layer (Fig. 10). Above the white basal zone the amount of black and mixed pumices equals that of white pumice lumps. This zone grades upward into a red-brown indurated zone with columnar jointing and black glassy collapsed pumice (Fig. 14). The capping upper red zone is more friable and contains less collapsed pumices than the zone immediately below it (Fig. 8). The upper unit is usually exposed (Fig. 12) or locally is covered by epiclastic deposits (Figs. 2 and 5). However, farther upstream in Squaw Creek a white ash-flow deposit and a lava flow respectively overlies McKenzie Canyon tuff. The true top of McKenzie Canyon tuff may have been eroded; if so, the true thickness is unknown. The McKenzie Canyon tuff has little internal stratification except for the reverse grading and concentration of pumice lumps (Fig. 12), lineation of collapsed pumices, and layering in the fine basal zone of each unit. The white basal zone in most members is 2 to 10 inches thick and is comprised of alternating layers of white pumice fragments (0.25 inch) and white ash.



Figure 14. Horizontal lineation of black collapsed pumice in upper MCT flow. (SE1/4, Sec. 17, T.14S., R.12E., west side of Deep Canyon.)

The most distinguishing feature of McKenzie Canyon tuff is the orange matrix of the upper flow (Figs. 2, 5, and 12). It contrasts sharply with a basal white to tan zone where the light basal zone is present. The color prevails laterally throughout the unit and is much too uniform to be explained by fumaroles (Williams, 1960). Because epiclastic deposits normally overlie the unit (Figs. 2 and 5) the color cannot be attributed to heating from an overlying ash-flow deposit or lava flow. The color is the result of a hematitic coating, probably caused by oxidation of iron as it reacted with the atmosphere and surface waters during cooling and degassing (Koch, 1970); i.e., vapor-phase oxidation.

The types of primary fragments in McKenzie Canyon tuff provide the second major criterion for identifying the McKenzie Canyon tuff. They include white vesicular rhyolite pumice, black scoriaceous andesite pumice, banded black and white pumice (Fig. 15), and black glassy elongate collapsed pumice. The white pumice in the lower flows is crystal-poor, friable and has the same general composition and characteristics as the white pumice in the upper unit. White pumice in the upper part of the upper member normally has an orange oxidized rim around a fresh core, but is commonly pervasively oxidized. The black pumice is usually scoriaceous and generally also has a red oxidized rim. Banded pumice occurs in at least



Figure 15. Banded black and white pumice in upper flow MCT. (SW1/4, Sec.13, T.13S., R.12E., NE side of Crooked River Canyon.)

minor amounts in the four McKenzie Canyon tuff flows in Squaw Creek (Fig. 11) which may indicate that all members are derived from the same source. Banded pumice is usually the largest pumice in the upper unit. It has a linear (Fig. 15) fabric but can also have a globular texture which may just be a cross-section of the linear fabric. Some banded pumice is a combination of black expanded cindery material and white nonfrothy pumice.

Collapsed pumices (Fig. 14) are not found in the nonwelded basal zone, but are concentrated in the dense compacted upper middle zone of the upper flow, and decrease upward into the red friable zone. Therefore, the collapsed pumices in this study are believed to be secondary features resulting from heat and compaction after deposition. They are probably not fiamme which are magmatic clots that have been degassed prior to eruption and deposited in various orientations (Taylor, 1984, pers. comm.). They also decrease in number distally where units are not as thick (Fig. 11) and appear not to have been as hot. They are well exposed on weathered surfaces and define a lineation (Fig. 14). Collapsed pumices retain the original black color, being too dense to be affected by oxidation. Some partly collapsed black pumices exhibit black glassy centers and expanded outer rims. Inflated pumice lumps lie in the same vicinity as collapsed pumices suggesting that some pumices might have

been cooler and failed to collapse. Chemical analyses show that collapsed pumices have the same composition as white or mixed pumices; therefore, flattening may not be based on chemical composition.

The pumice and collapsed pumice, in addition to lithic fragments, lie in a matrix (45% to 50%) that contains glass shards and crystal fragments. Lithic fragments are composed of basalt, andesite, and ash-flow tuff clasts.

Clasts of McKenzie Canyon tuff Below McKenzie Canyon tuff

At two locations in the distal reaches of McKenzie Canyon tuff (NW1/4, Sec. 32, T.12S., R.12E., and NE1/4, Sec. 10, T.13S., R.12E.) boulders of the red upper unit of McKenzie Canyon tuff are found in basaltic gravels below a thin (3 to 5 foot) ledge of the same red resistant ash-flow tuff (Fig. 16). Boulders of McKenzie Canyon tuff in the epiclastic units are up to three feet long and rounded; the basaltic cobbles are rounded and eight inches in maximum diameter. Clearly, McKenzie Canyon tuff boulders were not transported far. The sequence of events that produced this outcrop may be as follows: a hot ash flow was deposited, locally eroded, and pieces of the ignimbrite were deposited with stream gravels. A second hot flow of similar composition immediately covered the lower unit and locally covered



Figure 16. Clasts of a red upper flow of MCT in an epiclastic deposit below the upper flow of MCT. (NE1/4, Sec. 32, T.12S., R.12E., east side of Deschutes River Canyon.)

epiclastic deposits containing blocks of the initial flow. High heat content and compaction obliterated evidence of a contact between the two members. The entire known exposure of McKenzie Canyon tuff yields no observable evidence of two separate flow units within the red upper member except in these outcrops.

Another possible explanation is that one flow divided around an obstruction. The faster arm of the flow was deposited and broken up within sediments before the slower arm of the flow came around and covered the sediments. This seems unlikely considering the amount of sediment between the blocks and upper ledge of McKenzie Canyon tuff (Fig. 16) and the amount of time required to erode and deposit the blocks of McKenzie Canyon tuff.

LATERAL VARIATIONS AND SOURCE

Lateral variations in Lower Bridge tuff and McKenzie Canyon tuff indicate that they were derived from a source to the southwest. The ten largest pumice and lithic sizes were measured at many locations. Plate 1 shows that the largest pumice and lithic sizes of the Lower Bridge tuff ash-flow unit decrease distally. However, the thickness measurements do not show a consistent decrease; channeling has made them variable. Also, distinction between the two ash-flow deposits is lost at the distal end where the units become finer grained and

more homogeneous. The McKenzie Canyon tuff displays significant lateral variations. In the southwest part of the study area the McKenzie Canyon tuff is generally thicker (35 to 45 feet) and has a higher degree of induration. It contains up to four flow units with pumice and lithic clasts. McKenzie Canyon tuff becomes thinner (5 to 15 feet, Plate 1) and less indurated to the northeast and loses the lower silicic members (Plate 2). Also, to the northeast it is composed of fewer large pumice lumps, is lacking in collapsed pumice, and foreign lithic clasts decrease in size. Distally the white basal layer of the upper unit is lost, leaving a light orange, slightly welded upper flow.

Reversed topography observed in the study area may also indicate the direction from which the ash-flow tuffs originated. Many resistant rim lava flows in the Deschutes Formation now form linear ridges, representing the location of paleo-valleys to which they were once confined. Subsequent erosion removed the less resistant material forming the valley walls, thus leaving the lavas as topographic highs. La Follette Butte (Plate 1), which trends northeast-southwest, represents the northeast tip of one of these flows.

There is no evidence of a source at the southern exposure of McKenzie Canyon tuff in Deep Canyon and highway 126. A more probable source location is on the

west side of the Tumalo Fault about five miles south of the town of Sisters (Fig. 17). In fact, the source could lie even farther southwest of this proposed site.

However, the area has been down-dropped by the Tumalo Fault and buried by younger High Cascade deposits which has obscured any evidence of a volcanic source.

WELDING, ZONING, AND COOLING UNITS

Welding is defined as "that process which promotes the union or cohesion of glassy fragments" (Smith, 1960b). It ranges from the early stages with the cohesion of glassy fragments at points of contact to complete welding where glass surfaces are fused and all pore space is eliminated to form a dense black glass. The transition between initial and complete welding is marked by an increasing loss of porosity and a general darkening of pumice fragments followed by darkening of the shard-rich matrix. A thick section (45 feet) of McKenzie Canyon tuff in Squaw Creek (NW1/4, Sec. 3, T.14S., R.11E.) shows the highest degree of welding in McKenzie Canyon tuff with eutaxitic structure and a dark gray to black matrix.

A welded pyroclastic flow can be divided into five parts: a central densely welded zone grading into partially welded and nonwelded zones above and below. The lower two zones of incomplete welding are thinner

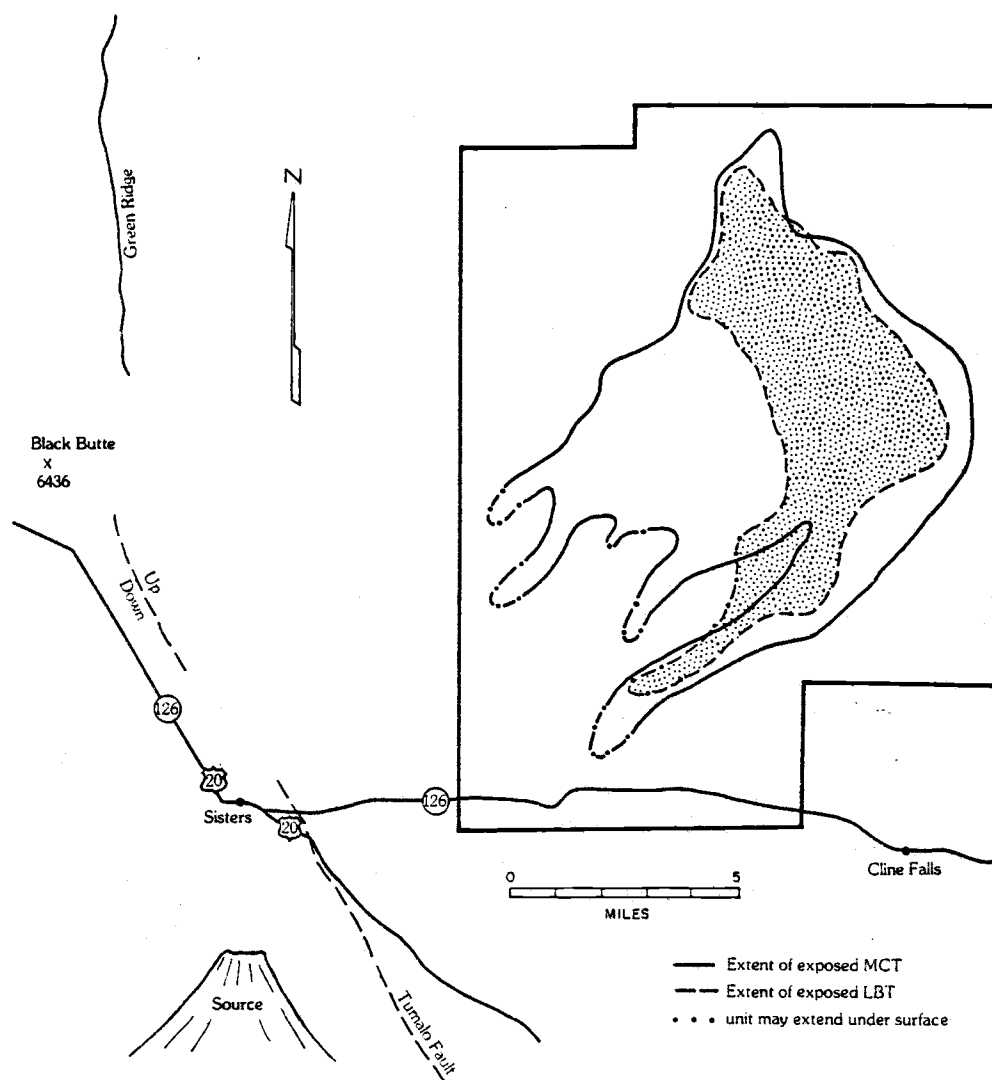


Figure 17. Possible location of source volcano for LBT and MCT.

than the upper ones and the sequence is called a simple cooling unit (Smith, 1960a). Multiple flows deposited in rapid succession can also form a simple cooling unit if they have undergone an uninterrupted cooling history to produce a welding pattern consistent with a single flow. It is often difficult to detect partings between flows in densely welded zones (e.g., upper flow McKenzie Canyon tuff) and often what appears to be a single flow actually consists of many flow units.

A compound cooling unit is recognized when there is a deviation in the zone patterns of a simple cooling unit which indicates a break in the cooling history. This may happen by: 1) unequal distribution of ash-flow deposits, and 2) emplacement of ash flows with very different temperatures.

McKenzie Canyon tuff is a compound cooling unit. The lower (1 to 3) silicic flows erupted, began to cool and were overlain by one or two hotter upper flows. This produced the lower nonwelded units, overlain by a moderately welded upper member with crude columnar jointing in the upper 10 to 30 feet (Fig. 12). In southern Deep Canyon, an area closest to the hypothesized source, McKenzie Canyon tuff is highly welded and individual flows are not detected although welding is still denser toward the top. Distally, only the upper McKenzie Canyon tuff is present and it forms a thin simple

cooling unit with only partial welding and a light orange color (Fig. 16). Between the proximal and distal sections, multiple flows of McKenzie Canyon tuff are recognizable because welding is not intense and the lower silicic flows are present.

The Lower Bridge tuff forms a simple cooling unit throughout the study area. At one locality (intersection of Deep Canyon and Deschutes River) the parting between Lower Bridge tuff flow units is marked by a one-inch epiclastic layer containing 50% pumice lapilli; however, this is still considered a simple cooling unit.

TEMPERATURE, VOLUME, TRANSPORT, SPEED, AND FLOW MECHANISMS

Temperature

Studies based on Fe-Ti oxides suggest that "quench temperatures for clasts in pumice flows can vary from 640° to 1000° C" (Lipman, 1971; Ewart et al., 1971). Based on degrees of welding, Smith (1960a, p. 824) estimated that flow temperatures range between 580° and 900° C. He also noted that the temperature of a pyroclastic flow depends on: 1) the amount of gas erupted as this affects the concentration of particles which is directly proportional to heat retention; 2) the initial velocity of the eruption which affects the maximum column height such that greater heights provide longer time for cooling; 3) the amount of air entrapped in the flow. With these variables, units of similar thicknesses and compositions may not have the same temperature of emplacement because of effects related to properties of the eruptive column.

Welding is an indication of flow temperature. The two units in this study show 1) low temperature emplacement (Lower Bridge tuff), and 2) a change in temperature during emplacement (McKenzie Canyon tuff).

Thick welded zones may be produced by rapid collapse of a short vertical column that conserves heat (Sparks et al., 1978). Sparks and Wilson (1976) note that air-fall tuffs do not commonly occur with welded tuffs; the formation of an air-fall tuff requires a large vertical column. Lower Bridge tuff includes a basal air-fall unit and two nonwelded ash-flow deposits suggesting a low temperature emplacement probably produced by a large vertical column. Additional evidence for deposition at a lower temperature is a weak signature of paleomagnetic polarity and the lack of a red color.

Alternatively, welded zones may be caused by an increase in temperature of the erupted material rather than just properties of the eruptive column. Some pyroclastic flows show a change in temperature during eruption (e.g., Upper Bandelier tuff, Smith and Bailey, 1966). The temperature increase of the Bishop tuff (Hildreth, 1979) and the Bandelier tuff may be the result of tapping deeper, hotter levels of the magma chamber. McKenzie Canyon tuff upper unit shows an increase in welding toward the top (Fig. 12) which may be caused by a similar mechanism.

Volume and Transport

Volume estimates are difficult to determine for Pliocene ash-flow deposits because erosion by wind and

water and deposition of younger beds prevents an accurate account of the original extent and thickness. Extrapolated thickness data between widely spaced exposures of a nonuniform unit yield imprecise estimates. Also, different degrees of vesiculation should be accounted for; however, this was not done for McKenzie Canyon tuff nor for the values in Table 1. A volume estimate for McKenzie Canyon tuff assuming a uniform eight foot thickness over an area 4.5 miles wide by 23 miles long (assuming a source five miles south of Sisters, Fig. 17) places the unit in an intermediate volume range; i.e., 0.1 to 1.0 km³, according to Sheridan (1979).

Table 1 lists distance and volume data for different units. Comparing the volume of McKenzie Canyon tuff with the Valley of 10,000 Smokes and Hakone, Japan, which have similar runout distances, McKenzie Canyon tuff volume estimate may be low. Mt. Lamington tuff (Taylor, 1958) has characteristics similar to McKenzie Canyon tuff: a large runout distance (16 km) and a low volume (0.1 km³). These facts may be explained by formation from a dome blast that boosted velocity. Smith and Roobol (1982) note that dome blasts are characteristically composed of dense lava clasts and ash. None are known to deposit welded tuff (Smith, 1960a, p. 818); consequently, this mechanism could not explain McKenzie Canyon tuff.

The probable transport mechanism for the ash-flow

Table 1. Estimated volumes and distances traveled by pyroclastic flows from their source.

Name of Pyroclastic Flow, Volcano	Distance (km)	Volume (km ³)
Ash Flow H, Guatemala	125	20-50
Aso, Japan	96	175
Crater Lake, Oregon	64	37
Valley of 10,000 Smokes	29	6.1
MCt, "Plio-Cascades"	37	0.7
Hakone, Japan	24	15
Bezymianny 1955-56	18	1.8
Mt. Lamington 1951-56	16	0.1
Asama 1783	11	0.1
Komagatake 1929	8	0.5
Soufriere, St. Vincent 1902-03	8	0.4-1.4

after Smith and Roobol, 1982

units in this study, considering the volume and distance traveled, is the gravitational collapse of an overloaded eruptive column. Eruptions often begin with a plume that is diverted by air currents and the material is deposited to form an air-fall tuff. Later, the volatile content decreases (Sparks and Wilson, 1976; Sparks and others, 1978) and the column density increases. It eventually exceeds the surrounding atmospheric density at which time ash and fragments begin to fall and initiate an ash flow. As the eruption continues, the column collapses and ash flow production proceeds.

Initially the flow moves in turbulent suspension and

immediately becomes separated into a lower zone (the pyroclastic flow) with a high concentration of particles and an upper turbulent cloud of ash and gas (Sparks, 1978). The lower layer moves by laminar and/or plug flow similar to a debris flow which does not allow sorting of particles because of high flow density. Fines are generated by crushing of larger particles within the high-concentration basal zone and are fluidized by exsolving gases (Sparks et al., 1978); an upward drag exerted on a particle by the rising gases is equal to gravitational forces. Gases exsolved during transport could be sufficient to fluidize small and medium size ash particles which should in turn support larger clasts.

Sheridan (1979) contends that ash flows can pass over topographic barriers at a great distance from the source. He describes an energy line that extends from the top of a "gas-thrust zone" in the eruptive cloud, which is the maximum elevation to which ash-flow particles are ejected, to the distal end of the unit. This outlines a triangular vertical zone in which the flow has enough energy to travel and explains flows that "surmount topographic barriers at a great distance from the vent". He assumes the top of the "gas-thrust zone" is 4 km for large pyroclastic flows yet it could be as much as 9 km (Sparks and others, 1978).

Table 2 compares the calculated slope of McKenzie

Table 2. Emplacement data on large pyroclastic flows.

Volcano	Deposit Slope	Runout (L, km)
"Plio-Cascades" MCt		
Intersection of Deep Canyon and Highway 126	0.4	21.8
Proposed source, 5 mi. S. of Sisters	0.4	37
Aira	0.9	35
Katmai, 1912	1.5	22
Valles Caldera	1.4	24
Bandelier Tuff	1.7	33
	2.2	29
Long Valley Caldera	2.2	37
Bishop Tuff	3.5	30

after Sheridan, 1979

Canyon tuff, based on modern elevations of basal contacts, with the slopes of other pyroclastic flows that have a similar runout length. Two sets of number are used in the calculations for McKenzie Canyon tuff. The first uses only the length (13.5 miles) and slope (0.4°) of the exposed McKenzie Canyon tuff. The calculation assumes that the source lay at the intersection of U.S. highway 126 and Deep Canyon (Plate 1 and Fig. 17), an unlikely situation because there is no evidence of a source vent there. The second set of numbers uses the proposed source of McKenzie Canyon tuff five miles south of Sisters (Fig. 17), making the flow length 23 miles and assumes the slope remains uniform (0.4°), although it is more likely to have increased closer to the source. Based on the flow distance, even at the minimum 13.5 miles (21.8 km), McKenzie Canyon tuff fits into the large pyroclastic flow category. Table 2 shows that the McKenzie Canyon tuff slope (0.4°) is much less than that of comparable ash-flow deposits (0.9° to 3.5°). The slopes of McKenzie Canyon tuff may have increased closer to the source volcano but the evidence is now covered by recent volcanics.

Speed and Flow Mechanisms

Observed speeds of pyroclastic flows vary depending on several criteria, including thickness and topographic

barriers. Estimates of velocities of observed pyroclastic flows range from 8 to 45 m/sec (Smith and Roobol, 1982). Sparks et al. (1978) suggest that initial velocities range from 60 to 30 m/sec.

An ash-flow deposit is not laid down in a block instantaneously but rather in parts. The lowest part of the tuff unit is deposited from the flow front while the middle and top are derived from the center and tail of the flow. The McKenzie Canyon tuff upper member may be explained by this mechanism. After less extensive lower silicic flows were deposited and slightly cooled, the upper flow was erupted. An initial silicic composition formed the flow front and was followed by a more mafic middle and tail of the flow as deeper parts of an inhomogeneous magma chamber were tapped.

MINERALOGY

Introduction

Samples analyzed for mineral content are compiled in Table 3 according to their vertical positions in the units. All of these minerals have been recovered from cleaned pumice, no samples are from the matrix. Samples numbers 191, 194, 195, and 196 represent the lower silicic flow units of McKenzie Canyon tuff; 198, 202, 206, 201, and 205 pertain to the upper red McKenzie Canyon tuff flow unit. Sample 3 is from the lower Lower Bridge tuff flow; 232, 234, 235, and 236 exemplify the upper Lower Bridge tuff flow.

Petrographic analyses of plagioclase grains indicate a lack of similarity in zoning patterns between crystals of the same unit. Most likely, thin sections are not cut through the core of each crystal and thus fail to display the same pattern. Although zoning patterns within plagioclase crystals of the same unit can often be used to speculate on the cooling history of the magma chamber, this type of conjecture cannot be used on the plagioclase of McKenzie Canyon tuff or Lower Bridge tuff. Gill (1981, p. 173) states

. . . the zoning, inclusions, and resorptions of plagioclase phenocrysts may provide the

Table 3. Analyzed mineral content of MCT and LBT relative to vertical position in the flow.

		% Volume Mafic Minerals	Olivine (Microprobe data)	Clinopyroxene Microprobe Data	Present? Y=Yes	Orthopyroxene Microprobe Data	Molecular % Ferrosilite	Amphibole	Plagioclase (An Content) (# of shards analyzed)
<u>MCT--White Pumice</u>									
upper	206	0.051		Augite	Y	Ferro-hyper.	42-49		37 (1)
	202	0.015			Y		45		28-31 (3)
	198	0.14			Y		38-40		29-31 (3)
	194	0.089		Augite	Y	Hypersthene	41		31-34 (2)
lower	191	0.053		Augite	Y		41-42		29-30 (2)
		Ave. = 0.07%					41-45 = Hypersthene		Ave. = 29-31 Oligoclase/ Andesine
<u>MCT--Black Pumice</u>									
	205	0.27	F ₀ ⁸²	Augite	Y		38-40		56-60 (3)
upper	201	0.23	F ₀ ⁸³	Augite	Y		37-39		61 (2)
	195	1.26			Y	Ferro-hyper.	40-41		61-65 (3)
lower	196	0.83		Augite	Y	Hypersthene	38		61-69 (2)
		Ave. = 0.6%					38-41 = Hypersthene		Ave. = 60-65 = Labradorite
<u>Lower Bridge Tuff</u>									
	236	5.7			Y		42-43	Pargasite	38-45 (3)
	235	10.4			Y		41	Pargasite	39-44 (3)
upper	234	7.2		Augite	Y		41-42	Pargasite	38-39 (2)
	232	3.1			Y		41	Pargasite	37-39 (2)
lower	3	3.2		Augite	Y		41-43	Pargasite	35 (3)
		Ave. = 5.9%					41-43 = Hypersthene		Andesine, increase in An upward

fullest available record of andesite magma history, but their ubiquity and bewildering complexity make their interpretation formidable.

The dacite and rhyolite of Lower Bridge tuff and the andesite and rhyolite of McKenzie Canyon tuff all contain augite and hypersthene. Normally two pyroxenes (augite and hypersthene) are present in an intermediate composition andesite whereas dacite and rhyolite may contain only a few hypersthene grains. Thus, McKenzie Canyon tuff rhyolite and Lower Bridge tuff are unusual in containing augite.

Clinopyroxenes from all the units are dark green and tabular. Analyses plot in the augite field (Fig. 18). Clinopyroxenes in black McKenzie Canyon tuff may have higher MgO and lower FeO than white McKenzie Canyon tuff samples. Microprobe analyses revealed inclusions of titanomagnetite (#3, #196), ilmenite (#234, #206), and what appeared to be feldspar (#196, #234, #206) trapped within the clinopyroxene grains (Charles Knowles, pers. comm.). High-K overgrowths capped one end of two clinopyroxene grains occurring in samples of McKenzie Canyon tuff black pumice (#205) and Lower Bridge tuff (#234). Chemical zonation was not observed within the clinopyroxenes. Intergrowths of orthopyroxene are observable within the clinopyroxene grains from samples #194, #196. These orthopyroxene intergrowths are hypersthene (Figs. 18 and 19) whereas single orthopyroxene crystals from

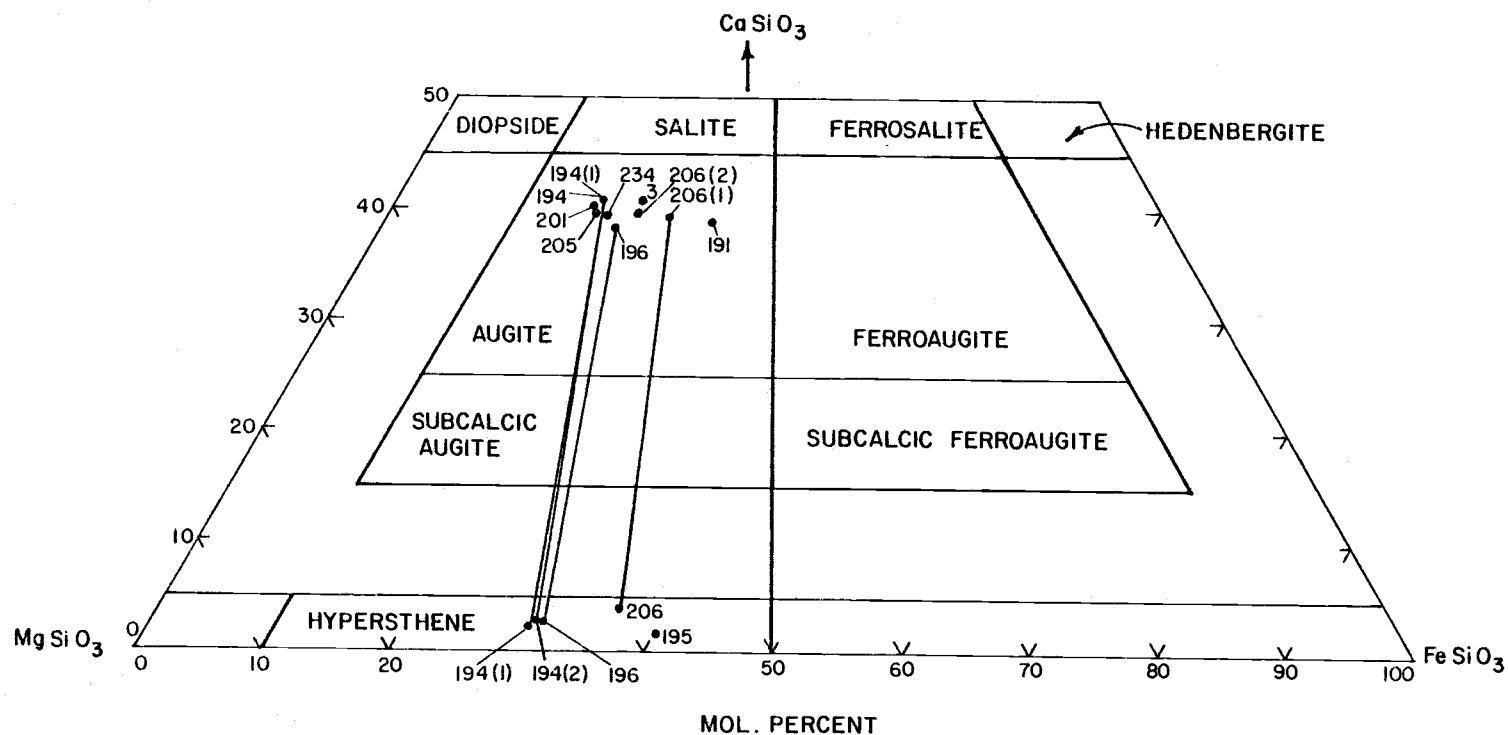


Figure 18. Clinopyroxenes in the system $\text{CaMgSi}_2\text{O}_6$ - $\text{CaFeSi}_2\text{O}_6$ - $\text{Mg}_2\text{Si}_2\text{O}_6$ - $\text{Fe}_2\text{Si}_2\text{O}_6$. (After Poldervaart, A. and Hess, H.H., 1951, Jour. Geol., vol. 59, p. 472) calculated by converting weight % oxide analyses of the pyroxene to a structural formula (Hutchison, 1974, p. 401-405). Lines connect coexisting phases in the same sample.

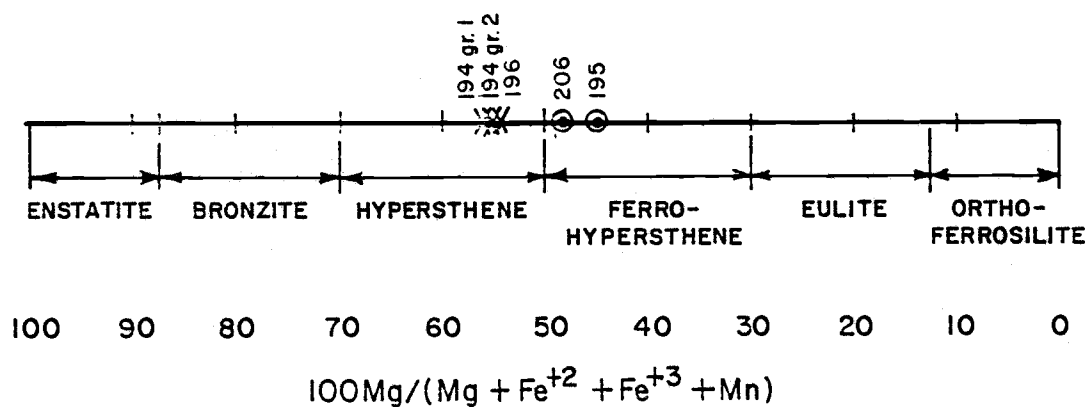


Figure 19. Nomenclature of orthorhombic pyroxenes and MCT microprobe orthopyroxene analyses using weight % oxides (after Deer, Howie, and Zussman, 1978, p. 112). An X is analyses of an orthopyroxene grain intergrowth with clinopyroxene. A circle represents a single orthopyroxene grain.

both McKenzie Canyon tuff black pumice (#195) and McKenzie Canyon tuff white pumice (#206) are ferro-hypersthene. Orthopyroxenes from all the samples are green to honey brown and often include magnetite.

Lower Bridge Tuff Pumice

Pumice from Lower Bridge tuff contains subhedral plagioclase grains which are larger and more abundant than the comparatively crystal poor McKenzie Canyon tuff pumice. Anorthite contents (all andesine) increase upward from An 35 in the white pumice of the lower pink flow to An 38-45 in the gray pumice of the upper purple flow. Plagioclase is further characterized by faint oscillatory zoning. Three grains have patchy zoning portrayed by a corroded core and rim filled with, and enclosed by, a euhedral plagioclase crystal of a lower or higher An content (Fig. 20). However, crystal textures are not consistent. Crystals are observed which have either no corrosion, a corroded rim, a corroded core with euhedral rim, or a corroded core and rim. The majority of grains display albite twins and about 20% exhibit Carlsbad twins. Inclusions of brown glass, crystals (mostly magnetite and apatite), and void spaces are typically abundant. The observed wide range of An contents may be due to contamination by these inclusions during analytical fusion of the plagioclase.

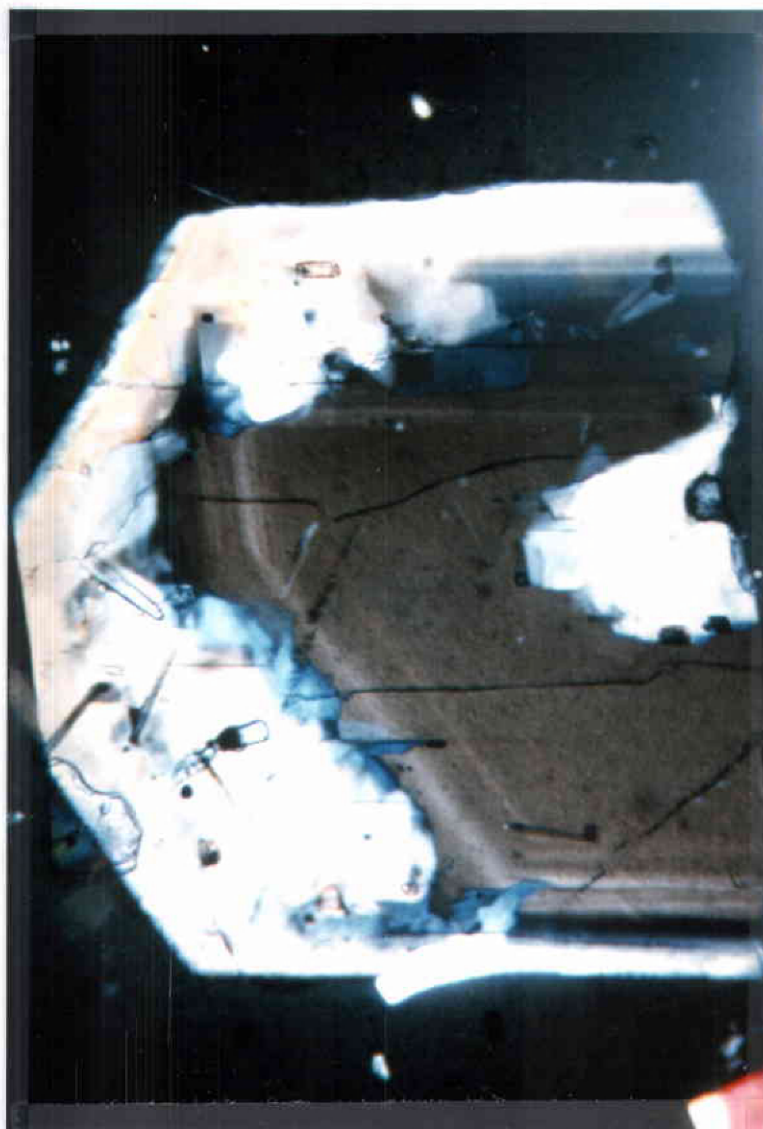


Figure 20. Photomicrograph of a plagioclase crystal from LBT pumice (#247). It shows a corroded core and rim, patchy zoning, oscillatory zoning, and clear lath-shaped inclusions (apatite) in the rim. The photograph shows about 3 mm of the slide.

The total weight percent of mafic minerals in the 14-48 mesh size fraction of Lower Bridge tuff pumice averages 6%, much higher than any McKenzie Canyon tuff pumice (Table 3). The heavy mineral suite consists of 35% amphibole, 50% hypersthene, 15% augite, and traces of ilmenite and magnetite (Fig. 21). The Mg content in augite (Appendix 1, samples #3 and #234) increases upward in the flow as expected. Brown laths of hypersthene (41-43 wt % Fs) contain magnetite inclusions.

Hornblende requires high water pressure to be stable and therefore generally does not crystallize under low-pressure shallow level conditions. Most amphiboles in volcanic rocks are common hornblende or are members of the pargasite-hastingsite series. Ti contents can be rather variable and all gradations to kaersutite (4% to 10% TiO_2) are found (Carmichael et al., 1974); kaersutites are normally found in alkali volcanic rocks (Deer, Howie, and Zussman, 1978). Amphiboles are only found in the upper flow of Lower Bridge tuff and in comparison with chemical compositions given by Leake (1968a), may be titaniferous pargasite (Appendix 1). The amphiboles have a distinctive black, vitreous luster; no glass, large, subhedral to euhedral grains showing good cleavage. The number of amphibole crystals in a sample varies from only two (#232) to many (#235).



Figure 21. The suite of mafic minerals in LBT under a binocular microscope. Pencil tip in lower right hand corner for scale.

McKenzie Canyon Tuff White Pumice

Minerals found in the crystal-poor white pumice of McKenzie Canyon tuff are plagioclase, hypersthene, augite, magnetite, ilmenite, and rare zircon. White pumice contains sparse plagioclase grains (An 29-31, oligoclase/andesine) that were probably broken during the eruptive event. A few grains have albite and Carlsbad twins, and faint oscillatory zoning is infrequently observed within continuously zoned crystals. Taylor (pers. comm., 1981) notes that intense oscillatory zoning arranged in distinct sets is common in volcanic feldspars and that the zone sets are probably formed in response to abrupt changes in pressure. A bright thin zone of low birefringence is seen in both samples #187 and #251 (Fig. 22); the composition is not known but it may indicate a similar chemistry or environment of crystallization existed for both crystals. Few, if any, inclusions are present within the crystals. This is a characteristic of plagioclase in the black pumice of McKenzie Canyon tuff. Corrosion of the plagioclase rim only occurs in 10% of the samples which may indicate variable pressure and temperature conditions. Overall, there appears to have been few sudden changes of pressure or other environmental effects.

The total weight percent of mafic minerals in the 14-48 mesh fraction of the white pumice is less than one



Figure 22. Photomicrograph under crossed nicols of plagioclase from MCT white pumice, (#251), southern Deep Canyon. Photo shows a lack of oscillatory zoning, sparse albite twins, and rare inclusions. The photograph shows about 3 mm of the slide.

percent (average of five samples). Hypersthene averages 3-4 grains per pumice fragment; the composition is verified by microprobe data (#206, #194, Appendix 1). Tabular ilmenite and rounded magnetite are also present in minor amounts. Olivine and amphibole are not found in the white McKenzie Canyon tuff pumice.

McKenzie Canyon Tuff Black Pumice

Black pumice from McKenzie Canyon tuff also contains sparse (4% by weight percent) plagioclase (An 60-65, labradorite), which is not unusual for Deschutes Formation andesites (Conrey, pers. comm.). The crystals generally have simple continuous zones (Fig. 23) and lack albite or Carlsbad twins. A few have faint oscillatory zones. Inclusions within the grains are absent except for magnetite and a few other crystals that occasionally displace the zones. Just 3 out of 24 examined crystals have a corroded or embayed core or rim which again suggests a simple history. Most crystals are broken, an effect which probably occurred during the explosive eruptive event.

The mafic suite of minerals consists of hypersthene, augite, olivine, and magnetite. The total weight percent of mafic minerals in the 14-48 mesh fraction of black pumice is about one percent (average of 4 samples). The hypersthene composition is verified by microprobe data



Figure 23. Photomicrograph of plagioclase under crossed nicols from a black MCT pumice (#252), southern Deep Canyon sample location. Albite and Carlsbad twins are unusual for plagioclase in black pumice of MCT. Note the slight zonation and few inclusions. The photograph shows about 3 mm of the slide.

(#195, #196). The augite contains some magnetite inclusions (#196) and feldspar (#196).

Black pumice from the upper orange flow of McKenzie Canyon tuff contains olivine crystals but they are missing from the black pumice of the lower light colored flows. One olivine grain was found in a lower silicic flow (#196) but this may have been caught in the screen from sieving previous samples. Gill (1981, p. 182) contends that olivine phenocrysts in andesite lie in the compositional range of Fo_{85-65} . Olivine crystals (#205 Fo_{82} and #201 Fo_{83} , Fig. 24) are large, euhedral, have an outer coating that has altered to iddingsite (Fig. 25) and fall into Gill's range for olivines in andesites. Iddingsite is red brown to orange brown and

is a continuous transformation in the solid state brought about by the diffusion of hydrogen atoms into the olivine structure where they become attached to oxygens and so release Mg^{+2} , Fe^{+2} and Si and allow their replacement by Fe^{+3} , Al and Ca ions (Deer, Howie, and Zussman, 1978, p. 5).

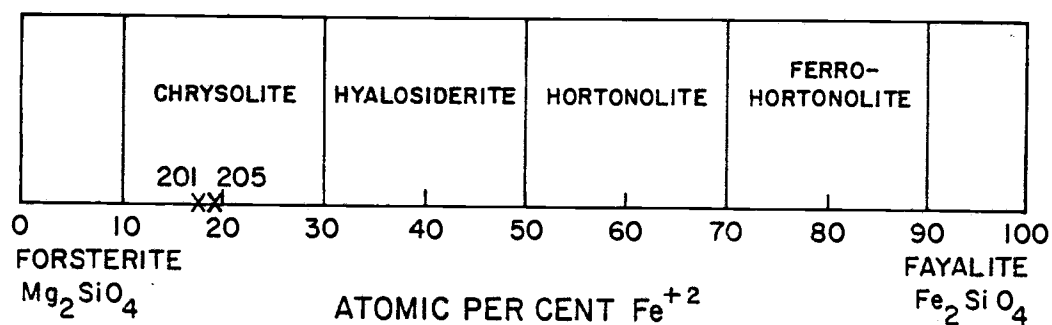


Figure 24. Nomenclature and chemical composition of olivines after Deer, Howe, and Zussman, 1978, p. 6. Atomic percent Fe²⁺ is determined from atomic ratios (Appendix 1).



Figure 25. An olivine crystal coated with iddingsite taken from a black MCT pumice (#201). Photograph is taken under a binocular microscope with magnification of 3X.

GEOCHEMISTRY

Introduction

Major element geochemistry shows that the Lower Bridge tuff contains rhyolitic and dacitic pumice lumps and the flows of McKenzie Canyon tuff contain rhyolitic and andesitic fragments. Appendix 2 lists the major element percentages and sample locations for Lower Bridge tuff, McKenzie Canyon tuff, Unit 0, and for two Deschutes Formation ash-flow tuff units analyzed by Rich Conrey, Units 5 (Fly Creek tuff) and 10 (Six Creek tuff). Only pumice fragments and collapsed pumices were analyzed for this study; they are assumed to represent primary magmatic compositions. The matrix was not analyzed due to the possibility of contamination by foreign material picked up from the surface during transport. Smith (1960a) observed that pumices, as in the upper welded flow of McKenzie Canyon tuff, may also be altered or contaminated by degassing, crystallization, and/or welding.

Lower Bridge tuff pumice fragments range from 64.7% - 72.1% SiO_2 . McKenzie Canyon tuff white pumices range from 69.7% - 73.4% SiO_2 and the black McKenzie Canyon tuff pumices range from 59.2% - 62.5% SiO_2 .

Sample #205 probably represents the mafic end member of black McKenzie Canyon tuff and sample #186 may represent the silicic end member of the white McKenzie Canyon tuff pumice (Appendix 2). Mixed pumices in McKenzie Canyon tuff range from 64% to 67.5% SiO_2 ; the McKenzie Canyon tuff ash-flow sheet spans a 14.2% SiO_2 range with a 7% SiO_2 gap. Collapsed pumices fall into the white pumice (#229) or mixed pumice (#225) compositions. The mixed pumice composition may be due to contamination during collection and analysis of the sample and may actually be rhyolite in composition. Rhyolite has a lower melting temperature than andesite and the silicic fragments may have become fused during welding of the hot andesitic tuff. Numerous geochemical analyses of collapsed pumices are required to verify that all are of rhyolitic composition.

Geochemical data obtained for white McKenzie Canyon tuff pumices from the Crooked River Canyon sample location (Plate 1, Fig. 3) were not included because of anomalous results due to contamination while sampling the small fragments. Other analyses of black and mixed clasts from this location were used; larger clasts are less susceptible to sample contamination.

Table 4 displays the average chemical compositions for McKenzie Canyon tuff and Lower Bridge tuff. Black and white Lower Bridge tuff pumice (64.7% to 70.8% SiO_2)

Table 4. Average chemical compositions and standard deviations for LBT and MCT.

Lower Bridge Tuff						McKenzie Canyon Tuff										
Lower Flow		Upper Flow				White Pumice			Black Pumice							
Top		Base	Middle			Top	3-4 Lower Flows			Upper Orange Flow			Lower Flows		Upper Orange Flow	
3		232	233	246		235	181	187	192	184	228	255	190	185	218	256
151		238	234	247		236	182	189	194	198	229	258	195	201	221	259
244		245	239			238	183	191	197	202	230		196	205		
						249				206	254					
SiO ₂	70.93	69.70	70.88		67.28	70.96	72.02		60.80	60.01						
	±0.40	±0.92	±0.77		±2.63	±0.99	±0.73		±1.05	±0.53						
TiO ₂	0.57	0.56	0.51		0.74	0.28	0.26		1.56	1.55						
	±0.06	±0.02	±0.06		±0.16	±0.03	±0.03		±0.11	±0.07						
Al ₂ O ₃	15.06	15.98	15.35		16.25	15.83	15.28		16.30	16.33						
	±0.31	±0.60	±0.71		±0.70	±0.76	±0.86		±0.09	±0.38						
FeO	3.21	3.04	2.84		3.76	2.63	2.45		7.39	7.71						
	±0.41	±0.09	±0.15		±0.69	±0.21	±0.18		±0.53	±0.34						
MgO	0.42	1.70	0.99		1.45	1.32	0.77		2.87	3.11						
	±0.39	±1.04	±0.30		±0.34	±0.32	±0.41		±0.30	±0.22						
CaO	1.75	1.91	1.42		2.85	1.65	1.44		5.31	5.72						
	±0.11	±0.17	±0.21		±0.84	±0.44	±0.35		±0.53	±0.33						
Na ₂ O	3.44	3.92	4.02		4.41	3.72	3.72		4.41	4.10						
	±0.80	±0.47	±0.40		±0.55	±0.82	±0.57		±0.21	±0.45						
K ₂ O	3.70	3.77	4.41		3.72	4.06	4.89		1.40	1.51						
	±0.67	±0.54	±0.19		±0.82	±0.37	±0.48		±0.12	±0.09						
Total	99.08	100.58	100.42		100.46	100.45	100.83		100.04	100.04						
K ₂ O/Na ₂ O	1.08	0.96	1.10		0.84	1.09	1.31		0.32	0.37						
CaO/FeO	0.55	0.63	0.50		0.76	0.63	0.59		0.71	0.74						

are averaged together for the value at the top of the upper flow, giving a noticeably lower SiO_2 content and higher standard deviation for SiO_2 than the rest of the flow. Only SiO_2 values from 59.2% to 60.5% were used in calculating the average composition of black McKenzie Canyon tuff pumices.

The McKenzie Canyon tuff is thick (35 feet) and welded in the southern Deep Canyon sample location (Plate 1, Fig. 26) and consequently does not have partings between flows (assuming that separate flows do exist). Values from the basal sample location are not calculated into black and white pumice averages (Table 4) because it is uncertain to which McKenzie Canyon tuff flow they belong. Due to the presence of the abundant banded pumices characteristic of the upper flow, values from sample locations 10 and 25 feet up from the base are used to determine the average of black and white McKenzie Canyon tuff from the upper flow (Table 4).

The white McKenzie Canyon tuff pumice from the upper and lower flows and all of the Lower Bridge tuff pumice show high $\text{K}_2\text{O}/\text{Na}_2\text{O}$ ratios ranging from 0.84 to 1.31 (Table 4); typically, most rhyolites have $\text{K}_2\text{O}/\text{Na}_2\text{O}=0.7$ and 1.0 is not uncommon (Cox, Bell, Pankhurst, 1979, p. 21). Black pumices in McKenzie Canyon tuff have a low $\text{K}_2\text{O}/\text{Na}_2\text{O}$ ratio for andesites.

The identification of a fragment as black or mixed



Figure 26. Southernmost sample location of MCT (35 feet thick). Partings are not visible within the flow. The unit at this proximal location is highly welded and columnar jointed. (SE1/4, Sec. 26, T14S, R11E)

in the field does not always hold true in the geochemical results. Sample #188 (64.0% SiO_2) is visually black although it has a mixed pumice chemistry. This indicates that either the white pumice was not detected in the fragment or there was a homogenization of the silicic and mafic magmas (i.e., magma mixing) prior to eruption. Considering that the majority of mixed pumices fall in the composition range between black and white pumice, any homogenized or mixed zones between two magma compositions in the magma chamber were small. Visually, samples #223 (61.6% SiO_2) and #231 (62.5% SiO_2) are mixed pumices but chemically they fall into the andesitic black pumice category. This may indicate that any black pumice composition with SiO_2 greater than the proposed mafic end member (#205, 59.2% SiO_2) may have encountered some small amount of mixing. Thus, there may be a small zone of mixing between andesite and rhyolite magmas in the magma chamber; however, the majority of andesitic pumice displays only a small amount of mixing with rhyolitic magma.

Table 5 compares the chemistry of pumices from blocks of McKenzie Canyon tuff that lie in an epiclastic deposit with the chemistry of the overlying orange McKenzie Canyon tuff flow as discussed in the ash-flow tuff descriptions section. The McKenzie Canyon tuff unit shows a similarity in pumice major-element chemistry

TABLE 5. A comparison of black and white pumice chemistries from blocks of MCT in sediments with the overlying MCT flow.

	White Pumice		Black Pumice	
	#270 MCT Blocks in Sediments	#273 Flow Above Blocks	#271 MCT Blocks in Sediments	#272 Flow Above Blocks
SiO ₂	71.50	72.80	64.00	61.80
Al ₂ O ₃	15.00	14.80	14.90	15.00
FeO	2.62	2.41	6.25	7.17
MgO	0.75	0.61	1.62	1.77
CaO	1.41	1.28	4.94	5.12
Na ₂ O	1.82	2.31	2.66	2.61
K ₂ O	5.02	4.76	2.19	1.90
TiO ₂	0.24	0.20	1.12	1.32
Total	98.30	99.19	97.69	96.63

between the blocks and the flow which suggests that they were derived from simultaneous volcanic eruptions.

The white component of a McKenzie Canyon tuff banded pumice has a similar composition to a singular white McKenzie Canyon tuff pumice (Table 6). The black component of a banded pumice produced a mixed composition. The mixed composition may be a result of mixing of the two magmas prior to eruption or contamination during sample preparation. Banded pumice fragments appear to be the combining of rhyolitic and andesitic magmas and represent the lack of a chemical continuum between the two composition.

Harker Diagrams

Harker diagrams are drawn for K_2O versus SiO_2 , TiO_2 versus SiO_2 , FeO versus SiO_2 , and CaO versus SiO_2 . Al_2O_3 , MgO , and Na_2O values are too variable to be of use plotted on a Harker diagram. In addition to McKenzie Canyon tuff and Lower Bridge tuff, values from two Deschutes Formation ash-flow tuffs (Units 5 and 10) were added for comparison. Chemistries from Units 5 and 10 are taken from Hales (1975) and Conrey (pers. comm., 1984). Yoder (1979) states that conformance to a variation (Harker) diagram does not make the rocks a "differentiation series". The diagram is only a plot of analyses in order of increasing silica and in itself

TABLE 6. A comparison of the chemistries of the components of MCT banded pumice with similar MCT pumice compositions.

	White Pumice		Mixed Pumice	
	#186W From Banded	Average From Up Flow MCT	#186B From Banded	#217 From Up Flow MCT
SiO ₂	73.4	72.02	65.6	65.6
Al ₂ O ₃	13.8	15.28	14.2	15.90
FeO	2.39	2.45	5.37	5.17
MgO	0.19	0.77	1.34	1.88
CaO	1.04	1.44	3.82	3.40
Na ₂ O	2.39	3.72	3.10	4.27
K ₂ O	5.12	4.89	2.45	2.61
TiO ₂	0.21	0.26	0.97	0.93
Total	98.54	100.83	96.78	99.76

carries no compelling implications of evolutionary development.

Linear regression lines, calculated and plotted by computer, are drawn through black, white, and all McKenzie Canyon tuff pumice values, and all Lower Bridge tuff pumice values. Linear regression lines were not calculated using the values from Units 0, 5, and 10. A regression line combining Lower Bridge tuff and McKenzie Canyon tuff was deleted because the line homogenized true values, insinuating a derivation from one magma. Pumices from both upper and lower flows were combined to determine the regression lines. White McKenzie Canyon tuff values are scattered making the validity of the regression line questionable.

Ewart (1979) proposes a division between high-K and medium-K andesite through rhyolite (Fig. 27). The McKenzie Canyon tuff rhyolite and all Lower Bridge tuff fall into the high-K category. Gill (1981) also proposed a division between high-K and medium-K andesites. McKenzie Canyon tuff andesite falls into the medium-K range of both Gill and Ewart. Mixed McKenzie Canyon tuff pumice compositions cross over the medium-K to high-K line of Ewart as expected, because it is a combination of a medium-K andesite and high-K rhyolite. Taylor (pers. comm., 1981) classifies rhyolite as greater than 68% SiO_2 with more than 4% K_2O . Rhyolite is a rare occurrence in

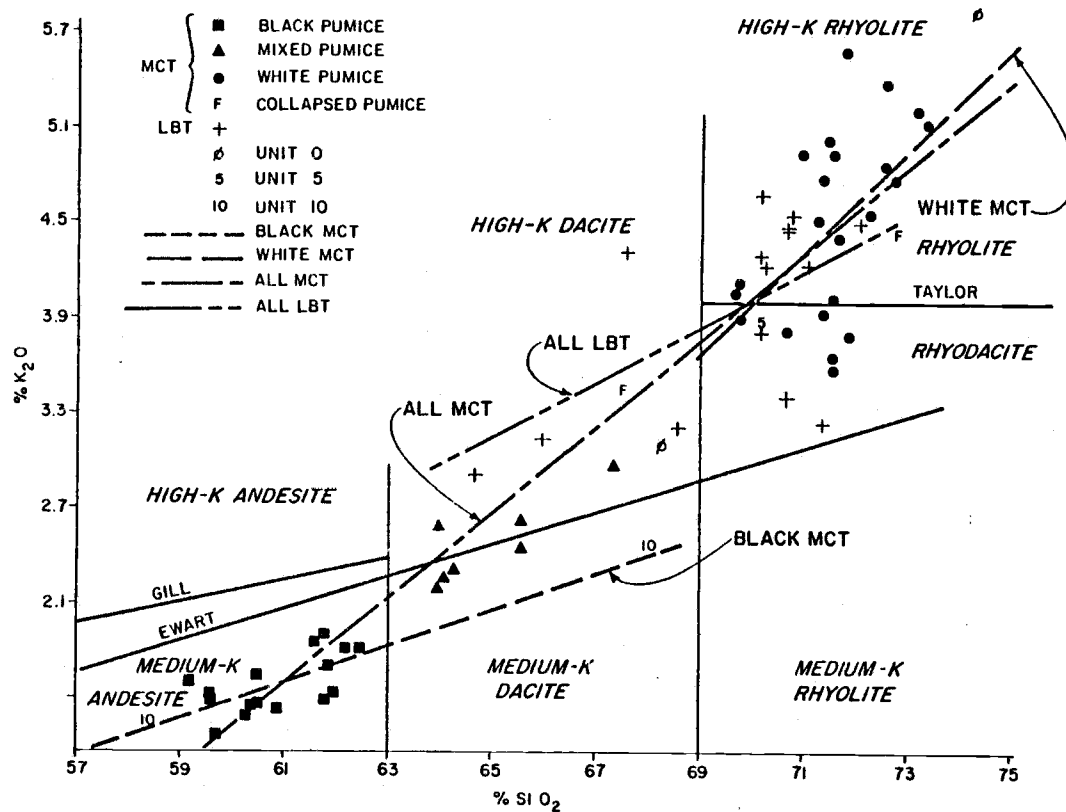


Figure 27. Harker diagram of % K₂O versus % SiO₂ with linear regression lines. Gill (1981, p. 6) and Ewart (1979) proposed divisions between medium-K and high-K andesites. Taylor (1981, pers. comm.) separates rhyolite and rhyodacite.

the Cascade calcalkalic suite. Rhyodacite with greater than 68% SiO_2 and less than 4% K_2O is usually the upper end of the calcalkaline series. McKenzie Canyon tuff and Lower Bridge tuff silicic rocks span the rhyolite-rhyodacite boundary and are called rhyolite in this study.

Units 0 and 5 have similar K_2O values to McKenzie Canyon tuff and Lower Bridge tuff rhyolite and dacite. The andesite of Unit 10 lies along the trend with McKenzie Canyon tuff andesite (Fig. 27). Unit 10 dacite also falls along the medium-K andesite trend rather than following a high-K trend similar to dacitic Lower Bridge tuff and rhyolitic McKenzie Canyon tuff and Lower Bridge tuff.

Gill (1981, p. 111) states that most orogenic andesites have 0.8% to 1.0% TiO_2 ; thus, black McKenzie Canyon tuff pumices are high-titanium andesites (Fig. 28). White McKenzie Canyon tuff pumices have a lower TiO_2 content than Lower Bridge tuff; TiO_2 may possibly be used to distinguish Lower Bridge tuff from McKenzie Canyon tuff white pumices. Units 0, 5 and 10 show a good correlation with Lower Bridge tuff and McKenzie Canyon tuff. The regression lines for white McKenzie Canyon tuff and Lower Bridge tuff do not follow the regression line for black McKenzie Canyon tuff.

The black McKenzie Canyon tuff regression line in

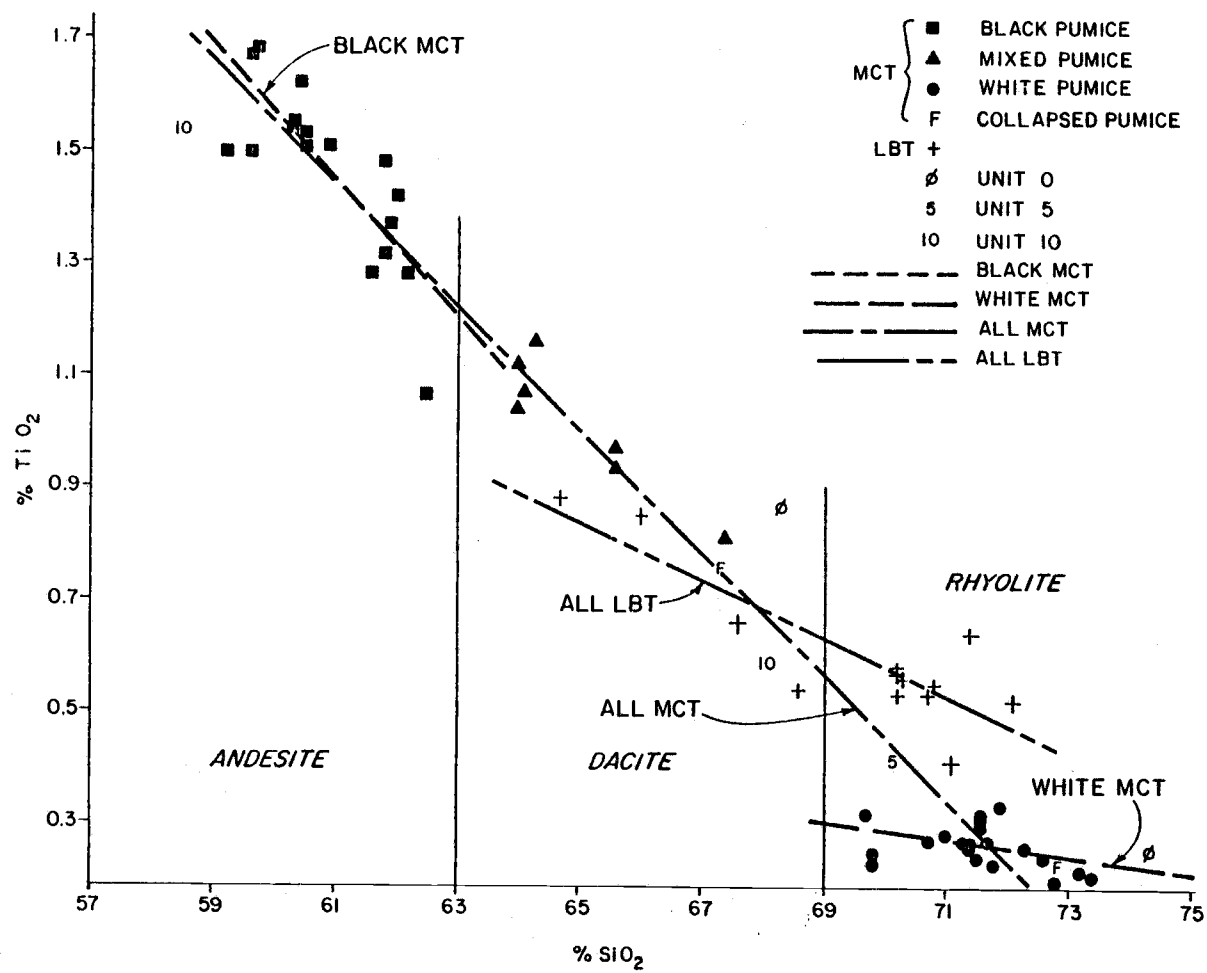


Figure 28. Harker diagram of % TiO₂ versus % SiO₂ with linear regression lines.

Figure 29, as in Figure 28, is almost parallel to the line of all McKenzie Canyon tuff. This suggests a trend of the black McKenzie Canyon tuff toward the silicic McKenzie Canyon tuff. However, the McKenzie Canyon tuff rhyolite and Lower Bridge tuff regression lines do not have the same trend as black McKenzie Canyon tuff pumice. The angle between the white McKenzie Canyon tuff and all McKenzie Canyon tuff regression lines (Fig. 28 and 29) indicates that high SiO_2 analyses may be inaccurate or that white McKenzie Canyon tuff may not be compositionally related to black McKenzie Canyon tuff. The rhyolitic Lower Bridge tuff has a slightly higher FeO content than rhyolitic McKenzie Canyon tuff and may be used to distinguish between the units.

Unit 0, 5, and 10 all fit within McKenzie Canyon tuff and Lower Bridge tuff CaO values (Fig. 30).

Calcalcalic Rocks and Ternary Diagrams

Gill (1981, p. 7) clarifies the use of the terms calcalcalic and calcalcaline: "'Calcalcaline' is a bastardized form of the adjective calcalcalic. . . and is used because it is a more euphonious adjective. . . ." A commonly used classification (Fig. 31) defines calcalcaline rocks as having an alkali-lime index of 56% to 61% SiO_2 . Gill's (1981) "average" calcalcaline andesites are plotted on the basis of $\text{FeO}+\text{MgO}$ versus SiO_2

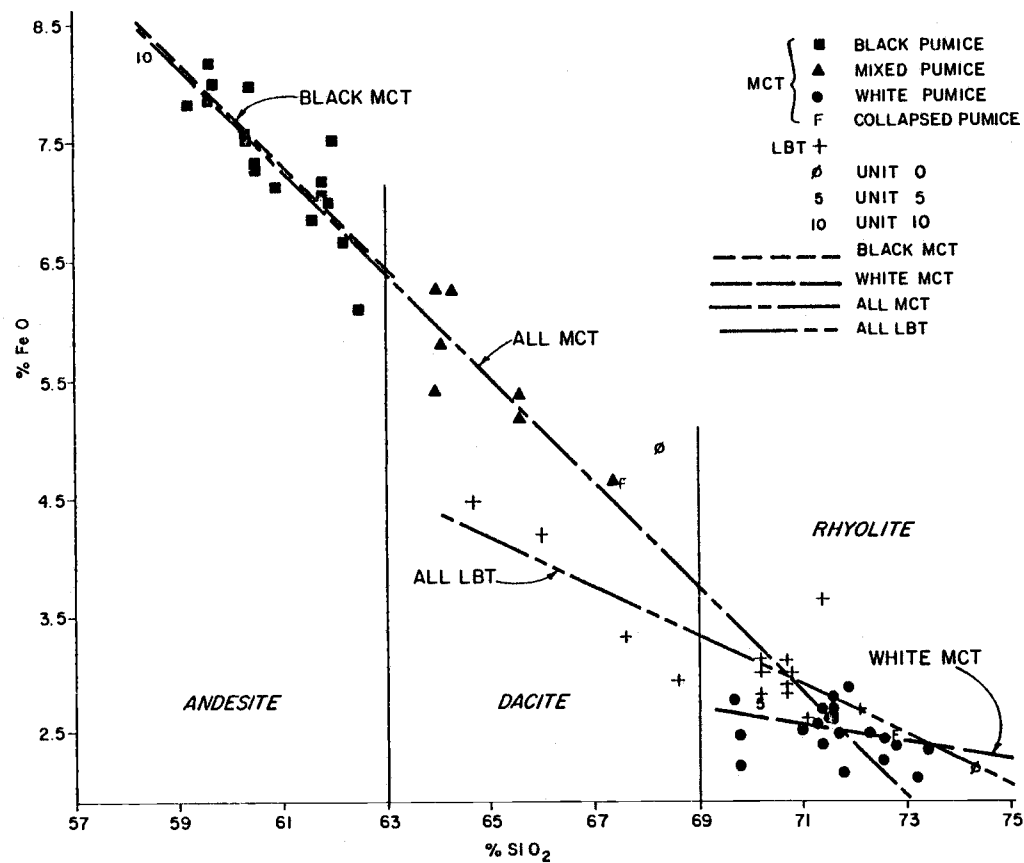


Figure 29. Harker diagram of % FeO versus % SiO₂ with linear regression lines.

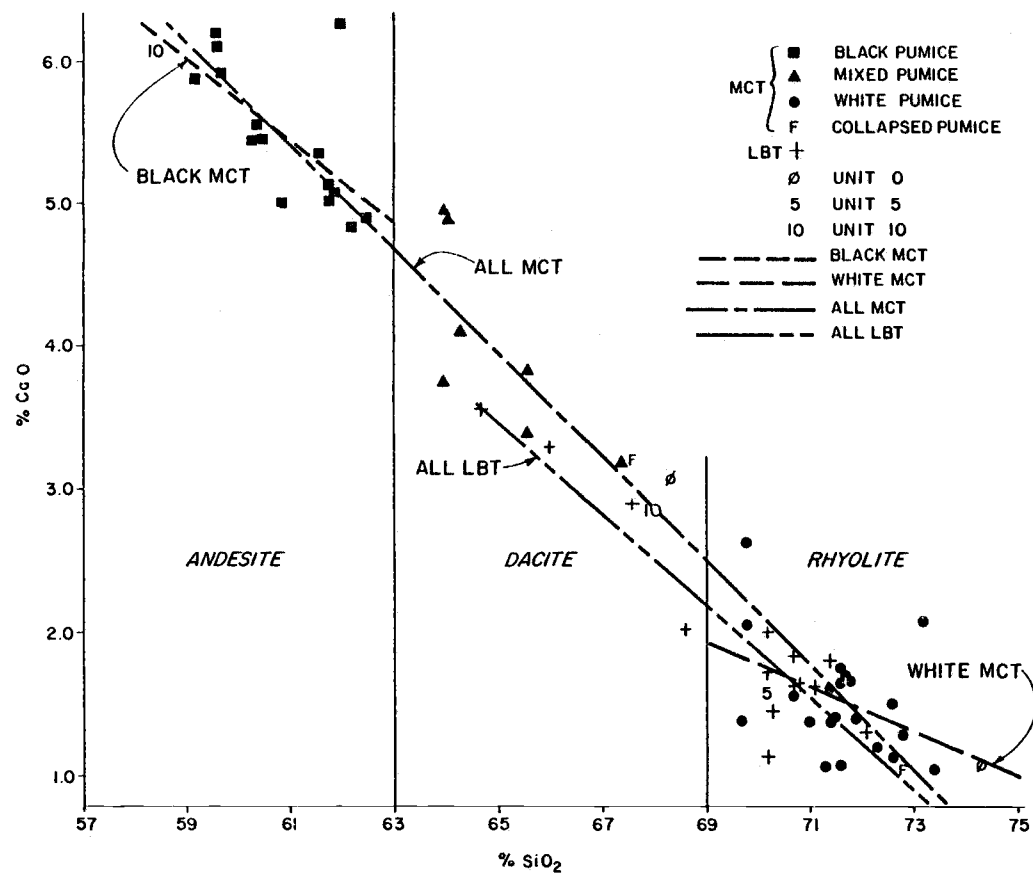


Figure 30. Harker diagram of % CaO versus % SiO₂ with linear regression lines.

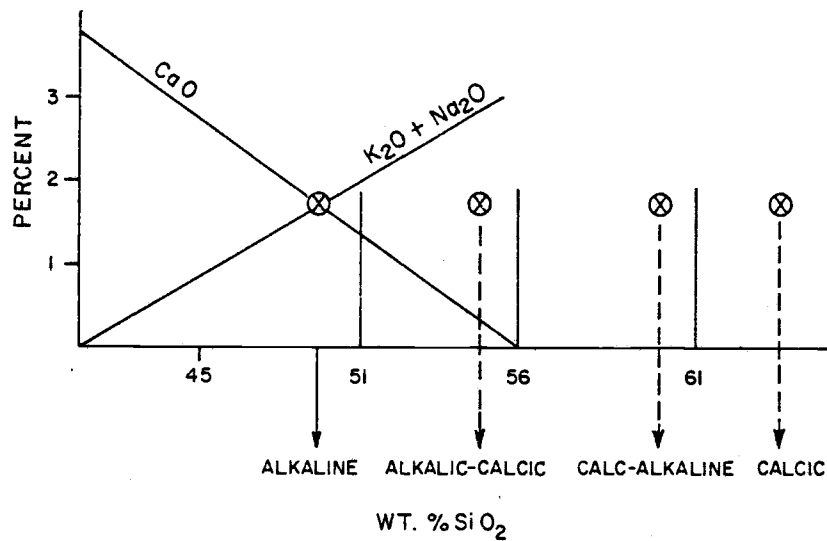


Figure 31. Chemical classification of volcanic rocks. If intersection of CaO and $\text{K}_2\text{O} + \text{Na}_2\text{O}$ is less than 51% SiO_2 =alkaline, 51-56%=alkaline-calcic, 56-61%=calc-alkaline, and less than 61%=calcic. (After Peacock, 1931)

in Figure 32 with McKenzie Canyon tuff black andesite values added for comparison. Hutchison (1974, p. 395) contends that weight percent silica is not a good index to use in variation diagrams because SiO_2 values do not change steadily throughout fractionation.

Figure 33 shows the relation of FeO and CaO to silica in McKenzie Canyon tuff andesites. Gill (1981, p. 107) states that in calcalkaline suites, FeO is less than or equal to CaO. Black McKenzie Canyon tuff does not follow this pattern and has higher FeO than average calcalkaline rocks.

Figures 34 and 35 show that it is highly unlikely for black McKenzie Canyon tuff and white McKenzie Canyon tuff to be related. The large compositional gap justifies the existence of two separate magmas. The subtraction by fractional crystallization of plagioclase, olivine, hypersthene, augite, and magnetite from black McKenzie Canyon tuff cannot lower the TiO_2 enough to derive white McKenzie Canyon tuff. Ilmenite and amphibole were not detected in black McKenzie Canyon tuff; however, the vectors are added to show the possible effect on the composition.

Yoder (1979, p. 210) states that triangular variation diagrams serve to bring into focus groups of chemical constituents considered to dominate the course of magma evolution. However, by excluding other major

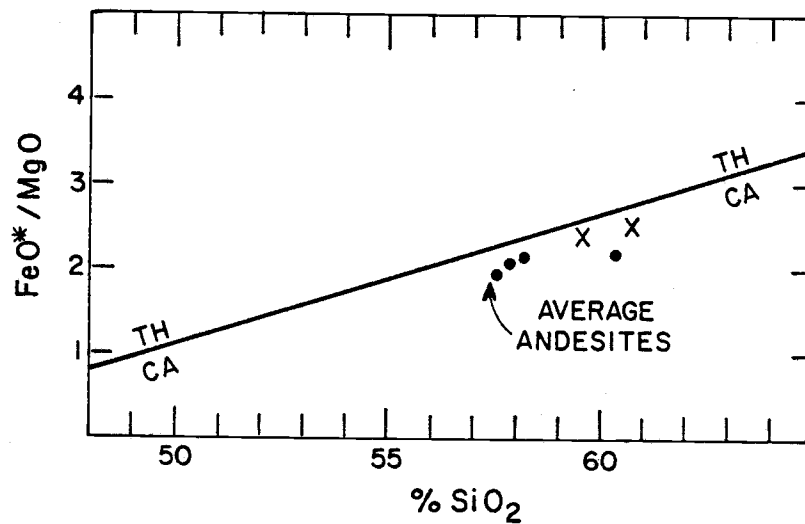


Figure 32. The definition of tholeiitic (TH) versus calcalkaline (CA) andesites. Dots indicate average andesite compositions (Gill, 1981, p. 8). X indicates average MCT andesite compositions (Table 3).
 *=total Fe

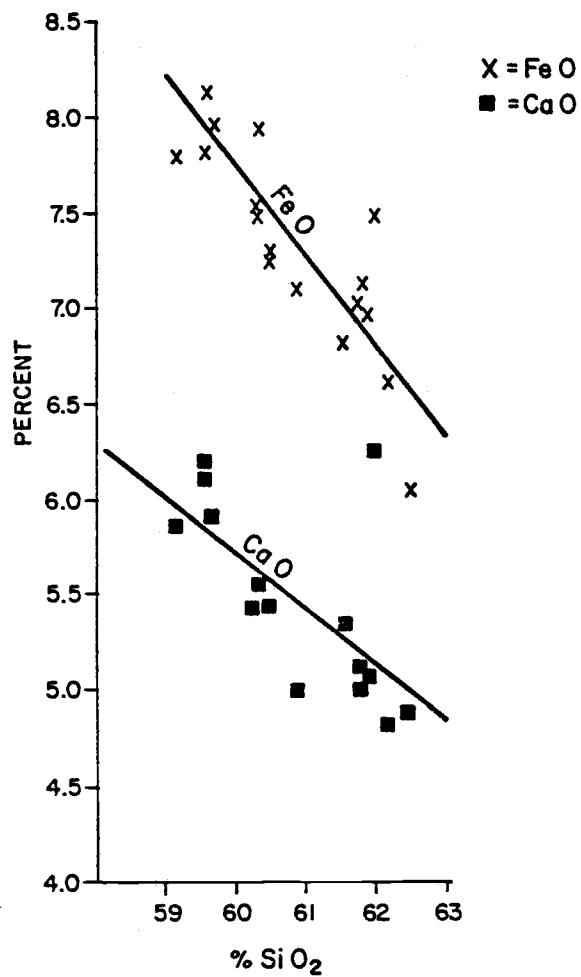


Figure 33. Relation of FeO and CaO versus SiO₂ in black andesite pumice of MCT. Gill (1981, p. 107) states that calcalkaline suites have Fe less than or equal to CaO.

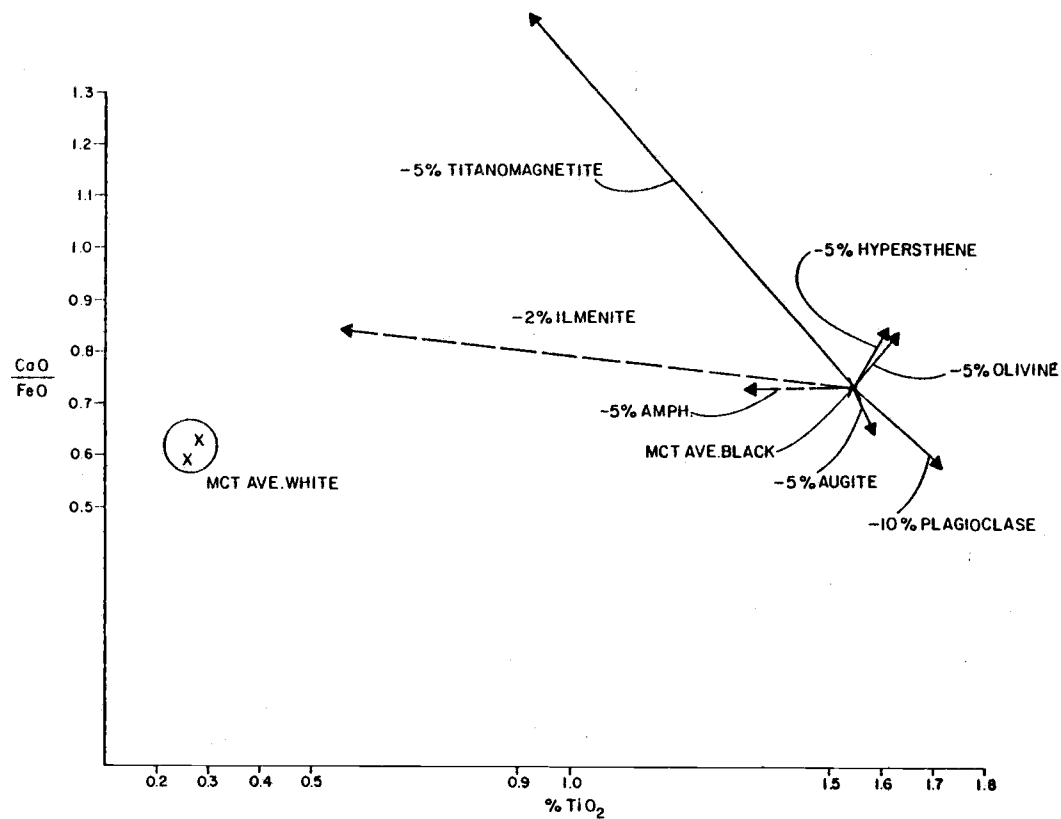


Figure 34. Arrows represent 10% fractional crystallization. It is highly unlikely that the sum of vectors or multiples of them will go from MCT-black to MCT-white pumice compositions. (pers. comm. Rich Conrey, 1984)

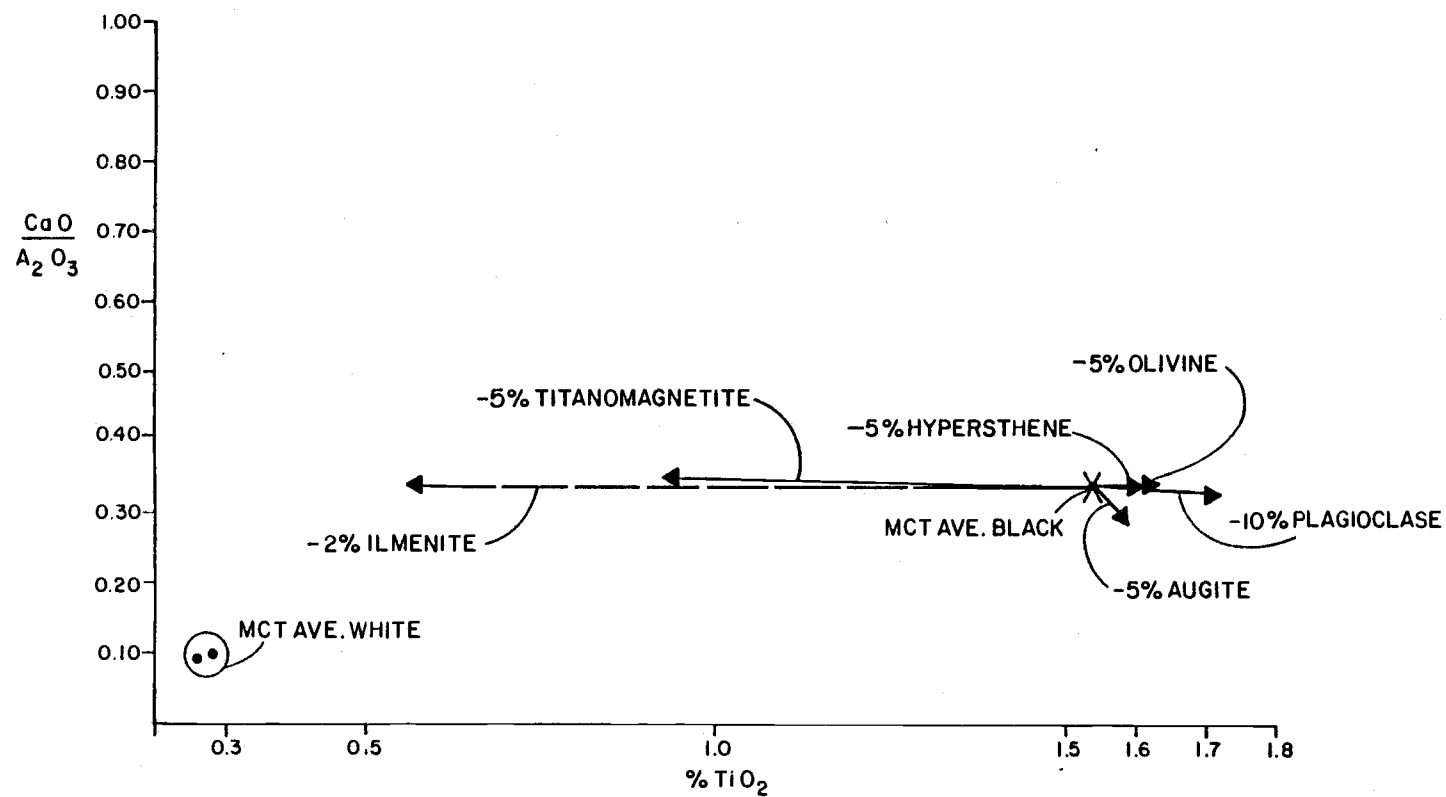


Figure 35. Arrows represent fractional crystallization of black MCT.

constituents the diagram shows only a partial picture. Where analytical error is relatively large in respect to total percentage of selected constituents, the recalculated percentages may plot in a wide scatter and give misleading trends.

The AMF diagram (Fig. 36) compares calcalkaline and tholeiitic divisions by Kuno (1968) and Irvine and Baragar (1971) with the rocks of this study. Kuno (1968) demonstrated that volcanic rocks of the calcalkalic rock series do not show iron enrichment. The Lower Bridge tuff and McKenzie Canyon tuff follow a similar chemical trend and fit well into the calcalkaline category, whereas Units 10 and 0 are richer in FeO and contain less MgO. Comparing McKenzie Canyon tuff and Lower Bridge tuff with the Bishop tuff, Carpenter Ridge, and Katmai, Figure 36 shows that the trend in McKenzie Canyon tuff is similar to the early and late flows of Katmai.

The plot of FeO-CaO-K₂O also shows a chemical similarity of McKenzie Canyon tuff with Katmai (Fig. 37). Compared to other ash-flow tuffs, McKenzie Canyon tuff spans a large compositional range.

Lateral and Vertical Chemical Variation

Plots of TiO₂ and FeO were made on a surface map to detect a horizontal variation in chemistry. The plots did not show any significant lateral chemical change

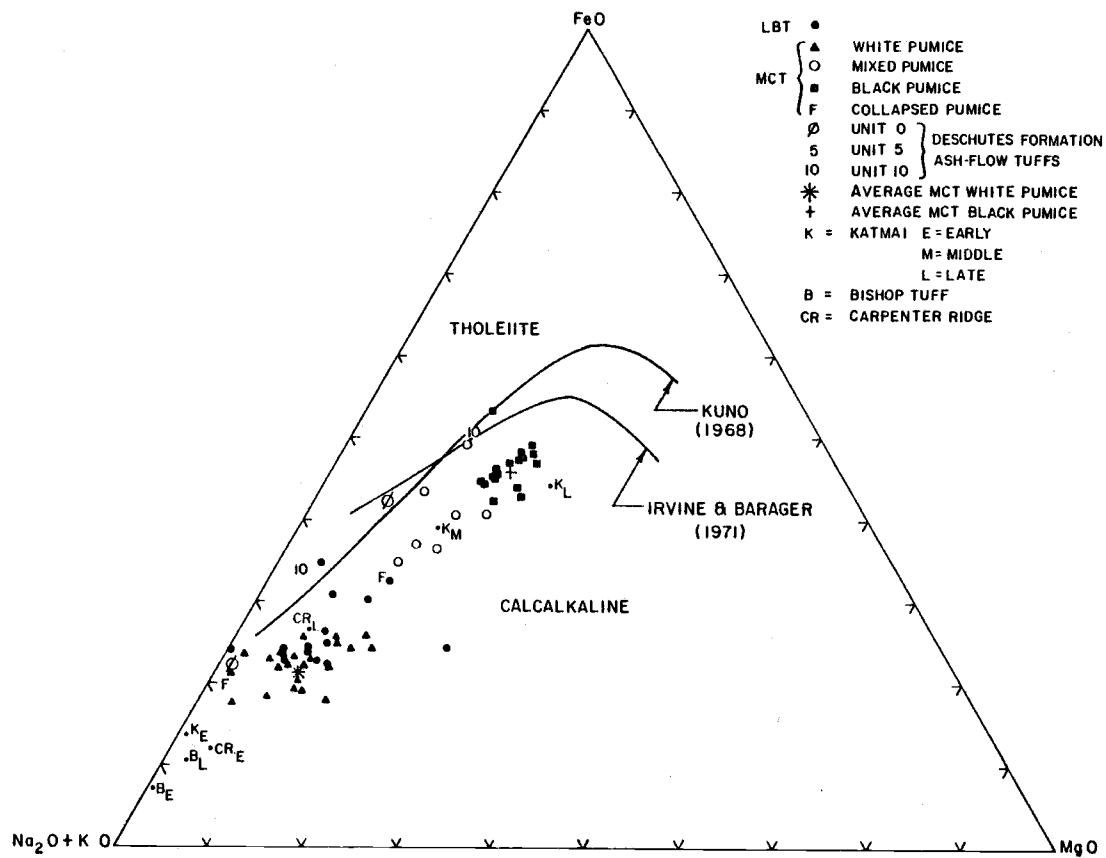


Figure 36. AMF diagram of oxide whole rock percentages by weight.

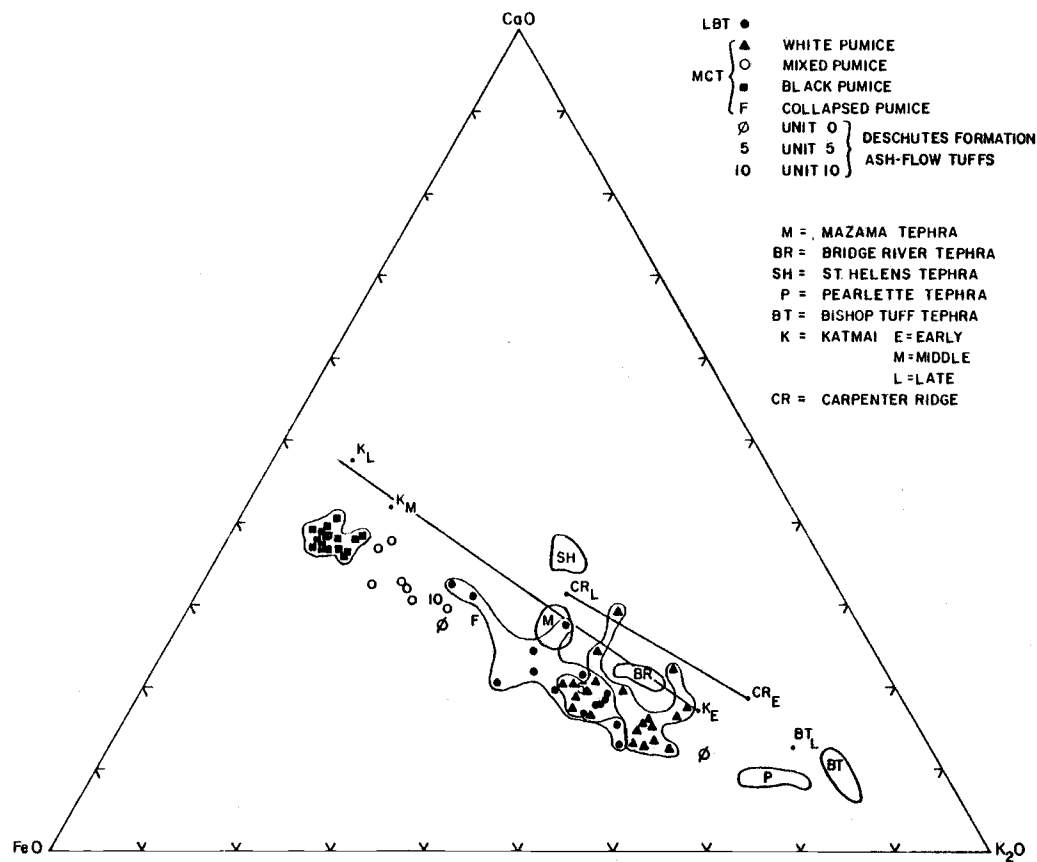


Figure 37. Plot of whole rock percentages.

probably because more than five data points (sample locations, Fig. 3) are needed to contour and produce useful information.

Pumice chemistries from single sample locations are plotted in their relative positions to identify a vertical variation within the units (Figs. 37-40). More samples are needed to find significant trends within the Lower Bridge tuff and McKenzie Canyon tuff; however, some generalities may be made based on these diagrams.

Lower Bridge tuff (Figs. 38 and 39) shows a distinct change in chemistries of the black and white pumice in the top part of the upper flow. A change in chemistries of the white pumices is not obvious between the upper and lower flows. K_2O and Na_2O for white McKenzie Canyon tuff pumices (Fig. 40 and 41) and Na_2O/K_2O (Fig. 40) show breaks between the lower silicic flows and the upper orange flow. Also K_2O in both figures shows a general decrease upward in the lower and upper flows. This may represent the tapping of deeper parts of the magma chamber. Black pumice (Fig. 40) on the average becomes more mafic.

Conclusion

Lower Bridge tuff is a high-K rhyolite that contains high-K dacite toward the top of the upper flow. Lower Bridge tuff regression lines do not parallel the "all

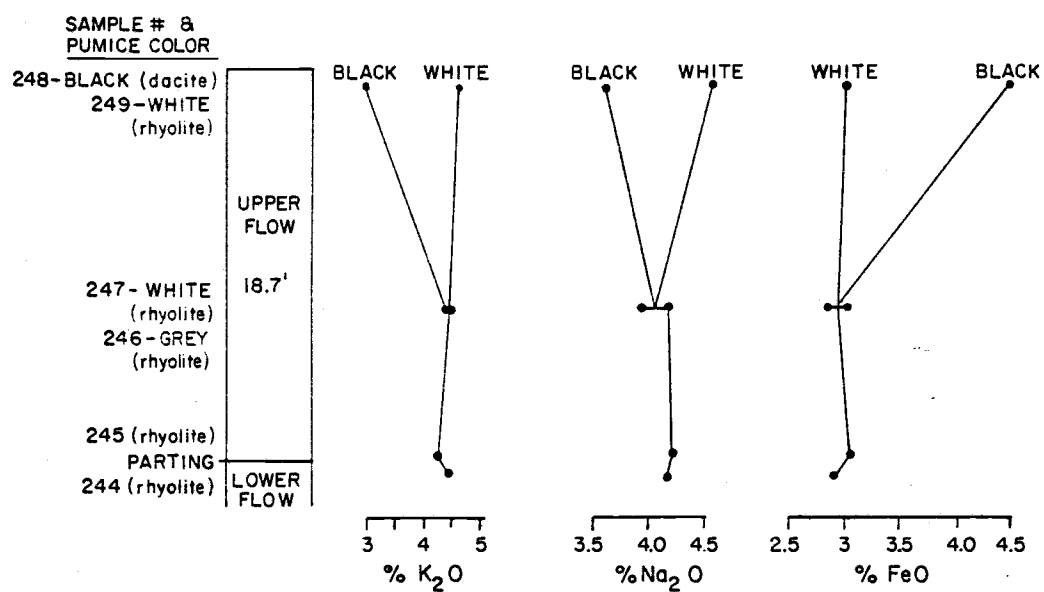


Figure 38. Vertical variation in chemistry, LBT at Deep Canyon sample location.

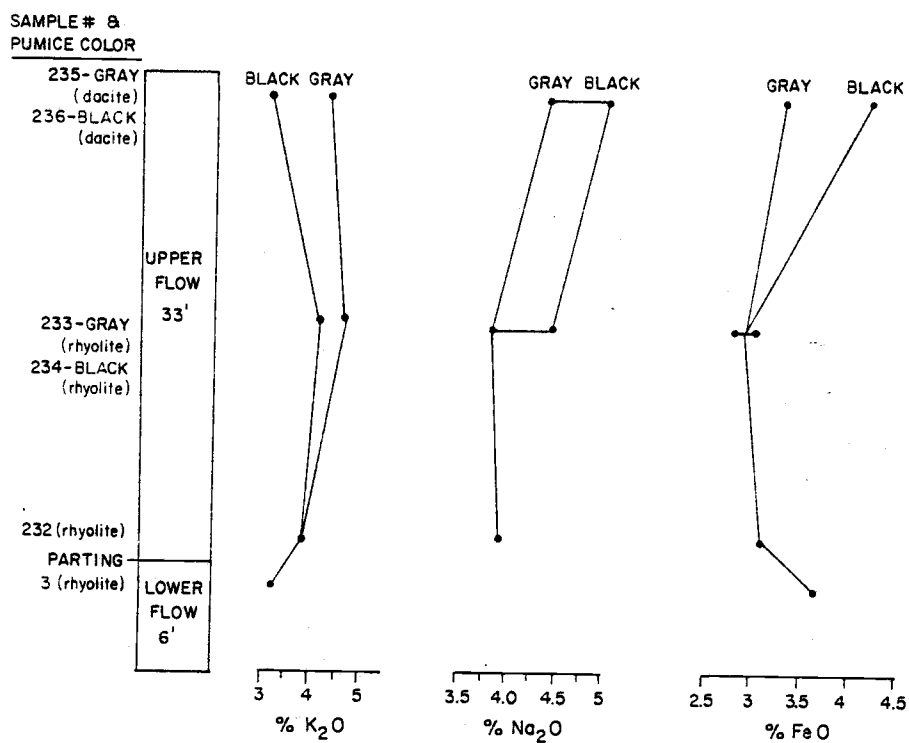


Figure 39. Vertical variation in chemistry, LBT at Deep Canyon and Deschutes River sample location.

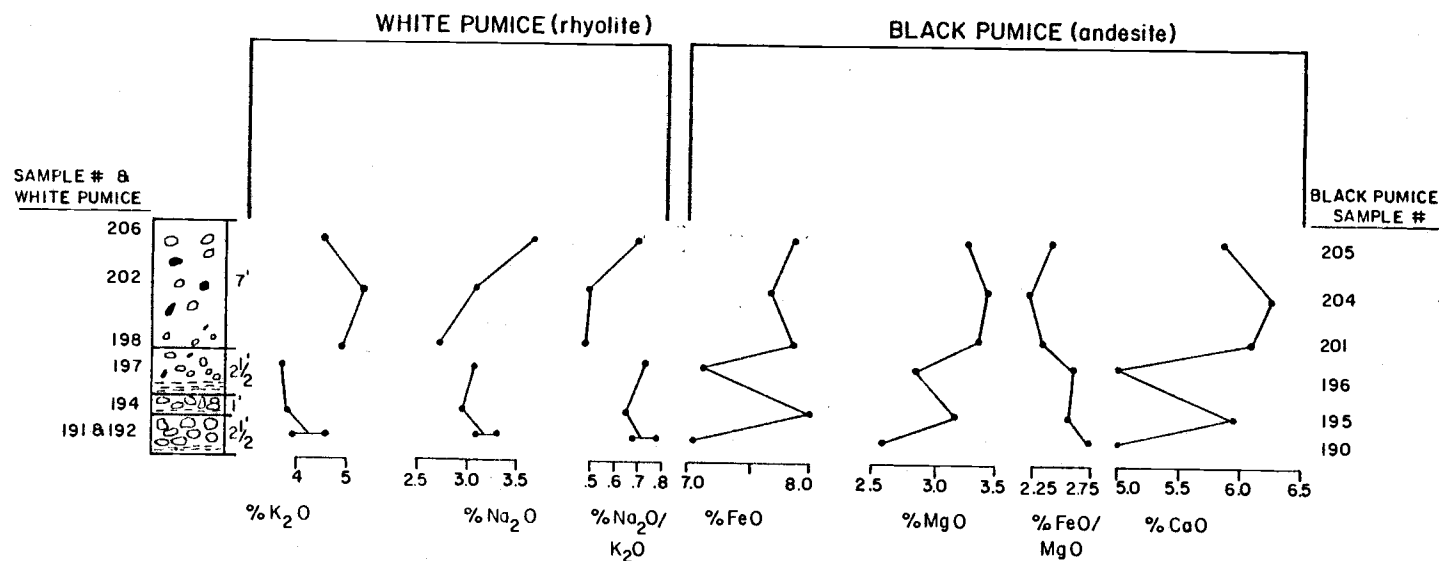


Figure 40. Vertical variation in chemistry, MCT at Squaw Creek Butte sample location.

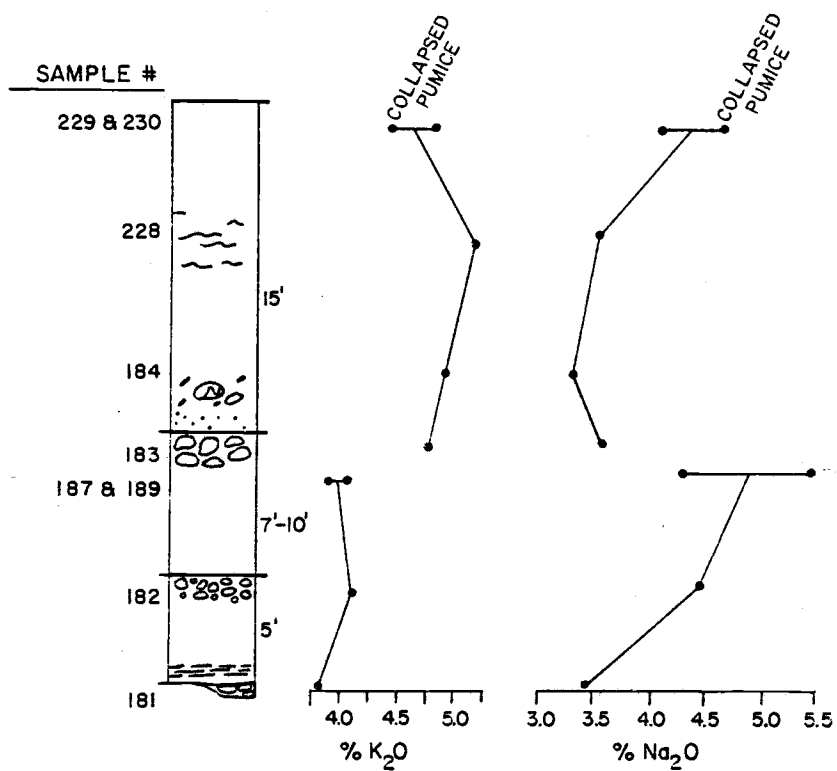


Figure 41. Vertical variation in chemistry of MCT white pumice at Deep Canyon and Lower Bridge sample location.

McKenzie Canyon tuff" regression lines and may suggest a different trend of evolution than that which produced the McKenzie Canyon tuff andesite. McKenzie Canyon tuff and Lower Bridge tuff rhyolite compositions are slightly different: Lower Bridge tuff has higher TiO_2 and possibly higher FeO .

The McKenzie Canyon tuff white pumice is a high-K rhyolite that shows little variation between the upper and lower flows. This supports the theory that the flows were derived from the same source. The vertical chemical variation that is present is a slight but significant break between K_2O and Na_2O at the boundary of the upper orange flow and a lower silicic flow. K_2O decreases slightly upwards (i.e., lower in the magma chamber) as expected.

Collapsed pumices have the same composition as McKenzie Canyon tuff pumice and were probably flattened during compaction and welding.

Black McKenzie Canyon tuff pumices do not have the scatter of points as found in the white McKenzie Canyon tuff pumices. The andesite becomes more mafic upwards and has high SiO_2 , TiO_2 , and FeO and medium K. Compared to an average andesite McKenzie Canyon tuff also has high NaO and low Al_2O_3 , MgO , and CaO . Conrey (pers. comm., 1984) suggests that this is a chemical signature characteristic of plagioclase (Al, Ca) and olivine (Mg)

fractionation in large quantities. Removal of Al, Ca, and Mg causes Si, Ti, Fe, Na, and K values to go up. White McKenzie Canyon tuff pumice regression lines never parallel black McKenzie Canyon tuff pumice lines, suggesting that the black and white pumice are chemically unrelated. Mixed McKenzie Canyon tuff pumices lie between rhyolitic and andesitic end members. A few homogeneous pumices also fall between the end members. These probably represent a small zone of mixing that formed between the magmas prior to eruption.

INTERPRETATION AND CONCLUSIONS

Table 7 summarizes the distinguishing features of the Lower Bridge tuff and McKenzie Canyon tuff. Any hypotheses proposed to explain the origin of McKenzie Canyon tuff and Lower Bridge tuff must account for the following facts:

- | | |
|-------------------------|---|
| A. Lower Bridge Tuff | Lower Bridge tuff is composed of two silicic flows with the upper one becoming more mafic toward the top. |
| B. McKenzie Bridge Tuff | <ol style="list-style-type: none"> 1. Mafic phenocryst abundances do not increase significantly from rhyolite (0.07%) to andesite (0.6%); both compositions are crystal poor. 2. Plagioclase reaction rims are not observed; they probably crystallized in a stable environment. 3. Phenocrysts are not mixed between flows: olivine is excluded from white pumices; plagioclase types are distinct for rhyolite and andesite pumices. |

Table 7. Characterization of the MCT and LBT.

	Lower Bridge Tuff	McKenzie Canyon Tuff
Physical Characteristics	<ol style="list-style-type: none"> 1. A multiple flow (2) simple cooling unit. 2. Commonly has a basal airfall with accretionary lapilli. 3. Nonresistant, easily weathered, lacks welding. 4. Contains light and dark gray pumice, dark gray pumice concentrated toward the top. 5. Massive, lacks grading. 	<ol style="list-style-type: none"> 1. The upper flow contains <u>mixed</u> pumice in addition to black and white. 2. A distinctive red color in the upper flow. 3. Crude columnar jointing occurs in the red resistant upper flow (cliff former). 4. Multiple flow compound cooling unit (up to four different flows). 5. Lower flows are silicic, light colored, nonresistant and contain white pumice and a few, if any, black or mixed pumice. 6. The upper flow is more extensive and resistant. 7. Elevation of lower flow surface decreases to the north. 8. Pumice and lithic clast size and thickness decrease to the north. 9. Massive, lacks grading.
Geochemistry of Pumice	<p>High-K rhyolite and dacite.</p> <p>Rhyolite has higher TiO_2 (0.55) than white MCT pumice (0.3).</p>	<p>White pumice: high-K rhyolite with lower TiO_2 than LBT.</p> <p>Black pumice: med-K, high TiO_2 and FeO andesite.</p>
Pumice	<p>Plagioclase (An 35-45, andesine)</p> <p>Augite</p> <p>Hypersthene</p> <p>Titaniferous pargasite</p> <p>Ilmenite</p> <p>Magnetite</p> <p>Apatite</p>	<p>Mineralogy of <u>Crystal rich</u> <u>Crystal poor</u></p> <p>White pumice: Plagioclase (An=29-31, oligoclase/andesine)</p> <p>Hypersthene</p> <p>Augite</p> <p>Magnetite</p> <p>Ilmenite</p> <p>Zircon</p> <p>Black pumice: Plagioclase (An=60-65, labradorite)</p> <p>Olivine (Fo⁸²)</p> <p>Augite</p> <p>Hypersthene</p> <p>Magnetite</p>
Stratigraphic Level	Often below MCT (tepiclastics) and above accretionary lapilli airfall.	
Paleomagnetism	Reverse	Reverse

4. The composition becomes more mafic upward in the upper flows and the degree of welding (i.e., temperature) increases upward in the upper flow.
5. A few mixed and black pumices are found in lower silicic flows.
6. A 7% SiO_2 compositional gap exists between rhyolite and andesite.
7. Homogeneously mixed fragments are scarce.
8. Figures 34 and 35 do not support a relation of rhyolitic and andesitic magmas by fractionation.
9. Figures 27 to 30 show that the white and black pumice compositions have divergent regression lines.

Many hypotheses have been proposed that speculate on existence, possible origins, and behaviors of the magma chamber. Two types of eruptive sequences are offered below which possibly explain the origin of Lower Bridge tuff and McKenzie Canyon tuff. One mechanism requires a small zoned magma chamber which repeatedly erupted and eventually tapped a deeper and more mafic composition magma, i.e., a zoned magma chamber. Alternatively, magmas from two separate sources, one rhyolite and one andesite, partly mixed during eruption and emplacement.

In the latter scenario eruption may have been caused by andesite injection into a rhyolitic magma chamber.

The Zoned Magma Chamber

All processes of differentiation in a single magma chamber lead toward compositional zonation. If eruptions tap the chamber from the top down, the most fractionated magma erupts first and the most mafic composition last (e.g., Lower Bridge tuff). An upward decrease in SiO_2 content of an ash-flow deposit often corresponds to an upward increase in crystal content, e.g., the Bandelier tuff, New Mexico (Smith and Bailey, 1966), the Paintbrush tuff, Nevada (Lipman, 1966), and flows at Crater Lake, Oregon (Williams, 1942). In addition to a compositional zonation the magma chamber may show an increase in temperature toward the bottom of the chamber (Bishop tuff, Hildreth, 1979, p. 46).

Compositional gaps in zoned pyroclastic eruptive units range from 2% to more than 10% SiO_2 : Valley of 10,000 Smokes (Fenner, 1950), Crater Lake, Oregon (Williams, 1942), Askja, Iceland (Smith, 1979), Bandelier tuff, New Mexico (Smith, 1979), Timber Mountain, Nevada (Christiansen and others, 1977), and the Yellowstone system (Smith, 1979). For reasons not yet clear, a silicic magma in the upper part of the chamber evolves independently from a lower less-silicic magma.

Hildreth (1981) described eight categories of zoned magma chambers producing compositionally zoned ash-flow tuffs. McKenzie Canyon tuff does not fit perfectly into any of the categories but has characteristics of two of them.

1) Rhyolite plus zoned intermediate magma with a large compositional gap. The Valley of 10,000 Smokes, Alaska, 1912 eruption is an example of a crystal-poor rhyolite (77% SiO_2) accompanied by a zoned crystal-rich intermediate (58-66% SiO_2) magma with a 10% gap in SiO_2 . Banded pumice in the Valley of 10,000 Smokes represents a commingling of magma from different levels during eruption. Evidence that the magmas commingled without mixing until eruption are: 1) the lack of complete mixing of the two compositions in the banded pumice, 2) the lack of exchange of phenocrysts between the two compositions.

McKenzie Canyon tuff does not have a crystal rich or highly zoned intermediate magma; andesite ranges from 59% to 62% SiO_2 . However, it does have a compositional gap of 7% SiO_2 . Banded pumice of McKenzie Canyon tuff does not show an exchange of phenocrysts between the two compositions or a relation of bulk chemistry (Figs. 27 to 30, 34 and 35). These observations and the lack of an increase in crystal content suggests that the two magmas are not related.

2) Zoned intermediate magmas commonly with a

compositional gap. Zoning ranges from rhyodacite to andesite and the SiO_2 gap may be up to 15%. Banded pumice is common in these eruptions and rarely indicates mafic injection into a silicic chamber. A large zoned magma chamber may never have the mafic component tapped, whereas a small chamber with a large eruption proves that compositional gaps are common e.g., Iceland (Sparks, 1977; Sigurdsson and Sparks, 1981). This is the most common type of large pyroclastic eruption from intermediate volcanoes of continental margins, e.g., Mazama. Crater Lake erupted 36 km^3 of rhyolite-rhyodacite and andesite to form a caldera; it displays a 10% SiO_2 gap. Banded pumices of mixed rhyodacite and basaltic andesite are present in which the rhyodacite is crystal poor (less than 10%) and the basaltic andesite is crystal rich (50-90%, Williams, 1942, p. 146). CaO versus SiO_2 plots of Crater Lake pumice (Smith, 1979, p. 12) show a strong relation between rhyodacite and andesite. McKenzie Canyon tuff and Mazama Ash of Crater Lake are very similar as far as the presence of a compositional gap and banded pumice but differ in crystal percent, relation of chemistry of the two compositions (Figs. 27 to 30), and mineralogy (Figs. 34 and 35).

Two Separate Magmas

Smith (1979, p. 8) states that a compositional gap is possible in a small-volume system as a result of mixing of two magmas from separate chambers. He also notes that banded pumice is common in calc-alkalic stratovolcanic systems. Hildreth (1981, p. 10158) states that only rarely does banded pumice warrant the inference that the mafic component had newly intruded the silicic magma chamber. He contends that a basaltic injection only occasionally is responsible for triggering an eruption; he is a proponent of a zoned magma chamber system. The data for McKenzie Canyon tuff indicate that the rhyolitic and andesitic magmas are not related and an unusual event probably brought them together.

The definition of magma mixing and the relation to banded pumice is germane to this discussion. Anderson (1975, p. 4-5) defines magma mixing as the development of a single uniform magma from the combination of two or more distinct magma compositions. Yoder (1973) contends that banded pumice is only a sign of contemporaneous extrusion of two magmas, not magma mixing. The presence of banded pumice only suggests that mafic magma was present and associated with the silicic magma. The lack of a uniform composition between the two magma types suggests the magmas were not in contact long.

Sparks and Sigurdsson (1977) proposed a mechanism of

triggering an eruption and of forming mixed mafic and silicic pumice. The injection of mafic magma into a silicic magma chamber causes convection, commingling of magmas, and vesiculation. The addition of more magma and vesiculation of the silicic magma increases the internal pressure and may cause an explosive eruption. Magma injection is not always evident if draw-down does not tap the intruding mafic magma. Anderson (1975, p. 4) describes banded pumice from Mt. Shasta and suggests that the eruption was initiated by a basalt injected into the magma chamber.

Conclusions

The lack of complete exposure of the ash-flow deposits and the source area(s) makes any conclusions speculative concerning the size, location and characteristics of the origin of the units. Data generated in this study is consistent with the hypothesis that the McKenzie Canyon tuff was derived from two separate magmas and Lower Bridge tuff was generated from a single zoned magma chamber. The only relation that can be made between McKenzie Canyon tuff and Lower Bridge tuff is that they originated from the same direction. Figures 27 to 30 show regression lines with different slopes indicating that the two chemistries are not related.

REFERENCES

- Allen, J. E., 1965, The Cascade Range volcano-tectonic depression of Oregon; Transactions of Lunar Geologic Field Conference: Oregon Dept. Geol. Min. Ind., p. 21-23.
- Anderson, A.T., 1976, Magma mixing: Petrological process and volcanological tool: Journal of Volcanology and Geothermal Research, v. 1, p. 3-33.
- Armstrong, R.L., Taylor, E.M., Hales, P.O., and Parker, D.J., 1975, K-Ar dates for volcanic rocks, central Cascade Range of Oregon: Isochron/West, no. 13, p. 5-10.
- Bloss, F.D., 1981, The spindle stage: principles and practices: Cambridge University Press, Cambridge, 340p.
- Boyle, A.C., 1921, Abstract of report to the chief engineer of the Union Pacific system on the diatomite deposit west of Terrebonne, in Stearns, H.T., 1930, Geology and water resources of the Middle Deschutes River Basin, Oregon: United States Geological Survey, Water-Supply Paper 637, p. 152-155.
- Chaney, R.W., 1938, The Deschutes flora of eastern Oregon in: Miocene and Pliocene Flora of Western North America: Carnegie Institute of Washington, Publication 476, p. 185-216.
- Chapin, C.E., and Elston, W.E., (eds), 1979, Ash-flow tuffs: U.S. Geol. Soc. Am., Spec. Pap. 180, 211p.
- Carmichael, I.S.E., Turner, F.J., and Verhoogan, J., 1974, Igneous Petrology, New York, McGraw-Hill Book Company, 739p.
- Christiansen, R.L., 1979, Cooling units and composite sheets in relation to caldera structure, in Chapin, C.E., and Elston, W.E., (eds.), Ash-flow tuffs: Geol. Soc. Am. Spec. Pap. 180 p. 29-42.

Christiansen, R.L., and others, 1977, Timber Mountain-Oasis Valley caldera complex of southern Nevada: Geol. Soc. of Am. Bull., v. 88, p. 943-959.

Conrey, Richard, 1983, Personal communication.

———, Richard, 1984, Volcanic stratigraphy of the Deschutes Formation, Green Ridge to Fly Creek, north-central Oregon: Master's Thesis, Oregon State University, Corvallis, Oregon, in preparation.

Cox, K.G., Bell, J.D., and Pankhurst, R.J., 1979, The interpretation of igneous rocks: London, Allen and Unwin, 450p.

Deer, W.A., Howie, R.A., and Zussman, J., 1967, Framework silicates, in Rock forming minerals: v. 4, Longman, Great Britain, 435p.

———, 1978, An introduction to the rock forming minerals: Longman, London, 528p.

Dill, Thomas, 1984, Volcanic stratigraphy along the Lower Metolius River, Jefferson County, central Oregon: Master's Thesis, Oregon State University, Corvallis, Oregon, in preparation.

Enlows, H.E., and Parker, D.J., 1972, Geochronology of the Clarno igneous activity in the Mitchell Quadrangle, Wheeler County, Oregon: Ore Bin, v. 34, p. 104-110.

Ewart, A., 1979. A review of the mineralogy and chemistry of Tertiary-Recent dacitic, latitic, rhyolitic, and related salic volcanic rocks, in Trondhjemites, dacites and related rocks: F. Barker, (ed), Elsevier. Amsterdam, p. 13-121.

———, Carmichael, I.S.E., Brown, F.H., and Green, D.C., 1971. Voluminous low temperature rhyolite magmas in New Zealand: Cont. Mineral. Petrol., v. 33, p. 128-144.

Farooqui, S.M., Beaulieu, J.D., Bunker, R.C., Stensland, D.E., and Thomas, R.E., 1981, Dalles Group: Neogene formations overlying the Columbia River Basalt Group in north-central Oregon: Oregon Geology, v. 43, no. 10, p. 131-140.

- Fenner, C.N., 1950, The chemical kinetics of the Katmai eruptions: American Journal of Science, v. 248, p. 593-627.
- Fisher, R.V., 1961, Proposed classification of volcanoclastic sediments and rocks: Geol. Soc. Am. Bull., v. 72, p. 1409-1414.
- , 1966, Rocks composed of volcanic fragments and their classification: Earth Sci. Rev., vol. 1, p. 287-298.
- Gill, J.B., 1981, Orogenic andesites and plate tectonics: Springer-Verlag, New York, 390p.
- Hales, P.O., 1975, Geology of the Green Ridge area, Whitewater River Quadrangle, Oregon: Master's Thesis, Oregon State University, Corvallis, Oregon, 90p.
- Hayman, G.A., 1983, Geology of a part of the Eagle Butte and Gateway Quadrangle East of the Deschutes River, Jefferson County, Oregon: Master's Thesis, Oregon State University, Corvallis, Oregon, 97p.
- Hewitt, S.L., 1970, Geology of the Fly Creek Quadrangle and the north half of Round Butte Dam Quadrangle, Oregon: Master's Thesis, Oregon State University, Corvallis, Oregon, 69p.
- Hildreth, West, 1979, The Bishop Tuff; evidence for the origin of compositional zonation in silicic magma chambers, in Chapin, C.E., and Elston, W.E., (eds.), Ash-flow tuffs: Geol. Soc. Am. Spec. Pap. 180.
- , 1981, Gradients in silicic magma chambers: implications for lithospheric magmatism: Jour. of Geophy. Res., v. 86, no. B11, p. 10153-10192.
- Hodge, E.T., 1928, Framework of the Cascade Range in Oregon: Pan-American Geologist, v. 49, p. 341-357.
- , 1940, Geology of the Madras Quadrangle: Oregon State Monographs, in Studies in Geology: no. 1. Oregon State Agricultural College, Corvallis, Oregon, 1 sheet.

- Hodge, E.T., 1942, Geology of north central Oregon: Oregon State Monographs, in Studies in Geology no. 3. Oregon State Agricultural College, Corvallis, Oregon, 76p.
- Hutchison, C.S., 1974, Laboratory handbook of petrographic techniques, Wiley & Sons, New York, 527p.
- Irvine, T.N., and Baragar, W.R.A., 1971, Guide to the chemical classification of the common volcanic rocks: Can. Jour. Earth Sci., v. 8, p. 523-548.
- Jay, J.B., 1982, The geology and stratigraphy of the Tertiary volcanic and volcanoclastic rocks, with special emphasis on the Deschutes Formation, from Lake Simtustus to Madras in central Oregon: Master's Thesis, Oregon State University, Corvallis, Oregon, 119p.
- Knowles, Charles, 1983, Personal communication.
- Koch, A.J., 1970, Stratigraphy, petrology and distribution of Quaternary pumice deposits of the San Cristobal Group, Guatemala City area, Guatemala: Ph.D. dissertation, University of Washington, Seattle.
- Kuno, H., 1968, Differentiation of basalt magmas, in Basalts: The Poldervaart Treatise on rocks of basaltic composition: H. H. Hess and A. Poldervaart, (eds.), Interscience, John Wiley and Sons, N.Y., p. 623-688.
- Leake, B.E., 1968a, A catalog of analyzed calciferous and subcalciferous amphiboles together with their nomenclature and associated minerals: Geol. Soc. Am., Spec. Paper 98, 210p.
- , 1968b, Optical properties and composition in the orthopyroxene series: The Mineralogical Mag., v. 36, p. 745-747.
- Lipman, P.W., 1971, Iron-titanium oxide phenocrysts in compositionally zoned ash-flow sheets from southern Nevada: Jour. of Geol. v. 79, p. 438-456.
- , Christiansen, R.L., and O'Connor, J.T., 1966, A compositionally zoned ash flow sheet in southern Nevada: U.S. Geol. Sur. Prof. Pap. 524-F, 47p.

- Macdonald, G.A., and Alcaraz, A., 1956, Nuee ardentes of the 1948-1953 eruption of Hibok Hibok: Bulletin Volcanologique, v. 18, p. 169-178.
- McBirney, A., Sutter, J.F., Nasland, H.R., Sutton, K.G., and White, C.M., 1974, Episodic volcanism in the central Oregon Cascade Range: Geology 2, p. 585-589.
- _____, and White, C.M., 1982, The Cascade Province, in Thorpe, R.S., (ed.), Andesites: orogenic andesites and related rocks: John Wiley, New York, p. 115-135.
- McDannel, Angela, 1984, Master's Thesis, Oregon State University, Corvallis, Oregon, in preparation.
- McKee, E.H., Swanson, D.A., and Wright, T.L., 1977, Duration and volume of Columbia River Basalt volcanism, Washington, Oregon, and Idaho: Geol. Soc. Am. Bull., v. 84, p. 537-546.
- Moore, J.G., and Peck, D.L., 1962, Accretionary lapilli in volcanic rocks of the western continental United States: Jour. of Geol., v. 70, p. 182-193.
- Oregon Community Profiles: Oregon Department of Economic Development, Salem, 1977.
- Peacock, M.A., 1931, Classification of igneous rock series, Jour. of Geol., v. 39, p. 54-67.
- Peterson, D.W., 1970, Ash-flow deposits - their character, origin, and significance: Jour. of Geol. Ed., v. 18, p. 66-76.
- Peterson, N.V., Groh, E.A., Taylor, E.M., and Stensland, D.E., 1976, Geology and mineral resources of Deschutes County, Oregon: Oregon Department of Geology and Mineral Industries, Bull. 89, 66p.
- Robinson, P.T., 1975, Reconnaissance geologic map of the John Day Formation in the southwest part of the Blue Mountains and adjacent area, north-central Oregon: U.S. Geol. Sur. Misc. Investigation Series Map I-872.
- _____, and Stensland, D.E., 1979, Geologic map of the Smith Rock Area, Jefferson, Deschutes, and Crook Counties, Oregon: U.S. Geol. Sur. Misc. Investigations Series Map I-1142.

- Robinson, P.T., and Brem, G.F., 1981, Guide to geologic field trip between Kimberly and Bend, Oregon with emphasis on the John Day Formation, in D.A. Johnson and J. Donnelly-Nolan, (eds.), Guides to some volcanic terrains in Washington, Idaho, Oregon, and northern California, eds., U.S. Geol. Sur. Cir. 838, p. 29-54.
- Ross, C.S., and Smith, R.L., 1961, Ash-flow tuffs: their origin, geologic relations and identification: U.S. Geol. Surv. Prof. Pap. 366.
- Russel, I.C., 1905, Preliminary Report on the geology and water resources of central Oregon: U.S. Geol. Sur. Bull. 252, 138p.
- Schairer, J.F., Smith, J.R., and Charyes, F., 1956, Refractive indices of plagioclase glasses: Annual Rep., Director Geophys. Lab., Carnegie Institute, Washington, Year Book, no. 55, p. 195.
- Schmid, R., 1981, Descriptive nomenclature and classification of pyroclastic deposits and fragments: recommendations of the IUGS subcommission on the systematics of igneous rocks: Geol., v. 9, p. 41-43.
- Sheridan, M.F., 1971, Particle-size characteristics of pyroclastic tuffs, Jour. of Geophy. Res., v. 76, no. 23, p. 5627-5634.
- _____, 1979, Emplacement of pyroclastic flows: a review, in Chapin, C.E., and Elston, W.E., (eds.), Ash-flow tuffs: Geol. Soc. Am. Spec. Pap. 180, p. 125-136.
- Sigurdsson, H., and Sparks, R.S.J., 1981, Petrology of rhyolitic and mixed magma ejecta from the 1875 eruption of Askja, Iceland: Jour. Petrol., v. 22, p. 41-81.
- Smith, A.L., and Roobol, M.J., 1982, Andesitic pyroclastic flows, in Thorpe, R.S., (ed.), Andesites: orogenic andesites and related rocks; John Wiley, New York, p. 415-433.
- Smith, Gary, 1984, Ph.D. dissertation, Oregon State University, Corvallis, Oregon, in preparation.
- _____, 1983, Personal communication.

Smith, Gary and Snee, Laurence 1984, Revised stratigraphy of the Deschutes basin, Oregon: implications for the Neogene development of the central Oregon Cascades, A.G.U. abstract, San Francisco, 1983.

Smith, R.L. 1960a, Ash flows: Geol. Soc. Am. Bull. 71, p. 795-842.

———, 1960b, Zones and zonal variations in welded ash flows: U.S. Geol. Sur. Prof. Pap. 354-F, p. 149-159.

———, and Bailey, R.A., 1966, The Bandelier Tuff, A Study of ash-flow eruption cycles from zoned magma chambers: Bull. Volcanologique, v. 29, p. 83-104.

———, 1979, Ash-flow magmatism, Geol. Soc. Am. Spec. Pap. 180, p. 5-27.

Sparks, R.S.J., 1976, Grain size variations in ignimbrites and implications for the transport of pyroclastic flows: Sedimentology, v. 23, p. 147-188.

———, 1978, Gas release rates from pyroclastic flows: an assessment of the role of fluidization in their emplacement: Bull. Volcanologique.

———, Sigurdsson, H., and Wilson, L., 1977, Magma mixing: a mechanism for triggering acid explosive eruptions: Nature, v. 267, p. 315-318.

———, and Walker, G.P.L., 1973, The ground surge deposit: a third type of pyroclastic rock: Nature, Physical Science v. 241, p. 62-64.

———, and Wilson, L., 1976, A model for the formation of ignimbrites by gravitational column collapse: J. Geol. Soc., Lon. 132, p. 441-451.

———, Wilson, L., and Hulme, G., 1978, Theoretical modeling of the generation, movement, and emplacement of pyroclastic flows by column collapse: J. Geophys. Res., v. 83, no. 84, p. 1727-1739.

Stearns, H.T., 1930, Geology and water resources of the Middle Deschutes River Basin, Oregon: U.S. Geol. Sur., Water-Supply Paper 637, p. 125-220.

- Stensland, D.E., 1970, Geology of part of the northern half of the Bend Quadrangle, Jefferson and Deschutes Counties, Oregon: Master's Thesis, Oregon State University, Corvallis, Oregon, 118p.
- Taylor, G.A., 1954, Volcanological observations of Mount Lamington, 29th May 1952: Bull. Volcanologique, v. 15, p. 81-97.
- _____, 1958, The 1951 eruption of Mt. Lamington, Papua: Aust. Dep. Nat. Devp. Bull., no. 38, 117p.
- Taylor, E.M., 1977, the Clarno Formation - A record of Early Tertiary volcanism in central Oregon: Geol. Soc. Amer. Abstracts with Programs, v. 9, p. 768.
- _____, 1978, Personal communication.
- _____, 1978, Field geology of S.W. Broken Top Quadrangle, Oregon: Oregon Dept. of Geol. and Min. Ind. Spec. Pap., no. 2, 50p.
- _____, 1980, Volcanic and volcanoclastic rocks on the east flank of the central Cascade Range to the Deschutes River, Oregon, in Geologic Field Trips in Western Oregon and Southwestern Washington: Oregon Department of Geology and Mineral Industries Bulletin 101, p. 1-7.
- _____, 1981, Central High Cascade roadside geology, in Johnson, D.A., and Donnelly-Nolan, J., (eds.), Guides to some volcanic terrains in Washington, Idaho, Oregon, and northern California, U.S. Geol. Sur. Cir., 838, p. 55-83.
- _____, 1981, Personal communication.
- _____, 1984, Personal communication.
- Walker, G.P., 1971, Grain-size characteristics of pyroclastic deposits: Jour. of Geol., v. 79, p. 696-714.
- Waters, A.C., 1961, Stratigraphic and lithologic variations in the Columbia River basalt: Am. Jour. Sci., v. 259, p. 583-611.
- _____, 1968, Reconnaissance geologic map of the Madras quadrangle, Jefferson and Wasco Counties, Oregon: U.S. Geol. Sur. Misc. Investigations Map I-555.

- Wendland, David, 1984, Master's Thesis, Oregon State University, Corvallis, Oregon, in preparation.
- Williams, Howel, 1957, A geologic map of the Bend quadrangle, Oregon, and a reconnaissance geologic map of the central portion of the High Cascade Mountains: Oregon Department of Geology and Mineral Industries Map with text.
- , 1942, The geology of Crater Lake National Park, Oregon, with a reconnaissance of the Cascade Range southward to Mount Shasta: Carnegie Institute of Washington Publication 540, 162p.
- , 1960, Volcanic history of the Guatemalan Highlands: Univ. of Calif. Pub. in Geol. Sci, v. 38, p. 1-86.
- , and McBirney, A.R., 1979, Volcanology: Freeman, Cooper and Co., San Francisco, 397p.
- Williams, I.A., 1924, Geology of the Pelton dam site, Oregon. Unpublished report in the files of the Federal Power Commission. in Stearns, H.T., 1930, Geology and water resources of the Middle Deschutes River Basin, Oregon: U.S. Geol. Surv. Water-Supply Paper 637, p. 132, 137.
- Wohletz, K.H., and Sheridan, M.F., 1979, A model of pyroclastic surge, in Chapin, C.E., and Elston, W.E., (eds.), Ash-flow tuffs: Geol. Soc. Am. Spec. Pap. 180 p. 177-194.
- Yoder, H.S. 1973, Contemporaneous basaltic and rhyolitic magmas: Am. Mineral, v. 58, 153-171.
- , (ed.), 1979, The evolution of the igneous rocks, Princeton University Press, New Jersey, 588p.
- Yogodzinski, Eugene, 1984, Master's Thesis, Oregon State University, Corvallis, Oregon, in preparation.

APPENDIX

Appendix 1. Microprobe Analyses

SAMPLE	Amphibole Microprobe Analyses (Weight %)						
	234	234	235	235			
	GR. 1	GR. 2	GR. 1	GR. 2	236	551	579
SiO ₂	41.32	40.12	39.88	39.17	41.14	40.69	39.96
Al ₂ O ₃	9.95	10.02	10.15	10.11	9.82	12.09	12.83
CaO	10.72	10.67	10.70	11.00	10.73	11.85	12.07
TiO ₂	4.16	4.09	3.99	4.13	4.04	2.98	4.05
MnO	0.16	0.22	0.14	0.15	0.22	0.70	-
MgO	14.56	14.35	13.98	14.52	13.82	14.34	12.92
FeO*	12.17	12.67	12.54	12.23	13.33	12.04	13.77
Na ₂ O	<u>2.92</u>	<u>2.83</u>	<u>2.80</u>	<u>2.82</u>	<u>2.77</u>	<u>2.45</u>	<u>2.28</u>
Total	<u>95.97</u>	<u>94.97</u>	<u>94.17</u>	<u>94.13</u>	<u>95.86</u>	<u>97.14</u>	<u>97.88</u>

Number of Ions on the Basis of 24 Oxygens

Si	6.4881	6.4002	6.4103	6.3121	6.5036	5.99	5.99
Al	1.8420	1.8830	1.9219	1.9201	1.8301	2.10	2.26
Ca	1.8037	1.8233	1.8421	1.8994	1.8162	1.87	1.94
Ti	0.4916	0.4904	0.4817	0.5001	0.4800	0.33	0.46
Mn	0.0215	0.0302	0.0194	0.0203	0.0290	0.09	0.00
Mg	3.4095	3.4129	3.3502	3.4880	3.2560	3.15	2.91
Fe	1.5985	1.6894	1.6848	1.6473	1.7614	1.34	1.64
Na	0.8876	0.8758	0.8723	0.8798	0.8487	0.70	0.66

234 gr. 1 and 2. Middle of upper flow LBT (Figure 37), titaniferous pargasite.

235 gr. 1 and 2. Top of upper flow LBT (Figure 37), titaniferous pargasite.

236 Top of upper flow LBT, titaniferous pargasite.

551 Titaniferous ferri-ferroan pargasite. Andesite. (Leake, 1968)

579 Titaniferous ferri-ferroan pargasite. Volcanic bomb. (Leake, 1968)

$$*FeO = \text{Total iron} = FeO + 0.9 \times Fe_2O_3$$

Appendix 1. Microprobe Analysis continued

SAMPLE	Orthopyroxene Microprobe Analyses				
	194 gr. 1	194 gr. 2	206	195	196
SiO ₂	48.86	48.56	49.26	50.88	51.28
Al ₂ O ₃	2.06	1.54	1.25	1.14	1.39
CaO	1.41	1.42	1.44	0.97	1.43
TiO ₂	0.36	0.42	0.27	0.19	0.33
MnO	1.01	1.01	2.33	1.09	1.33
MgO	25.18	25.13	23.13	21.29	25.47
FeO*	18.50	19.06	22.19	25.03	19.63
Na ₂ O	<u>0.00</u>	<u>0.00</u>	<u>0.00</u>	<u>0.00</u>	<u>0.00</u>
Total	<u>97.38</u>	<u>97.14</u>	<u>99.87</u>	<u>100.59</u>	<u>100.84</u>

Number of Ions on the Basis of 6 Oxygens

Si	1.8638	1.8645	1.8742	1.9237	1.8929
Al	0.0926	0.0698	0.0559	0.0509	0.0604
Ca	0.0576	0.0583	0.0587	0.0393	0.0566
Ti	0.0103	0.0122	0.0077	0.0053	0.0090
Mn	0.0325	0.0328	0.0750	0.0348	0.0414
Mg	1.4322	1.4384	1.3123	1.1999	1.4014
Fe	0.5902	0.6119	0.7059	0.7913	0.6058
Na	0.0000	0.0000	0.0000	0.0000	0.0000

194 gr. 1 and 2. White pumice, lower flow MCT, intergrowths with cpx., hypersthene.

206 White pumice upper flow MCT, single crystal from pumice lump, ferro-hypersthene.

195 Black pumice, lower flow MCT, single crystal from pumice lump, ferro-hypersthene.

196 Black pumice, lower flow MCT, intergrowth with cpx., hypersthene.

* FeO = Total iron = FeO + Fe₂O₃

Appendix 1. Microprobe Analyses Continued

SAMPLE	Clinopyroxene Microprobe Analyses				
	3	234	191	194 gr. 1	194 gr. 2
SiO ₂	50.22	50.11	48.76	47.29	46.39
Al ₂ O ₃	1.59	1.79	1.56	2.53	2.71
CaO	19.16	19.42	18.85	19.40	19.93
TiO ₂	0.40	0.52	0.36	0.85	0.84
MnO	1.15	0.59	1.01	0.46	0.53
MgO	14.15	15.52	12.57	15.05	15.17
FeO*	11.97	10.10	15.17	9.64	9.88
Na ₂ O	0.36	0.35	0.27	0.38	0.40
Total	99.01	98.41	98.54	95.60	95.85

Number of Ions on the Basis of 6 Oxygens

Si	1.9214	1.9101	1.9053	1.8621	1.8321
Al	0.0718	0.0805	0.0718	0.1173	0.1263
Ca	0.7852	0.7930	0.7890	0.8182	0.8432
Ti	0.0114	0.0148	0.0105	0.0252	0.0249
Mn	0.0374	0.0192	0.0332	0.0152	0.0175
Mg	0.8073	0.8821	0.7319	0.8837	0.8935
Fe	0.3830	0.3217	0.4957	0.3173	0.3264
Na	0.0268	0.0261	0.0201	0.0293	0.0307

134 Lower flow LBT, augite. 234 Upper flow LBT, augite.

191 White pumice, lower flow MCT, augite.

194 gr. 1 and 2. White pumice, lower flow MCT, augite.

* FeO = Total iron = FeO + Fe₂O₃

Appendix 1. Microprobe Analyses Continued

SAMPLE	Clinopyroxene Microprobe Analyses				
	206 gr. 1	206 gr. 2	196	205	201
SiO ₂	48.05	48.91	50.41	48.38	49.42
Al ₂ O ₃	2.22	2.15	2.69	2.91	3.15
CaO	19.21	19.64	19.20	19.76	19.39
TiO ₂	0.54	0.52	0.62	0.85	0.98
MnO	0.64	0.61	0.74	0.34	0.43
MgO	13.69	14.77	15.39	15.74	15.54
FeO*	13.28	11.87	10.58	9.59	9.76
Na ₂ O	<u>0.39</u>	<u>0.34</u>	<u>0.45</u>	<u>0.29</u>	<u>0.40</u>
Total	<u>98.02</u>	<u>98.82</u>	<u>100.08</u>	<u>97.87</u>	<u>99.07</u>

Number of Ions on the Basis of 6 Oxygens

Si	1.8740	1.8782	1.8912	1.8557	1.8680
Al	0.1020	0.0973	0.1189	0.1316	0.1404
Ca	0.8027	0.8079	0.7717	0.8121	0.7853
Ti	0.0157	0.0148	0.0173	0.0246	0.0277
Mn	0.0211	0.0199	0.0234	0.0109	0.0136
Mg	0.7956	0.8458	0.8605	0.9002	0.8758
Fe	0.4329	0.3812	0.3320	0.3075	0.3084
Na	0.0293	0.0256	0.0325	0.0216	0.0292

206 gr. 1 and 2. White pumice, upper flow MCT, augite.

196 Black pumice, lower flow MCT, augite.

201 Black pumice, upper flow MCT, augite.

205 Black pumice, upper flow MCT, augite.

* FeO = Total iron - FeO + Fe₂O₃

Appendix 1. Microprobe Analyses Continued

<u>Olivine Microprobe Analyses</u>			
<u>SAMPLE</u>	<u>201</u>	<u>205</u>	<u>2</u>
SiO ₂	38.31	36.53	39.87
MgO	44.72	44.35	45.38
FeO*	<u>16.76</u>	<u>17.94</u>	<u>14.06</u>
Total	<u>99.78</u>	<u>98.82</u>	<u>99.31</u>

<u>Number of Ions on the Basis of 4 Oxygens</u>		
Si	0.9741	0.9477
Mg	1.6953	1.7154
Fe	0.3563	0.3891

<u>Atomic Ratios</u>			
Mg	82.6	81.5	86.0
Fe ⁺² **	17.4	18.5	14.0

201 Black pumice, upper flow MCT, chrysolite.

205 Black pumice, upper flow MCT, chrysolite.

2 Chrysolite (Deer Howie and Zussman, 1978, p. 4).

*FeO = Total iron = FeO + Fe₂O₃.

**The amount of Fe₂O₃ is small in olivine and is included in with Fe⁺² for MCT samples.

Appendix 2. Major element geochemistry obtained by XRF and AAS.

Sample	3	151	232	233	234	235	236
SiO ₂	71.40	70.70	70.20	70.20	70.30	67.60	66.00
Al ₂ O ₃	15.00	15.40	16.50	14.54	15.55	15.36	16.22
FeO	3.65	3.12	3.14	2.85	3.03	3.33	4.20
MgO	0.49	0.78	1.10	1.24	0.72	1.34	1.65
CaO	1.80	1.83	1.72	1.13	1.45	2.90	3.29
Na ₂ O	3.15	2.83	3.89	3.68	4.53	4.38	4.97
K ₂ O	3.23	3.40	3.81	4.67	4.22	4.31	3.13
TiO ₂	<u>0.64</u>	<u>0.53</u>	<u>0.58</u>	<u>0.53</u>	<u>0.56</u>	<u>0.66</u>	<u>0.85</u>
Total	99.29	98.58	100.90	98.84	100.36	99.88	100.30

- 3 Rhyolite, white pumice, from pumice-rich zone at top of lower flow, LBT, Deep Canyon and Deschutes River. (SW 1/4, SE 1/4, Sec. 9, T14S, R12E)
- 151 Rhyolite, white pumice, from pumice-rich zone, 12' from base of 37' thick unit, in Squaw Creek, south of entrance to Deschutes River. (SE 1/4, NW 1/4, Sec. 18, T13S, R12E)
- 232 Rhyolite, gray pumice, from base of upper flow, LBT, Deep Canyon and Deschutes River. (SW 1/4, SE 1/4, Sec. 9, T14S, R12E)
- 233 Rhyolite, gray pumice, middle of upper flow, LBT, Deep Canyon and Deschutes River. (SW 1/4, SE 1/4, Sec. 9, T14S, R12E)
- 234 Rhyolite, black pumice, middle of upper flow, LBT, Deep Canyon and Deschutes River. (SW 1/4, SE 1/4, Sec. 9, T14S, R12E)
- 235 Dacite, gray pumice, top of upper flow, LBT, Deep Canyon and Deschutes River. (SW 1/4, SE 1/4, Sec. 9, T14S, R12E)
- 236 Dacite, black pumice, top of upper flow, LBT, Deep Canyon and Deschutes River. (SW 1/4, SE 1/4, Sec. 9, T14S, R12E)

Appendix 2. Major element geochemistry obtained by XRF and AAS.
Continued

Sample	238	239	244	245	246	247	248
SiO ₂	68.60	71.10	70.70	70.20	70.70	72.10	64.70
Al ₂ O ₃	16.13	16.37	14.78	15.32	14.82	15.45	17.05
FeO	2.96	2.65	2.85	3.03	2.93	2.73	4.47
MgO	2.90	1.37	0.00	1.10	0.80	0.80	1.78
CaO	2.02	1.63	1.63	2.00	1.61	1.30	3.55
Na ₂ O	3.47	3.65	4.35	4.41	4.35	3.91	4.62
K ₂ O	3.21	4.23	4.46	4.28	4.44	4.49	2.91
TiO ₂	<u>0.54</u>	<u>0.41</u>	<u>0.53</u>	<u>0.57</u>	<u>0.54</u>	<u>0.52</u>	<u>0.88</u>
Total	99.88	101.40	99.30	100.91	100.20	101.30	100.40

- 238 Dacite, white pumice, base of flow, LBT, Deschutes River. (NW 1/4, SW 1/4, Sec. 21, T13S, R12E)
- 239 Rhyolite, gray pumice, top of flow, LBT, Deschutes River. (NW 1/4, SW 1/4, Sec. 21, T13S, R12E)
- 244 Rhyolite, white pumice, top of lower flow, LBT, southern Deep Canyon. (NW 1/4, SE 1/4, Sec. 26, T14S, R11E)
- 245 Rhyolite, white pumice, base of upper flow, LBT, southern Deep Canyon. (NW 1/4, SE 1/4, Sec. 26, T14S, R11E)
- 246 Rhyolite, gray pumice, middle of upper flow, LBT, southern Deep Canyon. (NW 1/4, SE 1/4, Sec. 26, T14S, R11E)
- 247 Rhyolite, white pumice, middle of upper flow, LBT, southern Deep Canyon. (NW 1/4, SE 1/4, Sec. 26, T14S, R11E)
- 248 Dacite, black pumice, top of upper flow, LBT, southern Deep Canyon. (NW 1/4, SE 1/4, Sec. 26, T14S, R11E)

Appendix 2. Major element geochemistry obtained by XRF and AAS.
Continued

Sample	249	181	182	183	184	185	186
SiO ₂	70.80	70.70	69.80	71.40	71.60	60.50	65.60
Al ₂ O ₃	16.38	15.52	15.30	15.92	15.91	16.25	14.20
FeO	3.02	2.81	2.25	2.43	2.65	7.28	5.37
MgO	1.03	1.27	1.67	1.10	1.08	2.80	1.34
CaO	1.65	1.55	2.62	1.37	1.07	5.44	3.82
Na ₂ O	3.68	3.38	4.43	3.57	3.28	4.68	3.10
K ₂ O	4.54	3.82	4.12	4.77	4.93	1.64	2.45
TiO ₂	<u>0.55</u>	<u>0.27</u>	<u>0.23</u>	<u>0.26</u>	<u>0.30</u>	<u>1.51</u>	<u>0.97</u>
Total	101.65	99.32	100.42	100.80	100.80	100.10	96.78

249 Rhyolite, white pumice, top of upper flow, LBT, southern Deep Canyon. (NE 1/4, SE 1/4, Sec. 26, T14S, R11E)

181 Rhyolite, white pumice, MCT, lag deposit at base of three flows, Deep Canyon and Lower Bridge Road. (SE 1/4, Sec. 17, T14S, R12E)

182 Rhyolite, white pumice, from lowest of three flows, MCT, Deep Canyon and Lower Bridge Road. (SE 1/4, Sec. 17, T14S, R12E)

183 Rhyolite, white pumice from concentration of large pumice, at top of middle flow, MCT, Deep Canyon and Lower Bridge Road. (SE 1/4, Sec. 17, T14S, R12E)

184 Rhyolite, white pumice, from base of upper flow, MCT, Deep Canyon and Lower Bridge Road. (SE 1/4, Sec. 17, T14S, R12E)

185 Andesite, black pumice, cinders from base of upper flow, MCT, Deep Canyon and Lower Bridge Road. (SE 1/4, Sec 17, T14S, R12E)

186 Dacite, black pumice picked out of a mixed pumice block, MCT, Deep Canyon and Lower Bridge Road. (SE 1/4, Sec. 17, T14S, R12E)

Appendix 2. Major element geochemistry obtained by XRF and AAS.
Continued

Sample	186	187	188	189	190	191	192
SiO ₂	73.40	69.80	64.00	69.70	61.80	72.30	71.40
Al ₂ O ₃	13.80	15.05	15.90	15.37	16.20	15.32	16.58
FeO	2.39	2.51	5.40	2.80	7.05	2.52	2.72
MgO	0.19	1.37	2.31	0.93	2.58	0.80	1.46
CaO	1.04	2.05	3.75	1.37	5.01	1.20	1.60
Na ₂ O	2.39	5.38	4.45	4.30	4.61	3.30	3.08
K ₂ O	5.12	3.89	2.57	4.05	1.50	4.55	3.93
TiO ₂	<u>0.21</u>	<u>0.25</u>	<u>1.04</u>	<u>0.32</u>	<u>1.48</u>	<u>0.26</u>	<u>0.27</u>
Total	98.54	100.30	99.40	98.84	100.20	100.25	101.00

- 186 Rhyolite, white pumice picked from a mixed pumice, MCT, Deep Canyon and Lower Bridge Road. (SE 1/4, Sec. 17, T14S, R12E)
- 187 Rhyolite, white pumice, from top of the middle flow, MCT, Deep Canyon and Lower Bridge Road. (SE 1/4, Sec. 17, T14S, R12E)
- 188 Dacite, mixed pumice, from top of the middle flow, MCT, Deep Canyon and Lower Bridge Road. (SE 1/4, Sec. 17, T14S, R12E)
- 189 Rhyolite, white pumice, from top of the middle flow, MCT, Deep Canyon and Lower Bridge Road. (SE 1/4, Sec. 17, T14S, R12E)
- 190 Andesite, black pumice, from the bottom flow of four, MCT, Squaw Creek Butte. (NW 1/4, SE 1/4, Sec. 23, T13S, R11E)
- 191 Rhyolite, white pumice, one large fragment, from the bottom flow of four, MCT, Squaw Creek Butte. (NW 1/4, SE 1/4, Sec. 23, T13S, R11E)
- 192 Rhyolite, white pumice, from the bottom flow of four, MCT, Squaw Creek Butte. (NW 1/4, SE 1/4, Sec. 23, T13S, R11E)

Appendix 2. Major element geochemistry obtained by XRF and AAS.
Continued

Sample	194	195	196	197	198	201	202
SiO ₂	71.90	59.70	60.90	71.60	71.00	59.60	72.60
Al ₂ O ₃	17.25	16.38	16.32	16.35	16.40	16.48	15.18
FeO	2.90	8.00	7.12	2.73	2.55	7.85	2.30
MgO	1.53	3.17	2.85	1.72	1.37	3.35	1.14
CaO	1.40	5.92	5.00	1.65	1.37	6.10	1.50
Na ₂ O	2.92	4.19	4.42	3.08	2.73	3.68	3.10
K ₂ O	3.79	1.27	1.43	3.66	4.93	1.50	5.37
TiO ₂	<u>0.33</u>	<u>1.68</u>	<u>1.51</u>	<u>0.31</u>	<u>0.28</u>	<u>1.50</u>	<u>0.24</u>
Total	102.00	100.30	99.55	101.10	100.60	100.06	101.40

- 194 Rhyolite, white pumice, from the second flow up of four, MCT, Squaw Creek Butte. (NW 1/4, SE 1/4, Sec. 23, T13S, R11E)
- 195 Andesite, black pumice, one large cinder, from the second flow up of four, MCT, Squaw Creek Butte. (NW 1/4, SE 1/4, Sec. 23, T13S, R11E)
- 196 Andesite, black pumice, from the third flow up of four, MCT, Squaw Creek Butte. (NW 1/4, SE 1/4, Sec. 23, T13S, R11E)
- 197 Rhyolite, white pumice, from the third flow up of four, MCT, Squaw Creek Butte. (NW 1/4, SE 1/4, Sec. 23, T13S, R11E)
- 198 Rhyolite, white pumice, from the base of the top flow, MCT, Squaw Creek Butte. (NW 1/4, SE 1/4, Sec. 23, T13S, R11E)
- 201 Andesite, black pumice, from the base of the top flow, MCT, Squaw Creek Butte. (NW 1/4, SE 1/4, Sec. 23, T13S, R11E)
- 202 Rhyolite, white pumice, from the middle of the top flow, MCT, Squaw Creek Butte. (NW 1/4, SE 1/4, Sec. 23, T13S, R11E)

Appendix 2. Major element geochemistry obtained by XRF and AAS.
Continued

Sample	204	205	206	217	218	220	221
SiO ₂	62.00	59.20	71.30	65.60	60.40	64.30	60.30
Al ₂ O ₃	15.20	15.93	16.89	15.90	16.01	16.17	16.26
FeO	7.53	7.83	2.60	5.17	7.99	6.25	7.53
MgO	3.41	3.25	0.57	1.88	3.22	2.93	3.07
CaO	6.25	5.87	1.06	3.40	5.55	4.10	5.44
Na ₂ O	3.55	3.78	3.65	4.27	3.63	3.83	3.92
K ₂ O	1.54	1.60	4.51	2.61	1.45	2.31	1.40
TiO ₂	<u>1.42</u>	<u>1.50</u>	<u>0.27</u>	<u>0.93</u>	<u>1.62</u>	<u>1.16</u>	<u>1.54</u>
Total	100.90	98.96	100.85	99.76	99.87	101.05	99.46

- 204 Andesite, black pumice, from the middle of the top flow, MCT, Squaw Creek Butte. (NW 1/4, SE 1/4, Sec. 23, T13S, R11E)
- 205 Andesite, black pumice, from the top of the top flow, MCT, Squaw Creek Butte. (NW 1/4, SE 1/4, Sec. 23, T13S, R11E)
- 206 Rhyolite, white pumice, one 2 1/2" pumice, from the top of the top flow, MCT, Squaw Creek Butte. (NW 1/4, SE 1/4, Sec. 23, T13S, R11E)
- 217 Dacite, mixed pumice, from the base of the upper orange flow (the only flow present), MCT, Crooked River. (NW 1/4, NE 1/4, Sec. 36, T13S, R12E)
- 218 Andesite, black pumice, from the base of the orange flow, MCT, Crooked River. (NW 1/4, NE 1/4, Sec. 36, T13S, R12E)
- 220 Dacite, mixed pumice, from the middle of the orange flow, MCT, Crooked River. (NW 1/4, NE 1/4, Sec. 36, T13S, R12E)
- 221 Andesite, black pumice, from the middle of the orange flow, MCT, Crooked River. (NW 1/4, NE 1/4, Sec. 36, T13S, R12E)

Appendix 2. Major element geochemistry obtained by XRF and AAS.
Continued

Sample	223	224	225	226	229	229	230
SiO ₂	61.60	62.20	67.50	61.90	73.20	72.80	72.60
Al ₂ O ₃	16.05	16.25	15.51	16.15	14.23	14.79	14.50
FeO	6.85	6.66	4.57	7.00	2.15	2.42	2.48
MgO	3.22	3.38	1.54	2.77	0.83	0.16	0.22
CaO	5.34	4.83	3.18	5.07	2.07	1.09	1.12
Na ₂ O	3.65	3.65	4.13	3.94	3.60	4.64	4.12
K ₂ O	1.85	1.81	3.46	1.71	5.20	4.46	4.85
TiO ₂	<u>1.28</u>	<u>1.28</u>	<u>0.74</u>	<u>1.37</u>	<u>0.22</u>	<u>0.23</u>	<u>0.24</u>
Total	99.84	100.06	100.63	99.91	101.50	100.60	100.13

- 223 Andesite, mixed pumice, from the top of the orange flow, MCT, Crooked River. (NW 1/4, NE 1/4, Sec. 36, T13S, R12E)
- 224 Andesite, black pumice, from the top of the orange flow, MCT, Crooked River. (NW 1/4, NE 1/4, Sec. 36, T13S, R12E)
- 225 Dacite, collapsed pumice, from the middle of the upper flow, MCT, Deep Canyon and Lowder Bridge Road. (SE 1/4, Sec. 17, T14S, R12E)
- 226 Andesite, black pumice, from the middle of the upper flow, MCT, Deep Canyon and Lower Bridge Road. (SE 1/4, Sec. 17, T14S, R12E)
- 228 Rhyolite, white pumice, from the middle of the upper flow, MCT, Deep Canyon and Lower Bridge Road. (SE 1/4, Sec. 17, T14S, R12E)
- 229 Rhyolite, collapsed pumice, from the top of the upper flow, MCT, Deep Canyon and Lower Bridge Road. (SE 1/4, Sec. 17, T14S, R12E)
- 230 Rhyolite, white pumice, from the top of the upper flow, MCT, Deep Canyon and Lower Bridge Road. (SE 1/4, Sec. 17, T14S, R12E)

Appendix 2. Major element geochemistry obtained by XRF and AAS.
Continued

Sample	231	251	252	253	254	255	256
SiO ₂	62.50	72.60	60.30	67.40	71.60	71.70	60.50
Al ₂ O ₃	15.61	16.13	16.60	15.05	14.89	15.27	16.29
FeO	6.10	2.82	7.57	4.64	2.68	2.51	7.32
MgO	2.71	1.17	2.85	1.67	1.12	0.74	2.83
CaO	4.91	1.64	5.45	3.18	1.75	1.70	5.45
Na ₂ O	3.67	3.38	4.57	3.97	3.92	3.82	4.55
K ₂ O	1.82	3.57	1.39	2.95	4.02	4.40	1.46
TiO ₂	<u>1.07</u>	<u>0.32</u>	<u>1.55</u>	<u>0.81</u>	<u>0.30</u>	<u>0.27</u>	<u>1.53</u>
Total	98.40	100.63	100.28	99.67	100.28	100.41	99.93

- 231 Andesite, mixed and black pumice, from the top of the upper flow, MCT, Deep Canyon and Lower Bridge Road. (SE 1/4, Sec. 17, T14S, R12E)
- 251 Rhyolite, white pumice, from the base of the 35' thick MCT section, southern Deep Canyon. (NE 1/4, SE 1/4, Sec. 26, T14S, R11E)
- 252 Andesite, black pumice, from the base of the 35' thick MCT section, southern Deep Canyon. (NE 1/4, SE 1/4, Sec. 26, T14S, R11E)
- 253 Dacite, mixed pumice, from the base of the 35' thick MCT section, southern Deep Canyon. (NE 1/4, SE 1/4, Sec. 26, T14S, R11E)
- 254 Rhyolite, white pumice, from 10' up in the 35' section, MCT, southern Deep Canyon. (NE 1/4, SE 1/4, Sec. 26, T14S, R11E)
- 255 Rhyolite, white pumice, from 10' up in the 35' section, MCT, southern Deep Canyon. (NE 1/4, SE 1/4, Sec. 26, T14S, R11E)
- 256 Andesite, black pumice, from 10' up in the 35' section, MCT, southern Deep Canyon. (NE 1/4, SE 1/4, Sec. 26, T14S, R11E)

Appendix 2. Major element geochemistry obtained by XRF and AAS.
Continued

Sample	257	258	259	270	271	272	273
SiO ₂	64.10	71.80	59.60	71.50	64.00	61.80	72.80
Al ₂ O ₃	16.00	14.70	17.09	15.00	14.90	15.00	14.80
FeO	5.80	2.20	8.18	2.62	6.25	7.17	2.41
MgO	2.26	0.47	3.22	0.75	1.62	1.77	0.61
CaO	4.88	1.66	6.20	1.41	4.94	5.12	1.28
Na ₂ O	3.92	4.30	4.46	1.82	2.66	2.61	2.31
K ₂ O	2.26	5.58	1.53	5.02	2.19	1.90	4.76
TiO ₂	<u>1.07</u>	<u>0.23</u>	<u>1.67</u>	<u>0.24</u>	<u>1.12</u>	<u>1.32</u>	<u>0.20</u>
Total	100.29	100.94	101.95	98.30	97.69	96.63	99.19

- 257 Dacite, mixed pumice, from 10' up in the 35' section, MCT, southern Deep Canyon. (NE 1/4, SE 1/4, Sec. 26, T14S, R11E)
- 258 Rhyolite, white pumice, from 25' up in the 35' section, MCT, southern Deep Canyon. (NE 1/4, SE 1/4, Sec. 26, T14S, R11E)
- 259 Andesite, black pumice, from 25' up in the 35' section, southern Deep Canyon. (NE 1/4, SE 1/4, Sec. 26, T14S, R11E)
- 270 Rhyolite, white pumice, from MCT boulders below the orange MCT flow, MCT, southern Deep Canyon. (NE 1/4, SE 1/4, Sec. 26, T14S, R11E)
- 271 Dacite, black pumice, from MCT boulders below the orange MCT flow, southern Deep Canyon. (NE 1/4, SE 1/4, Sec. 26, T14S, R11E)
- 272 Andesite, black pumice, from the orange MCT flow above the MCT boulders, southern Deep Canyon. (NE 1/4, SE 1/4, Sec. 26, T14S, R11E)
- 273 Rhyolite, white pumice, from the orange MCT flow above the MCT boulders, southern Deep Canyon. (NE 1/4, SE 1/4, Sec. 26, T14S, R11E)

Appendix 2. Major element geochemistry obtained by XRF and AAS.
Continued

Sample	170	170	Unit 10	Unit 10	Unit 5	Uncertainties %
SiO ₂	74.30	68.30	68.93	59.10	70.60	4- 8
Al ₂ O ₃	13.30	13.20	15.71	16.70	15.72	4-10
FeO	2.23	4.91	4.14	7.78	2.84	4-10
MgO	0.16	0.89	0.66	2.33	0.48	10-20
CaO	1.08	3.08	2.24	5.79	1.67	4- 8
Na ₂ O	2.01	2.66	5.31	4.78	4.00	4- 8
K ₂ O	5.82	3.10	2.29	1.21	3.77	4- 8
TiO ₂	<u>0.26</u>	<u>0.87</u>	<u>0.56</u>	<u>1.54</u>	<u>0.40</u>	2- 5
Total	99.15	97.05	99.84	99.23	99.48	

- 170 Rhyolite, white pumice, Unit 0, from middle of flow. (NW 1/4, NE 1/4 Sec. 10, T13S, R12E)
- 171 Dacite, mixed pumice, Unit 0, from middle of flow. (NW 1/4, NE 1/4 Sec. 10, T13S, R12E)
- Unit 10 Dacite, white pumice, average of 7 analyses, "Six Creek Tuff."
- Unit 10 Andesite, black pumice, average of 5 analyses, "Six Creek Tuff."
- Unit 5 Rhyolite, white pumice, average of 11 analyses, "Fly Creek Tuff."